

Stellingen

1. Bij de heterogene Wacker oxidatie van etheen werd door Forni *et al.* een lineair verband gevonden tussen de reactiesnelheid en de V^{4+} concentratie. Op grond hiervan concluderen zij ten onrechte tot een promoterende werking van V^{4+} .
L. Forni and G. Terzoni, *Ind. Eng. Chem. Process Des. Dev.*, 16 (1977) 288.
2. Uit het feit dat Moro-oka *et al.* bij Wacker (?) oxidatie van propen acroleïne als produkt vonden, kan geconcludeerd worden dat op hun katalysator geen Pd(II) maar nulwaardig palladium aanwezig geweest is.
Y. Moro-oka, T. Ohhata, Y. Takita and A. Ozaki, *Bull. Chem. Soc. Jpn.*, 46 (1973) 681.
3. Gezien de overeenkomst in overgangstoestand bij Wacker oxidatie van crotonalkohol en 3-propen-2-ol is het verwonderlijk dat Jira zich sterk maakt om de overeenkomst in produktselektiviteit te verklaren uit een voorafgaande evenwichtinstelling tussen beide uitgangsstoffen.
R. Jira, *Tetrahedron Lett.*, 17 (1971) 1225.
4. Het is onwaarschijnlijk dat het dimeer van vanadium oxide alleen op het (111) vlak van $\gamma\text{-Al}_2\text{O}_3$ voor zal komen, zoals door Haber *et al.* voorgesteld wordt. Bovendien wordt door Haber's metingen de gelijktijdige aanwezigheid van monomere en polymere eenheden op het $\gamma\text{-Al}_2\text{O}_3$ oppervlak niet uitgesloten.
J. Haber, A. Kozlovska and R. Kozlovski, *J. Catal.*, 102 (1986) 52.
5. Busca *et al.* berekenen ten onrechte de vanadaat-bezettingsgraad op $\text{TiO}_2(\text{a})$ per eenheid van gewicht katalysator. Men moet de bezettingsgraad per eenheid van gewicht drager uitrekenen.
G. Busca, G. Centi, L. Marchetti and F. Trifiro, *Langmuir*, 2 (1986) 568.
6. Dat transport van waterstof over het oppervlak van een Pd/SiO₂ katalysator voornamelijk via de gas-fase verloopt is nog geen reden om te veronderstellen dat spillover in het algemeen op deze wijze verloopt.
E. Baumgarten, C. Lentjes-Wagner and R. Wagner, *J. Catal.*, 117 (1989) 533.
7. De relatieve druk waarbij water als monolaag zal adsorberen op alumina wordt door Peri zeker te laag geschat.
J.B. Peri, *J. Phys. Chem.*, 69 (1965) 211.
8. Het wekt verwondering dat er nog weinig onderzoek is gedaan naar de synthese en katalytische activiteit van heteronucleaire bimetallische complexen. Het is immers in principe mogelijk om met dergelijke complexen meerdere elementaire reaktiestappen gelijktijdig te versnellen.

9. Goede titels kunnen vaker gebruikt worden.

S. Malinowski, S. Szczepanska and J. Sloczynski, J. Catal., 4 (1965) 324.
S. Malinowski, S. Szczepanska and J. Sloczynski, J. Catal., 7 (1967) 67.

10. De veelheid aan katalytische reacties die in de levende natuur voorkomen, onder milde omstandigheden en gelijktijdig verlopend, wekt verwondering, en toont aan dat onze huidige kennis en kunde in de technologische katalyse beschouwd moet worden als een eerste onbeholpen aanzet.
11. In het creationisme speelt het verklaren van geologische verschijnselen uit de gevolgen van katastrofes in het verleden een centrale rol. Het verdient daarom aanbeveling om de term creationisme te vermijden en te veranderen in katastrofisme.
12. Het weergeven van chemische reacties in termen uit het dagelijks leven voert ons binnen in een sprookjeswereld, waarin onsterfelijke wezentjes de meest flitsende avonturen beleven en met elkaar een veelheid van bruisende relaties aangaan en weer verbreken.
13. Eén goede moeder leert ons meer dan tien schoolmeesters.
14. Tuinders weten dat CO_2 in broeikassen effect heeft.

Stellingen
behorende bij het proefschrift:
Heterogeneous Wacker Oxidation
van
Evert van der Heide

TU Delft, 13-9-1990.

10/20/78
3/7/79
S. R. 10/1/79

Heterogeneous Wacker Oxidation

Heterogeneous Wacker Oxidation

Proefschrift

Ter verkrijging van
de graad van doctor
aan de Technische Universiteit Delft,
op gezag van de Rector Magnificus,
prof. drs. P.A. Schenck,
in het openbaar te verdedigen
ten overstaan van een commissie
aangewezen door het College van Dekanen
op 13 september 1990
te 16.00 uur

door

Evert van der Heide

geboren te Zwartsluis

scheikundig doctorandus.



Delft University Press, 1990.

**Dit proefschrift is goedgekeurd door de promotor
prof. dr. J.J.F. Scholten**

Als ik naar de hemel kijk, het werk van uw vingers,
naar de maan en de sterren door U daar vastgezet
dan denk ik:

Wat is toch de mens dat U om hem geeft,
wat betekent hij dat U voor hem zorgt ?
U hebt hem bijna goddelijk gemaakt
hem met glorie en eer gekroond.

Psalm 8

Contents

1. Introduction to Wacker oxidation

Discovery and industrial application	1
Kinetics and mechanism	3
Reoxidation of Pd(0) to Pd(II)	15
Reoxidation of CuCl to CuCl ₂ by O ₂	20
Wacker oxidation of higher and substituted alkenes	21
Heterogeneous Wacker oxidation	26
Oxidation reactions over V ₂ O ₅ containing catalysts	29
Preparation of supported vanadate catalysts	31
The structure of vanadate monolayers	33
Scope of the thesis	39
References	40

2. Some experimental aspects of heterogeneous Wacker oxidation

Catalyst preparation	47
The catalytic performance	52
References	56

3. Solid-state ⁵¹V NMR and DRIFT structural studies of vanadate monolayers on γ -Al₂O₃

Abstract	57
Introduction	58
Experimental	59
Results	60
Discussion	65
Conclusions	67
References	68

4. Kinetics and mechanism of the gas phase oxidation of ethylene to acetaldehyde over a new heterogenized surface vanadate Wacker catalyst

Abstract	69
Introduction	70
Experimental	70
Results and discussion	72
Conclusions	78
References	79

5. Kinetics and mechanism of the gas phase oxidation of 1-butene to butanone over a new heterogenized surface vanadate Wacker catalyst

Abstract	81
Introduction	82
Experimental	83
Results and discussion	85
References	92

6. Mechanism of the gas phase oxidation of cyclohexene over a new heterogenized surface vanadate Wacker catalyst

Abstract	93
Introduction	93
Experimental	94
Results and discussion	95
Conclusions	99
References	100

7. Kinetics and mechanism of the gas phase oxidation of styrene to benzaldehyde, acetophenone and cinnamaldehyde over a new heterogenized surface vanadate Wacker catalyst

Abstract	101
Introduction	102
Experimental	103
Results and discussion	104
Conclusions	110
References	110

8. Kinetics and mechanism of the gas phase oxidation of ethylene to acetaldehyde over a TiO_2 (anatase) supported surface vanadate Wacker catalyst

Abstract	111
Introduction	112
Experimental	113
Results and discussion	114
Conclusions	121
References	121

9. Kinetics and mechanism of the reduction of vanadate monolayers by hydrogen spillover in the presence of palladium chloride

Abstract	123
Introduction	124
Experimental	125
Theory	126
Results and discussion	131
Conclusions	135
List of symbols	136
References	136

10. Oxidation of ethylene to acetaldehyde over a heterogenized surface vanadate Wacker catalyst in the presence and in the absence of gaseous oxygen

Abstract	137
Introduction	138
Experimental	139
Results and discussion	140
Conclusions	146
References	146

11. Heterogeneous Wacker oxidation; outline and outlook

Abstract	147
Outline	149
Outlook	154
References	155

Summary 157

Samenvatting 159

Uitleg voor niet-vakgenoten 161

Dankwoord 163

Curriculum vitae 165

Publications:

Chapter 3: E. van der Heide, R. Janssen and J.G. van Ommen, submitted to J. Molec. Catal..

Chapter 4: E. van der Heide, M. de Wind, A.W. Gerritsen and J.J.F. Scholten, Proc. 9th Int. Congr. Catal., Calgary, 4 (1988) 1648.

Chapter 5: E. van der Heide, J.A.M. Ammerlaan, A.W. Gerritsen and J.J.F. Scholten, J. Molec. Catal., 55 (1989) 320.

Chapter 7: E. van der Heide, J. Schenk, A.W. Gerritsen and J.J.F. Scholten, Recl. Trav. Chim. Pays-Bas, 109 (1990) 93.

Chapter 9: E. van der Heide, M.F.M. Zwinkels, A.W. Gerritsen and J.J.F. Scholten, submitted to J. Molec. Catal..

Chapter 10: E. van der Heide, A.W. Gerritsen and J.J.F. Scholten, submitted to J. Molec. Catal..

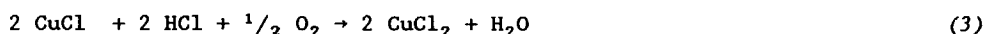
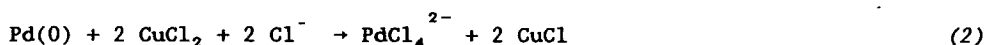
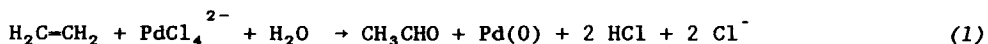
drawings: J.J.B. van Holst

1

Introduction to Wacker oxidation

Discovery and industrial application

The formation of acetaldehyde during the reduction of palladium chloride by ethylene was already noticed in 1894 by Phillips [1], but the reaction remained practically unknown until the late nineteen fifties, when a new catalytic process for the oxidation of ethylene to acetaldehyde, based on



the Phillips reaction, was introduced by Smidt and co-workers, working with the Consortium für elektrochemische Industrie, a research company of Wacker Chemie [2]. They found that the oxidation of ethylene by palladium chloride dissolved in hydrochloric acid became a catalytic process by addition of CuCl_2 to the palladium chloride/hydrochloric acid solution. The reaction runs under the mild conditions of one atmosphere pressure and 293 - 333 K. In the presence of CuCl_2 , the zero-valent palladium formed simultaneously with acetaldehyde (eq. (1)) is reoxidized *in situ* to palladium chloride (eq. (2)), whereafter CuCl reacts with oxygen and returns to CuCl_2 (eq. (3)).

- 1. Wacker oxidation -

When the reaction equations are added, the net reaction is oxidation of ethylene with oxygen to acetaldehyde (eq. (4)). Higher (terminal) alkenes can be oxidized to the corresponding (methyl-) ketones (eq. (5)).

The Wacker process was a technological improvement on the existing processes. Usually the oxidation of alkenes to ketones and aldehydes was performed in two steps: hydration of the alkene to the corresponding



alcohol, followed by dehydrogenation (or oxidative dehydrogenation) to the corresponding ketone or aldehyde. Until now, in spite of new developments [3], Wacker oxidation is the only important one-stage oxidation reaction of ethylene to acetaldehyde and of higher (terminal) alkenes to (methyl-) ketones [4].

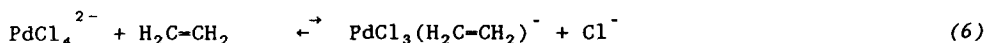
Shortly after the Wacker invention, acetaldehyde was already produced on a large scale as a raw material for the production of acetic acid and related compounds. It is estimated that in 1976 29 companies, with more than 82 % of the world's 2.3 megaton acetaldehyde per year plant capacity, used the Wacker process for the direct oxidation of ethylene [5].

Two technologically different production methods are in use: in the single-stage process a mixture of ethylene and oxygen is led through the catalyst solution, while in the two-stage process first ethylene is oxidized to acetaldehyde, according to eqs. (1) and (2), whereafter the reduced catalyst is oxidized by air (eq. (3)) [6]. Economic considerations determine the choice between the two. The selectivity in both processes is high (> 95 %); byproducts include chlorinated and higher oxidized compounds. In both processes the catalyst deactivates due to precipitation of insoluble copper oxalate, and therefore a small part of the catalyst solution is regenerated continuously [7]. Nowadays acetic acid can be produced by the rhodium catalyzed carbonylation of methanol (Monsanto process [8]) and therefore the need for production of acetaldehyde is strongly decreasing.

The commercial Wacker oxidation of higher alkenes (e.g. of propene and of the butenes) still seems to be attractive, but, although detailed process schemes have been published [9], these processes have never been practised on a large scale until now. The reasons for this will be discussed in a later paragraph.

Kinetics and mechanism

The kinetics of the Wacker reaction have been studied profoundly. In the initial stage a rapid ethylene uptake by the Pd(II) solution is observed, the rate of which is not influenced by the acid concentration, but which decreases with increasing chloride ion concentration by a first order inhibition. The initial uptake exceeds that required to saturate the reaction solution with ethylene. This clearly points to the formation of an ethylene-palladium complex and is in agreement with equilibrium (6) [10].

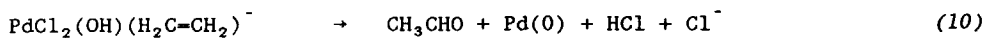
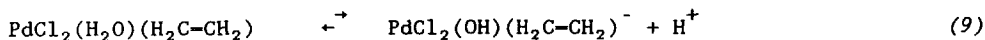
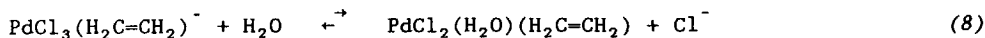


After this initial uptake of ethylene a slower uptake occurs, and a second order inhibition in chloride is found, next to a first order inhibition with respect to the proton concentration. Furthermore the reaction rate is first order with respect to the palladium as well as the alkene concentration. Combining these results the experimental net rate expression becomes (eq. (7)) [11]:

$$r = k \cdot \frac{[\text{PdCl}_4^{2-}][\text{H}_2\text{C}=\text{CH}_2]}{[\text{H}^+][\text{Cl}^-]^2} \quad (7)$$

Equation (7) is valid within the concentration ranges: $0.005 \text{ M} < \text{Pd(II)} < 0.04 \text{ M}$; $0.1 \text{ M} < \text{Cl}^- < 1.0 \text{ M}$ and $0.04 \text{ M} < \text{H}^+ < 1.0 \text{ M}$.

The equilibria (6), (8) and (9), including the rate determining step



(eq. (10)), give a good description of the observed kinetics. From equilibrium (8) also a first order with respect to the water concentration

- 1. Wacker oxidation -

is to be expected. However, water as the solvent is present in excess and therefore the influence of the water concentration on the reaction rate cannot be measured.

Further evidence of the correctness of the above mechanism is obtained from isotope experiments (Table I). When the reaction takes place in D₂O an isotope effect k_H/k_D of 4.05 is found [12]. This isotope effect is

Table I. Isotope experiments in Wacker oxidation.

<u>reaction</u>	<u>k_H/k_D</u>	<u>products</u>	<u>ref.</u>
H ₂ C=CH ₂ + D ₂ O	4.05	H ₃ C-CHO	[12]
D ₂ C=CD ₂ + H ₂ O	1.07	D ₃ C-CDO	[11]
DHC=CHD + H ₂ O	≈ 1	H ₂ DC-CDO/HD ₂ C-CHO = 1.7, 1.86	[11,13]
D ₂ C=CH ₂ + H ₂ O	-	H ₂ DC-CDO/HD ₂ C-CHO = 0.89	[13]

consistent with equilibrium (9), since acids, PdCl₂(H₂O)(H₂C=CH₂) in this case, are weaker in D₂O than they are in H₂O. It is also found that no deuterium is incorporated in the product [14], thus all of the hydrogen atoms in the aldehyde originate from ethylene. This result excludes a hydration of the alkene followed by dehydrogenation, because in that case deuterium would have been incorporated in the product. Moreover, under equal reaction conditions, dehydrogenation of ethanol is slow relative to Wacker oxidation [14].

Other isotope experiments have been carried out with 1,2-dideutero-ethylene (both *cis* and *trans*). The overall reaction rate is essentially the same for C₂H₄ and C₂H₂D₂. The product ratio of CH₂DCDO to CHD₂CHO was found to range between 1.70 [11] and 1.86 [13]. Analogous results are found in the case of oxidation of C₂D₄: it leads to CD₃CDO exclusively and an isotope effect k_H/k_D of only 1.07 is found [11]. For hydrogen transfer from one carbon to the other, a kinetic isotope effect k_H/k_D of about 1.7 is found and the same kinetic isotope effect in the reaction rate should be anticipated when hydrogen transfer is involved in the rate determining step.

- 1. Wacker oxidation -

The value of 1.07 found indicates that in the course of the rate determining step C-H bond breaking does not occur. It should be noted that the magnitude of the difference between 1.7 and 1.07 is not large enough to be conclusive; it gives only an indication that no C-H bond breaking is involved in the rate determining step [15,16].

Also 1,1-dideuteroethylene has been oxidized; a ratio of CH₂DCDO to

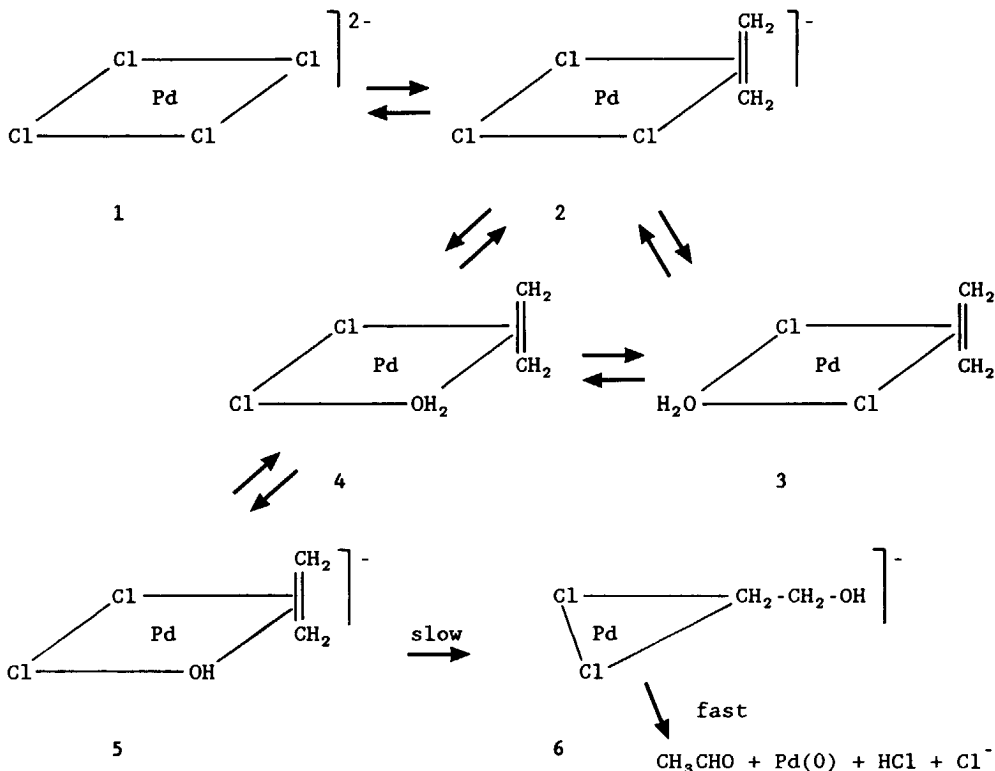


Figure 1. Reaction mechanism of the Wacker oxidation [15].

CHD₂CHO of 0.89 was found [13]. Later on, this result will be discussed in detail; for the time being it is sufficient to say that also in this case hydrogen is more easily transferred from one carbon to another than deuterium.

- 1. Wacker oxidation -

On the basis of the above results a reaction mechanism can be formulated as depicted in Fig. 1, and this will now be discussed further.

When PdCl_2 is dissolved in hydrochloric acid, PdCl_4^{2-} (complex 1) is almost exclusively available [17]. This d^8 Pd(II)-complex is sp^2 hybridized and therefore square planar [18]. After reaction with ethylene, complex 2 is formed, which has the same square planar structure as its platinum analogue, Zeise's salt. Although a few in-plane palladium-alkene complexes are known [19], ethylene is bound perpendicular to the Pd-Cl (or Pt-Cl) plane [6,20]. Evidence for the relation between the properties of Zeise's salt and the

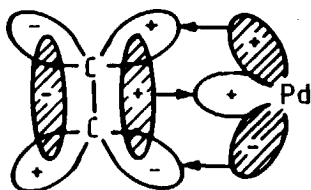


Figure 2. Coordination of ethylene to a palladium centre [13].

Wacker reaction is the fact that also Zeise's salt, if decomposed by water, exudes acetaldehyde [21].

The bond between ethylene and palladium can be described according to the donation-back-donation principle (Fig. 2) [22]. The π -electrons of ethylene are partly transferred to an sp^2 hybridized orbital of palladium and the filled d_{yz} orbital of palladium donates electrons back to the antibonding π -orbitals of ethylene. A decrease of the π -electron density and an increase of the antibonding electron density result in a lowering of the bonding strength and an increase of the C-C distance in ethylene. Moreover coordinated ethylene is more sensitive towards nucleophilic attack than free ethylene.

The next step comprises exchange of a chlorine ligand for a water ligand (eq. (8)), in which both a *cis* and a *trans* hydrated palladium complex (3 and 4) can be formed. For steric reasons only the *cis*-form is expected to be reactive. About 10 % of the corresponding $\text{PtCl}_2(\text{H}_2\text{O})(\text{C}_2\text{H}_4)$ complex is in the *cis*-form [23]. As Pd(II) shows less of a *trans* effect than

- 1. Wacker oxidation -

Pt(II) does, it should be expected that more than 10 % of the *cis* isomer is present in the case of Pd(II).

The next step is an acid-base equilibrium: the coordinated water molecules are in equilibrium with coordinated hydroxyl groups and H_3O^+ is set free (Fig. 1 and eq. (9)).

The rate-determining step is assumed to be the nucleophilic attack of the coordinated ethylene molecule by a hydroxyl group (eq. (10)). This step

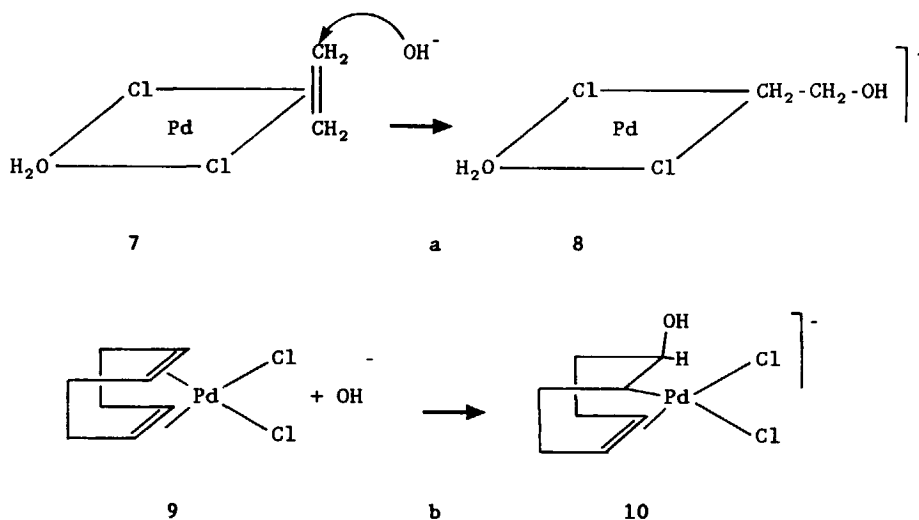


Figure 3. Intermolecular *trans* hydroxypalladation of a: coordinated ethylene (hypothetical); b: coordinated 1,5-cyclooctadiene [24].

is called 'hydroxypalladation'. However, two possibilities exist for hydroxypalladation. The first involves an intermolecular (*trans*) reaction between a hydroxyl anion from the solution and the coordinated ethylene molecule (Fig. 3, a). The second possibility is an intramolecular (*cis*) attack of the coordinated ethylene by the coordinated hydroxo group as indicated in Fig. 1. Both mechanistic possibilities lead to the same final kinetics.

It is difficult to make a choice between both possibilities. Under extreme reaction conditions, where Wacker oxidation is slow, indications are found for the occurrence of a *trans* hydroxypalladation. 1,5-Cyclooctadiene can be hydroxypalladized [24] and in this case surely a *trans*

- 1. Wacker oxidation -

hydroxypalladation occurs, as explained in Fig. 3b. In this case a *trans* addition is preferred for two reasons: first the original bidentate π complex 9 is neutral and exchange of a chlorine ligand for H_2O leads to a cation, which is unlikely. Further, attack of the neutral complex by external hydroxide is not influenced by charge effects, as is the case when OH^- reacts with the negatively charged $PdCl_3(C_2H_4)^-$ complex.

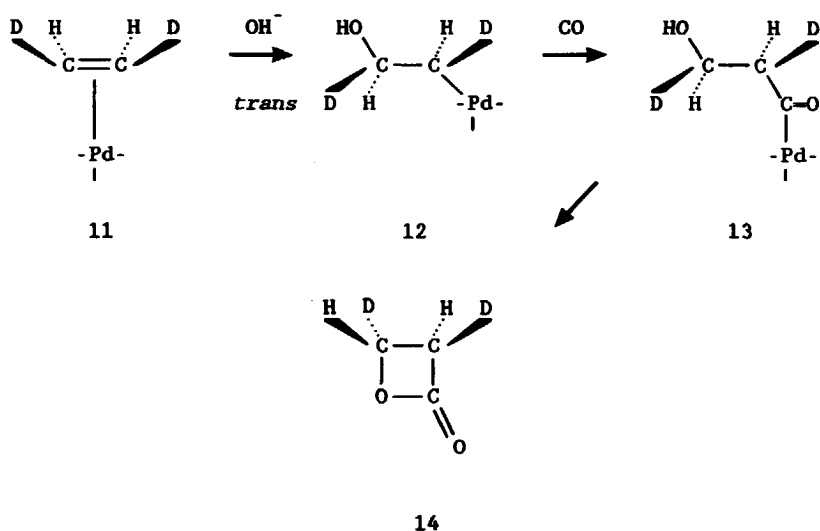


Figure 4. Hydroxypalladation of *cis*-1,2-dideuteroethylene, followed by carbonylation and lactone formation [25].

Further evidence in favour of *trans* addition stems from experiments with deuterated ethylene. As indicated in Fig. 4 a σ -bonded species like complex 12 can be captured by insertion of CO into the Pd-C bond. When this reaction is carried out starting from *cis*-1,2-dideuteroethylene, followed by lactone formation, the stereochemical structure of the product can be determined. The result indicates that we are dealing with a *trans* hydroxypalladation [25]. However, the conditions of this reaction differ strongly from normal Wacker oxidation conditions, as the starting material, the bis-ethylene palladium complex, is uncharged and can be *trans* attacked for the same reasons as the cyclooctadiene complex discussed above. Furthermore palladium

- 1. Wacker oxidation -

carbonyl complexes, quite different from the palladium complexes which occur under Wacker conditions, are likely to be the reactive form in the presence of CO.

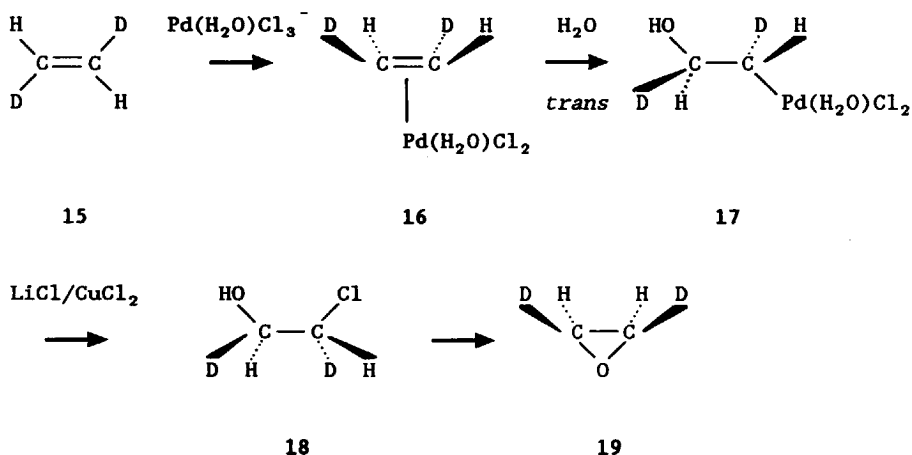


Figure 5. Hydroxypalladation of *trans*-1,2-dideuteroethylene, followed by chlorination and epoxide formation [26].

Another example of *trans* hydroxypalladation will be discussed now. When *trans*-1,2-dideuteroethylene is hydroxypalladated, followed by chlorination and epoxide formation (Fig. 5), the stereochemical configuration of the product can be established. Both *threo* chlorohydrin and *cis* epoxide are formed, which is indicative of a *trans* hydroxypalladation [26]. Some comments can be made with respect to this reaction: in Fig. 5 the chlorination is indicated to occur via inversion of the configuration. This may be true, and is the case when acetic acid is used as a solvent, but it is not necessarily the case in an aqueous solution as used in this experiment. Another objection can be made in connection with the very high chloride concentration used in this experiment. When such high chloride concentrations are used, any *cis* hydroxypalladation would be suppressed by equilibrium (8) being shifted to the left and therefore the results cannot be extrapolated to normal Wacker conditions [27].

In our view (see also [15]), under Wacker conditions the occurrence of

- 1. Wacker oxidation -

a *cis* hydroxypalladation is more likely, as will be explained now. Evidence of a *cis* addition can be derived from Wacker oxidation experiments in the presence of ethylenediamine or diethylenetriamine (Fig. 6). After reaction with the alkene, complexes 20 and 21 are formed. Complex 20 contains a water ligand coordinated *cis* to the olefine and decomposes 100 times faster than complex 21 does, under formation of acetaldehyde. In complex 21 no position is available for water coordination; the formation of acetaldehyde proceeds

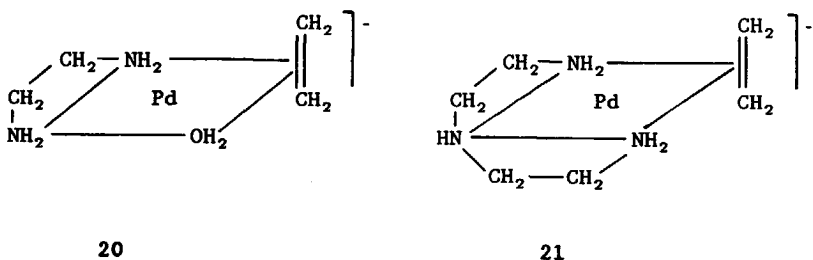


Figure 6. Pd(II) complexes with ethylenediamine and diethylenetriamine [28].

in this case via *trans* hydroxypalladation [28]. Although the comparison of these results points to a *cis* hydroxypalladation, one must take into account that different amine ligands influence the reactivity of the palladium centre differently.

Further information which supports an intramolecular *cis* hydroxypalladation is available. Under normal Wacker conditions the concentration of hydroxyl ions is only 10^{-15} times that of water. The less nucleophilic water is present in such abundance that reaction with H_2O will prevail [15]. But when water is reactant no retardation of the reaction rate by an increase of the hydrogen ion concentration is to be expected. Palladium coordinated water is more acidic than water itself and in this way a sufficiently high hydroxyl concentration is created.

From the low hydroxyl concentration in solution still another argument for *cis* hydroxypalladation can be put forward. Combining the experimental reaction rate with the equilibrium constant K_{water} and the equilibrium constant of equilibrium (6), it is found that the reaction rate of the

- 1. Wacker oxidation -

hydroxyl attack on $\text{PdCl}_2(\text{H}_2\text{O})(\text{C}_2\text{H}_4)$ must be 10^3 times faster than the rate of a diffusion controlled process in order to arrive at the measured rate of reaction [15].

It has to be concluded that the reaction proceeds via an intramolecular *cis* hydroxypalladation. As mentioned already, the number of coordinated

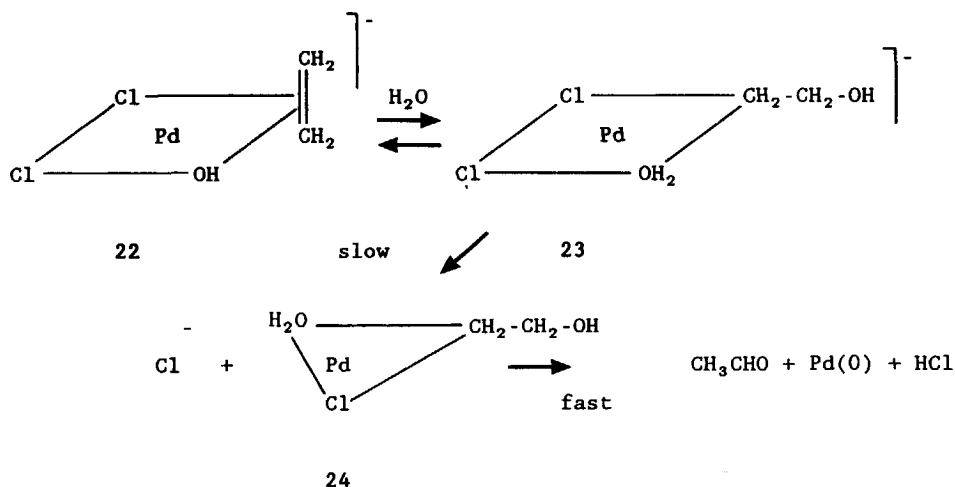


Figure 7. Reaction mechanism involving a reversible hydroxypalladation [26].

hydroxyl groups is much higher than the number of free hydroxide ions. It goes without saying that intramolecular *cis* addition of a hydroxyl ligand is not influenced by any form of diffusional retardation.

Recently, an alternative mechanism was proposed wherein a reversible hydroxypalladation occurs, followed by a rate-determining loss of a chloride ligand and product formation (Fig. 7). The reversible nature of the hydroxypalladation is supported by the fact that a reversible oxymercuration and also a reversible aminopalladation are known which are supposed to be related to Wacker oxidation [26].

There is, however, evidence against this mechanism. A strong argument for a non-reversible hydroxypalladation step stems from experiments carried out with 2-propene-1-ol (allyl alcohol) as the reactant. If a reversible

- 1. Wacker oxidation -

hydroxypalladation occurred, then the oxidation of allyl alcohol should proceed via the equilibria presented in Fig. 8 and isomerisation of the deuterated alcohol, simultaneously with product formation, would be expected. Although under conditions where the oxidation reaction is slow a fast isomerisation is observed [27], under fast oxidation conditions only very little isomerisation of 1,1-dideutero-2-propene-1-ol is found during

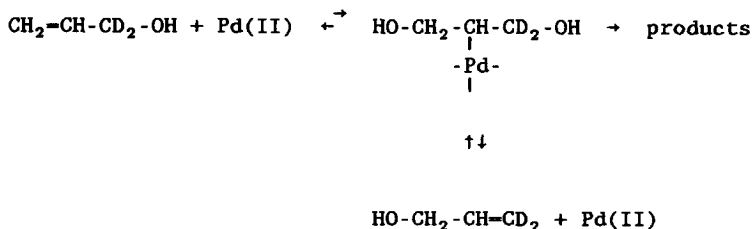


Figure 8. Proposed equilibria during Wacker oxidation of deuterated allyl alcohol oxidation [29].

the course of the reaction. Hence, a reversible hydroxypalladation reaction has to be rejected [29].

It is impossible to determine the structure of the transition state in the rate-determining step; we can only speculate about it. When 1,1-dideuteroethylene is oxidized, the product ratio $\text{CH}_2\text{DCDO} : \text{CHD}_2\text{CHO}$ is 0.89. This isotope distribution is consistent with a transition state structure involving a non-symmetrical π -coordinated ethylene molecule (Fig. 9) [30]. Theoretical calculations confirm this proposal [31].

After the rate-determining hydroxypalladation step, rapid rearrangement and decomposition gives the aldehyde and palladium metal (Fig. 1 and eq. (10)). The details of this rearrangement are still subject to speculation. We recall that, starting from C_2D_4 and H_2O , CD_3CDO is formed exclusively, which means that all H or D atoms in the ethylene end up in the acetaldehyde. Hence, one H or D atom has to be transferred from one carbon to the other. Some mechanisms have been published in the literature which allow for this fact (Fig. (10)).

- 1. Wacker oxidation -

The first proposal, designated a in Fig. 10, involves a hydrogen shift from one carbon to the other via the coordination sphere of palladium. This mechanism is not supported by experimental evidence. Replacement of ethylene by higher alkenes does not strongly influence the reaction rate. Hence, the

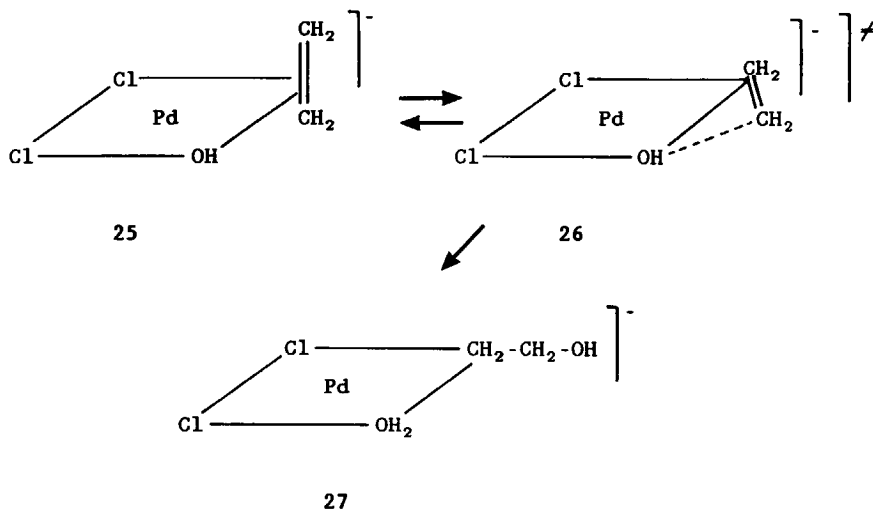


Figure 9. Transition state (26) in the rate determining step in Wacker oxidation [30,31].

rate-determining step shows little carbonium ion character in the transition state. Further, it is unlikely that low-coordinated carbon (30) exists near the palladium coordination sphere; a double bond formation would be more likely. In that case, starting from complex 29, a β -H elimination occurs and a palladium-vinylalcohol, complex 31, is formed. This complex undergoes a π - σ -rearrangement and the product formed, 32, is subjected to a β -H elimination over oxygen. Acetaldehyde is liberated and the simultaneously formed palladium hydride is unstable so that zero-valent palladium and HCl are formed. The reactions mentioned, β -H elimination, π - σ -rearrangement and hydride formation, are well-known palladium catalyzed reactions [15,26].

- 1. Wacker oxidation -

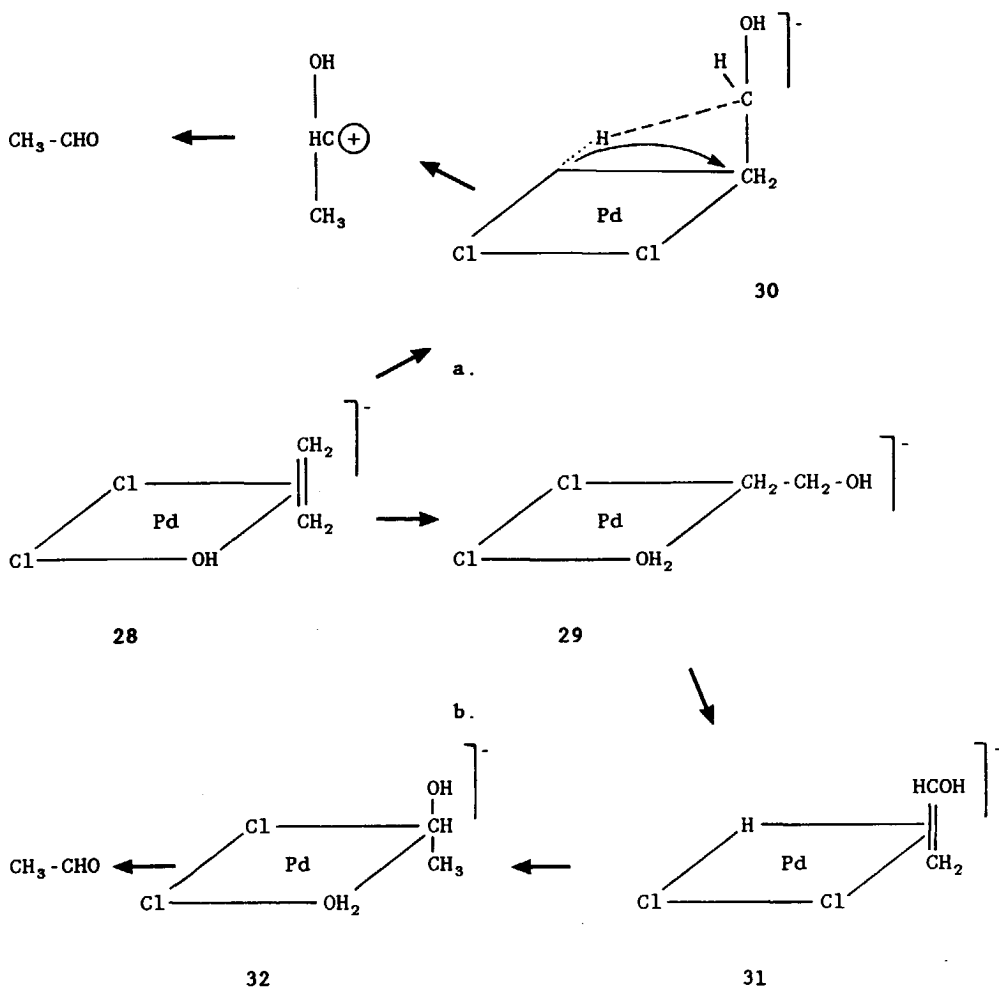


Figure 10. Reactions proceeding after the rate determining step.
 a: ref. [6]; b: ref. [15].

Summarizing the results discussed up to here, the reactions depicted in Fig. 1 represent the reactions actually occurring during Wacker oxidation. The rate-determining step involves a *cis* hydroxypalladation reaction, as represented in Fig. 9, followed by a series of fast reactions running probably according to route b, Fig 10, and leading to the product acetaldehyde.

- 1. Wacker oxidation -

Table II. Reduction potentials of some (Wacker oxidation) half reactions.

<u>half reaction</u>	<u>standard reduction potential [15,32,33]</u>
$\text{Cu}^{2+} + \text{e}^- \rightleftharpoons \text{Cu}^+$	0.158 (0.167,
$\text{PdI}_4^{2-} + 2 \text{e}^- \rightleftharpoons \text{Pd}(0) + 4 \text{I}^-$	0.18 0.153)
$\text{H}_3\text{C-CHO} + 2 \text{H}^+ + 2 \text{e}^- \rightleftharpoons \text{H}_2\text{C=CH}_2 + \text{H}_2\text{O}$	0.21
$\text{Cu}^{2+} + \text{Cl}^- + \text{e}^- \rightleftharpoons \text{CuCl}$	0.465
$\text{PdBr}_4^{2-} + 2 \text{e}^- \rightleftharpoons \text{Pd}(0) + 4 \text{Br}^-$	0.49
$\text{PdCl}_4^{2-} + 2 \text{e}^- \rightleftharpoons \text{Pd}(0) + 4 \text{Cl}^-$	0.623
$\text{Benzoquinone} + 2 \text{H}^+ + 2 \text{e}^- \rightleftharpoons \text{Hydroquinone}$	0.699
$\text{Fe}^{3+} + \text{e}^- \rightleftharpoons \text{Fe}^{2+}$	0.770
$\text{Pd}(\text{ClO}_4)_4^{2-} + 2 \text{e}^- \rightleftharpoons \text{Pd}(0) + 4 \text{ClO}_4^-$	0.92
$\text{VO}_2^+ + 2 \text{H}^+ + 2 \text{e}^- \rightleftharpoons \text{VO}^{2+} + \text{H}_2\text{O}$	1.00
$\text{O}_2 + 4 \text{H}^+ + 4 \text{e}^- \rightleftharpoons 2 \text{H}_2\text{O}$	1.229
$\text{Cr}_2\text{O}_7^{2-} + 14 \text{H}^+ + 6 \text{e}^- \rightleftharpoons 2 \text{Cr}^{3+} + 7 \text{H}_2\text{O}$	1.33
$\text{MnO}_4^- + 8 \text{H}^+ + 5 \text{e}^- \rightleftharpoons \text{Mn}^{2+} + 4 \text{H}_2\text{O}$	1.507

Pd(II), like bromide or iodide. The use of poorly interacting ligands, like sulphate, phosphate, fluoride, acetate, nitrate and chlorate results in a high reaction rate.

The reduction potential of Pd(II) is influenced in the same way. With strongly interacting ligands, the Pd(II) valence state is stabilized and a low potential results and *vice versa*. As a consequence, when more active palladium salts are used, the electrochemical gap between the Pd(II)/Pd(0) and the O₂/H₂O redox couples decreases and it becomes more difficult to find satisfactory redox couples and conditions.

Among the metals of the platinum group, palladium gives the highest activity. Nevertheless, Wacker oxidation can also be performed using the other platinum metals. The order of these metals according to decreasing

- 1. Wacker oxidation -

reaction rate is: $\text{PdCl}_2 > \text{RhCl}_3 > \text{RuCl}_3 > \text{IrCl}_3 > \text{PtCl}_4$ [34,35]. Rh has the advantage that it can be reoxidized by oxygen without the use of a co-catalyst like copper [36].

Other redox couples may be used as well. Next to Cu(I)/Cu(II) , a well-known redox couple is Fe(II)/Fe(III) [2] and the highly efficient benzoquinone/hydroquinone redox couple is usually applied in kinetic experiments [15]. Further advantages of the use of benzoquinone are that, under normal conditions, no influence of the quinone concentration on the reaction rate is found and that the hydrogen ions produced during the alkene oxidation (eq. (2)) are efficiently removed in the reoxidation step. This leads to hydroquinone, and no change of the pH occurs during the reaction. However, for kinetic reasons, hydroquinone cannot be reoxidized by oxygen. When copper is used, the pH can change during the course of the reaction, because the hydrogen produced (eq. (2)) is only removed in the third reaction step (eq. (4)). Copper also influences the concentration of free chloride by complexation.

Less known redox couples include vanadyl sulphate [37], NO_x complexes (where it is found that the oxygen incorporated in the product originates from the NO_x group, and not from water) [38], the surface of active carbon (where, in our opinion, the surface quinone groups may act as a reversible redox agent) [34,39], and strongly oxidizing agents, like H_2O_2 , $\text{Cr}_2\text{O}_7^{2-}$ and MnO_4^- . These strongly oxidizing agents have the disadvantage that, after use, no reoxidation by oxygen takes place [2,15,40]. More recently also heteropoly acids (HPA's) came into use as redox systems [41].

It is difficult to measure the influence of the redox compound on the reaction rate: as can be seen from eq. (11) an insufficient redox reaction leads to an increase of the Pd(0) concentration and catalyst deactivation through the formation of inactive metallic palladium. When high concentrations of the redox compound are used, no influence on the reaction rate is to be expected at all.

Summarizing, the degree of stability of the Wacker catalyst is determined by the rate of reoxidation of Pd(0) to Pd(II) , as compared to the rate of delivery of Pd(0) , but, following the generally accepted mechanism,

- 1. Wacker oxidation -

Table III. Influence of some redox couples on the kinetics in Wacker oxidation.

<u>redox compound</u>	<u>number of electrons transferred</u>	<u>order to be expected¹</u>	<u>measured order</u>	<u>remarks</u>	<u>references</u>
CuCl ₂	1	2	2	in MeOH positive	[42] [15]
benzoquinone	2	1	1	oxidation of π -allyl-PdCl ₂	[43] [15,33]
Cr ₂ O ₇ ²⁻	6	0.33	0.5		[44]
HPA ²	many	low	0.2		[33]

¹ Wacker oxidation involves a two-electron oxidation.

² HPA = heteropoly acid, H_xPM_xM'_yO₄₀; M, M' are usually Mo and V; x depends on the total charge of the metal atoms.

no influence of the reoxidation reaction on the oxidation rate of the alkene is to be expected.

A difficulty encountered here is that it is doubtful whether atomic Pd(0) may exist in solution. We think it is much more likely that Pd(0) is present in some coordinated form. A more elegant solution of this problem is

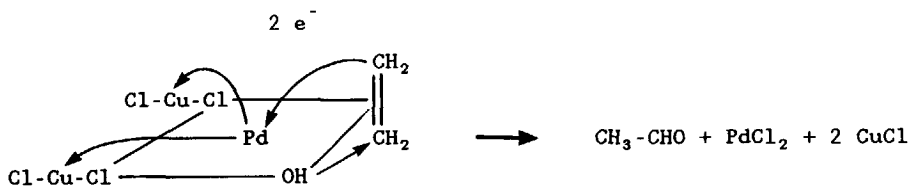


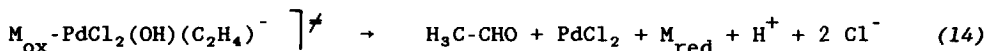
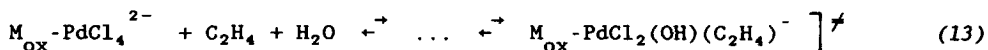
Figure 11. Structure of a palladium reaction intermediate with coordinated copper [42].

the introduction of the idea that the redox component is chemically coordinated to the H₂PdCl₄ from the very beginning of the reaction. If this

- 1. Wacker oxidation -

is true we no longer have to think in terms of the formation of Pd(0). Indeed, in some cases an influence of the redox couple concentration on the kinetics is found (Table III).

In case of an influence of the redox couple on the reaction rate there should be an interaction between that couple and the catalytically active complex (Fig. 11). The reaction order in redox concentration is in agreement with what is to be expected (Table III). For instance in the case of copper, one electron originating from the palladium complex will be transferred per copper ion, thus two copper ions are needed in one oxidation step. The redox influence on the activity can be explained by introduction of an additional equilibrium, eq. (12), in which the palladium complex interacts with a redox compound M. The rate-determining step is represented by eq. (14).

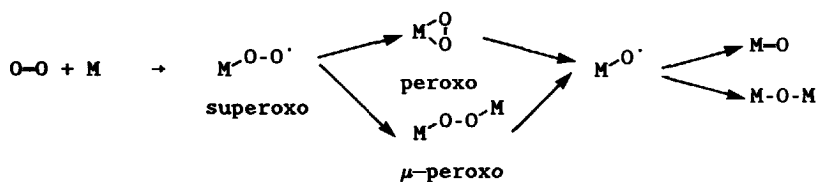


The reaction now proceeds via simultaneous oxidation of the alkene and reduction of the redox compound. When this mechanism is adhered to, zero-valent palladium no longer plays a role in the mechanism. At high redox concentrations equilibrium (12) is shifted strongly to the right and the Pd(II) complexes are almost completely available in the $\text{M}_{\text{ox}}\text{-Pd(II)}$ complex form. Such a structure has been put forward in the case of copper (Fig. 11) [6,42], see also [45]. It is well known that with benzoquinone strong complex bonding between quinone and Pd(II) or Pd(0) occurs [15,33,46,47].

More research is needed to clarify the way redox couples are involved in the Wacker mechanism.

Reoxidation of CuCl to CuCl₂ by O₂

A typical feature of the literature on homogeneous Wacker oxidation is the lack of attention paid to the mechanism of the Cu(I) oxidation to Cu(II) by dioxygen (see, for instance, Henry [15]). Nevertheless, this mechanism is an essential part of the Wacker process. It is also important to see whether reactive oxygen intermediates can interfere with Wacker product formation.



M - (transition) metal. Valence states are not indicated.

Figure 12. Reduction of O₂ to O²⁻.

Generally speaking, the reduction of the biradical dioxygen to O²⁻ proceeds in four steps (Fig. 12). First, through the uptake of one electron from a metal atom, the dioxygen molecule is reduced to the superoxo ligand, O₂⁻. After uptake of another electron a peroxo or μ-peroxo complex is formed. The bond length increases by the foregoing reductions; the length is 1.21 Å in the case of dioxygen, whereas a length of 1.24 - 1.28 Å is found for O₂⁻. The peroxo- and μ-peroxo bond lengths range from 1.30 to 1.55 Å [48,49].

This general reaction scheme will be valid in the case of oxidation of Cu(I) to Cu(II) as well. The reactions proceed rapidly, but the various steps can be studied by making use of complexing ligands. Reversible binding of oxygen in the form of a μ-peroxo ligand is observed for the complex depicted in Fig. 13 [50]. When pyridine is used as a solvent one of the products is the polymeric $[\langle \text{PY} \rangle \text{Cu} \langle \text{O} \rangle \text{Cu}]_n$ [51]. The formation of this product, next to py₂CuCl₂, proceeds rapidly and no intermediates are

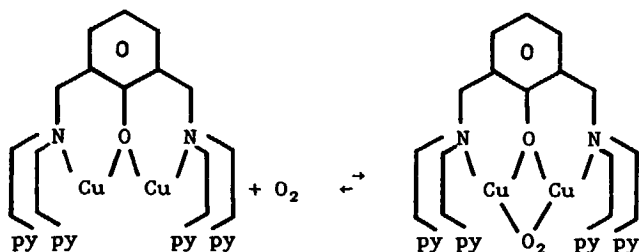


Figure 13. Reversible binding of dioxygen by complexed copper [50].

detected.

When water is used as a solvent, Cu(I) has to be stabilized by ligands like Cl^- , otherwise a rapid disproportionation to Cu(II) and Cu occurs. The first reaction steps of the reaction of CuCl, dissolved in water, with oxygen is proposed to occur via eqs. (14) - (17) [52]. Although very



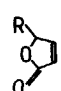
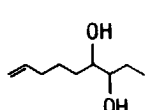
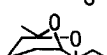
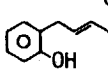
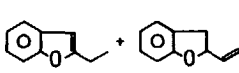
reactive intermediates are involved, their decomposition in the presence of Cu(I) proceeds rapidly and during Wacker oxidation no interference with the Wacker oxidation of alkenes is found.

Wacker oxidation of higher and substituted alkenes

Wacker oxidation is applicable to most alkenes; examples from the literature have been brought together in Table IV. Whereas oxidation of ethylene leads to acetaldehyde, terminal alkenes are mainly oxidized to methylketones. However, when electron-withdrawing groups are bound to the olefin, formation of the aldehyde is preferred, as is the case when styrene is oxidized, resulting in a mixture of acetophenone and phenylacetaldehyde [55,60].

- 1. Wacker oxidation -

Table IV. Products formed by Wacker oxidation of several alkenes.

<u>alkene</u>	<u>product</u>	<u>remarks</u>	<u>references</u>
$H_2C=CH_2$	CH_3-CHO		[2]
$R-CH=CH_2$	$R-C(O)-CH_3$		[2]
$R-CH=CH-COOH$	$R-C(O)-CH_3 + CO_2$		[2,4]
$CH_2=C(CH_3)-COOH$	$CH_3-CH_2-COOH + CO_2$		[2]
$R-CH=CH-COOR$	$R-C(O)-CH_2-COOR$		[40]
$R-CHX-CH=CH_2$	$R-CHX-CH_2-CHO$	X = electron withdrawing group	[4,29,53,54]
$Ph-CH=CH_2$	$Ph-C(O)-CH_3 +$ $Ph-CH_2-CHO$		[2,53,55]
$HO-CH_2-CH=CH_2$	$OHC-CH=CH_2 +$ $HO-CH_2-CH_2-CHO +$ $HO-CH_2-C(O)-CH_3$	Not a simple dehydrogenation	[29]
$CH_2=CH-CH=CH_2$	$CH_3-CH-CH-CHO$		[2]
$CH_3-CH=CH-CH=CH_2$	$CH_3-CH-CH-C(O)-CH_3$		[2]
$CH_2=CH-CH_2-CH=CH_2$	$CH_3-CH_2-CH=CH-CHO$		[2]
$CH_2=CH-(CH_2-)_nCH=CH-R$	$CH_3-C(O)-(CH_2-)_nCH=CH-R$		[40]
cyclohexene	cyclohexanone		[57]
benzene	fenol		[58]
$R-CH=CH-CH_2-COOH$			[40,59]
			[56]
			[45]

Nitroethylene gives nitroacetaldehyde [4]. Whether a ketone or an aldehyde is formed is a matter of subtle experimental differences: when, for instance, acrylonitrile is oxidized in ethylene glycol as the solvent, 1,3-

- 1. Wacker oxidation -

dioxolan-2-ylacetonitrile is formed, this last compound being the acetal of the corresponding aldehyde [4]. But oxidation in methanol leads to 2,2-dimethoxy-propanenitrile, which is the ketal of the ketone (Fig. 14) [53]. Also the reaction temperature [60] and the hydrochloric acid concentration [57] may influence the aldehyde/ketone ratio.

Wacker oxidation of the higher alkenes has been investigated less thoroughly than that of ethylene. For all terminal alkenes the same mechanism is supposed to play a part, by analogy of the kinetics

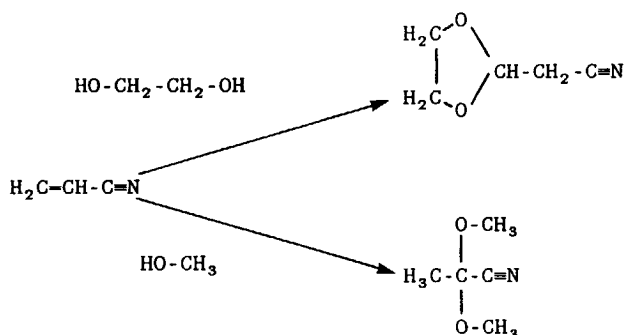


Figure 14. Wacker oxidation of acrylonitrile [4,53].

[11,57,61,62]. The formation of aldehydes and of ketones runs according to the same mechanism, and the stereochemistry of the hydroxypalladation step determines the selectivity.

Interestingly, for internal alkenes the reaction rate retardation by an increase of the proton concentration is of an order far below unity [57,63]. In our opinion the rate of hydroxypalladation is slowed down by steric hindrance (Fig. 15), dependent on the size of the substituents bound to the olefine (Fig. 17). The lower order in the retardation by an increase of the hydrogen ion concentration may be explained from a reaction between coordinated olefine and water. This experimental result strongly demands for

- 1. Wacker oxidation -

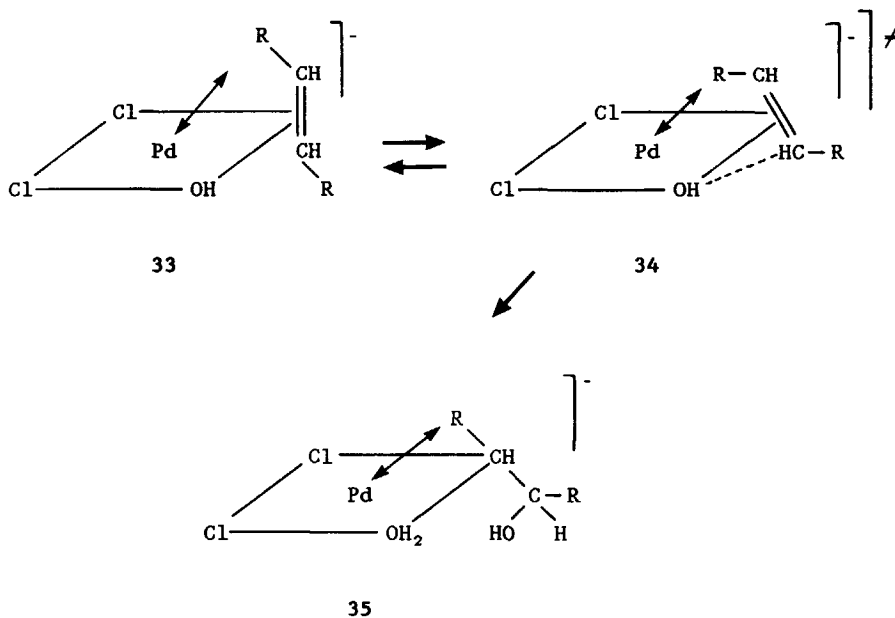


Figure 15. Steric hindrance in the formation of the transition state during hydroxypalladation of an alkyl-substituted alkene. The double arrow (\leftrightarrow) indicates the hindrance.

further research.

Other reactions can interfere with the Wacker oxidation reaction. During Wacker oxidation of propylene, for instance, next to acetone and propionaldehyde [60] acrolein is formed via a π -allyl mechanism [64]. Also deactivation, due to formation of π -allyl complexes [65], may occur, especially when 1,1-disubstituted alkenes like 2-methyl-1-butene are oxidized. In the case of 2-methyl-1-butene, the formed stable π -allyl complex can react with oxidation agents like Pd(II) salts, CrO_3 and MnO_2 . Via a 4-electron oxidation, both 2-methylcrotonaldehyde and 2-methyl-1-butene-3-one are formed (Fig. 16) [15,66].

Double bond isomerisation during Wacker oxidation of higher alkenes can cause problems as it leads to a mixture of carbonyl compounds [53,62,67]. The isomerisation is related to the presence of zero-valent palladium. No

- 1. Wacker oxidation -

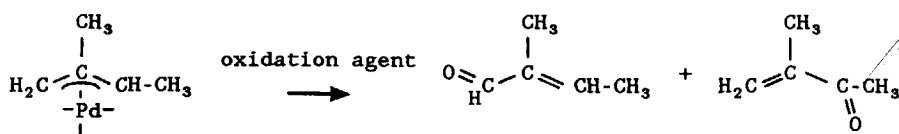


Figure 16. Oxidation of coordinated 2-methyl-1-butene [15,66].

sign of such isomerisation is found when the formation of significant amounts of Pd(0) is prevented by the use of an efficient redox couple [57].

The reactivity of the alkenes decreases with increasing chain length as given in Fig. 17 [57]. This effect is relatively strong, proceeding from ethylene to propylene. Obviously, the electron-donating methyl group in propylene reduces the sensitivity of coordinated propylene towards nucleophilic attack by a coordinated hydroxyl group. Increasing steric

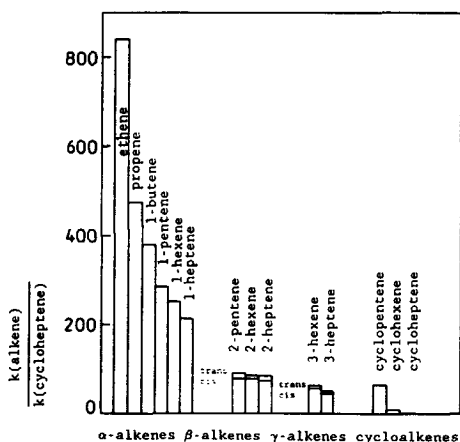


Figure 17. Reactivity of alkenes in the Wacker oxidation relative to cycloheptene [57].

hindrance with increasing chain length also plays a part. For these reasons, the over-all reaction rate slows down. It is also seen from Fig. 17 that internal olefins show an appreciably slower rate of reaction, in accordance with the foregoing reasoning.

Cis-alkenes react a little slower than *trans*-alkenes, which is likely to be related to the fact that the *cis*-isomer, for sterical reasons, is more

strongly coordinated to the palladium, *i.e.* equilibrium (6) shifts to the left. From this shift it was calculated that the energy content of coordinated *trans*-2-butene is about 2.5 kJ/mol higher than the energy content of coordinated *cis*-2-butene. The same is found for the pentenes, and the result may be applied in general [68].

Heterogeneous Wacker oxidation

The discovery of the Wacker reaction is a typical case of serendipity. Smidt [69], developing heterogeneous catalytic epoxidation of ethylene over supported palladium catalysts, observed the formation of small amounts of acetaldehyde. Further research indicated that this was related to the amount of water available and that a higher stability was reached when CuCl_2 or FeCl_3 was added. Finally, the well-known stable homogeneous Wacker catalyst resulted [2].

In its homogeneous form the Wacker process has a number of technological disadvantages. The combination of hydrochloric acid and oxygen forms a very corrosive agents and titanium or enamel-lined reactors, piping and pumps are needed. Furthermore, undesired chlorinated byproducts are formed, particularly when the higher alkenes are oxidized. For instance, in the case of 1-butene oxidation, 3-chloro-2-butanone is formed at selectivities as high as 25 % [9,70]. With increasing chain length the boiling points of the products increase to above that of water and separation of the products from the aqueous catalyst solution becomes a problem. The solubility of alkenes in water decreases with increasing chain length and, as a consequence, the overall rates of reaction decline.

These disadvantages can be largely circumvented by heterogenizing the catalyst. From the literature it appears that many attempts in this direction have been made. Filling of the pores of a porous carrier material with the homogeneous Wacker catalyst, leading to a supported liquid phase (SLP) catalyst, is the most obvious attempt. However, although a good activity is reached, most SLP catalysts suffer from diffusional retardation and even deactivation, due to lack of reoxidation of zero-valent palladium [2,71,72]. The same is true for SLP catalysts with zeolite as a support [73]. Another possible reaction, related to Wacker oxidation, is oxidation

- 1. Wacker oxidation -

of CO to CO₂, which proceeds over a heterogeneous PdCl₂/CuCl₂ catalyst [74], whereas preparation of dialkyl oxalates from carbon monoxide and an alcohol is possible over heterogeneous PdCl₂/V₂O₅ catalysts [75,76].

An interesting recent example involves SLP systems containing a Wacker catalyst solution in the form of molten salts. The supported salt mixture consists of PdCl₂, CuCl₂, CuCl and KCl and the reaction runs above 423 K, the melting point of the salt mixture [77]. However, it is questionable if at such high temperatures higher alkenes can be oxidized with the same high selectivity as found with ethylene in the feed.

Heterogeneous catalysts with redox agents other than copper have also been investigated. Good activities and selectivities were arrived at by Fujimoto *et al.* [34,39] with catalysts based on a palladium compound adsorbed on the surface of activated carbon. No other metal salts are added and quinone groups on the surface of the carbon are believed to function as the redox couple. Among the platinum group metals palladium is favoured and among the palladium salts PdCl₂ is favoured over PdSO₄, Pd(OAc)₂ and Pd(NO₃)₂ [34,39]. A remarkably high third order dependence of the reaction rate on the partial water vapour pressure is found, as well as a negative apparent activation energy [76]. Both phenomena are caused by capillary condensation or evaporation of water in the micropores of the active carbon [39].

It is also possible to replace the Cu(I)/Cu(II) redox couple by V₂O₄/V₂O₅. Heterogeneous catalysts based on palladium-doped vanadium pentoxide on an α-Al₂O₃ support have been investigated by Evnin and Forni [78-80]. Good activities and high selectivities were reached and byproducts included acetic acid and carbon dioxide. At higher temperatures acetic acid became the main product [81]. The dependence of the reaction rate on the partial ethylene, oxygen and water vapour pressures has been measured; orders of 0.4, 0.9 and 0.7, respectively, have been found. When the amount of V⁴⁺ on the catalyst was varied by addition of germanium or molybdenum, a positive influence of V₂O₄ on the reaction rate was found.

The catalyst life time is relatively short (< 150 h). Regeneration of the catalyst at a higher temperature in a stream of air is possible [78]. In our opinion the low stability of the catalyst is caused by the absence of chemical fixation of V₂O₅ to the surface of α-alumina, this surface being

virtually inert. It follows that the V_2O_5 cohesion forces surmount the adhesion forces and hence the large V_2O_5 crystallites grow at the expense of the smaller ones. This sintering process is accompanied by a loss of V_2O_5 surface area, and hence the redox capacity, and the catalyst stability will decrease. Furthermore the catalyst failed to oxidize alkenes higher than propylene [79].

A group of Chinese investigators [82] studied the performance of a supported catalyst consisting of a mixture of Pd-Ti-V-oxide supported on silica. Starting from ethylene, mixtures of acetaldehyde and acetic acid were obtained with a total selectivity as high as 90 %. In this case also a

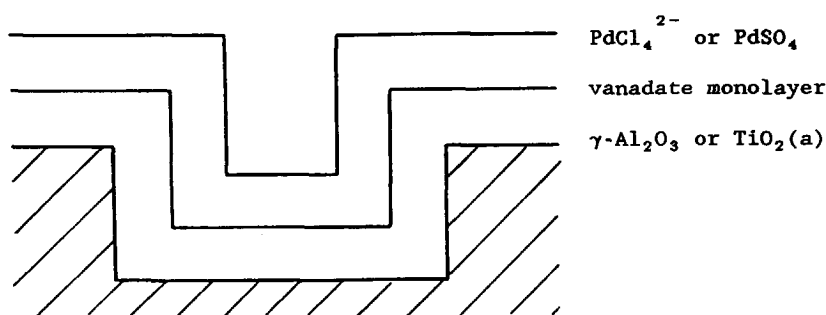


Figure 18. A vanadate monolayer Wacker catalyst.

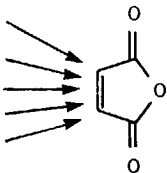
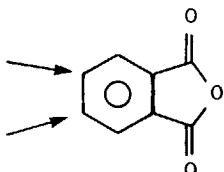
linear relation between the amount of V^{4+} and the activity was observed. Regeneration was performed by heating the catalyst in air [82]. The stability of the catalyst was disappointingly low, plausibly for the same reasons as indicated above for the $\alpha-Al_2O_3$ supported catalyst.

Recently a more stable heterogeneous Wacker catalyst, schematically represented in Fig. 18, has been introduced by van der Steen *et al.* [83,84]. Their catalyst consists of a porous support, γ -alumina, with a high surface area covered by a molecularly dispersed chemically bound vanadate monolayer on which a sub-monolayer of palladium chloride is affixed. Preliminary experiments showed the activity and selectivity of this catalyst to be promising. Further development of such catalysts forms the subject of the present thesis. Furthermore, we will report on experiments which are aimed at gaining a deeper fundamental insight into the processes on and the structure of these catalysts on a molecular scale.

Oxidation reactions over V_2O_5 containing catalysts

Only a few cases of the occurrence of vanadium in living nature are known. Vanadium is found in the bacterium *Azobacter chroococcum* [85], in the seaweed *Laminaria muscaria* [86], in *Ascidella aspersa*, a member of the group

Table V. Oxidation reactions performed over V_2O_5 catalysts.

<u>reaction</u>	<u>catalyst</u>	<u>reaction temperature</u>	<u>references</u>		
$CH_3-CH_2-CH_2-CH_3$ $CH_2=CH-CH_2-CH_3$ $CH_2=CH-CH=CH_2$ furan benzene	 $V_2O_5-P_2O_5$	643-753 K	[89] [90,91] [91,92] [91] [91]		
o-xylene naphthalene		 $V_2O_5-TiO_2$	583-673 K	[93] [94]	
$CH_3-CH_2-CH_3 \rightarrow CH_2=CH-CH_3$ $CH_3-CH_2-CH_2-CH_3 \rightarrow CH_2=CH-CH_2-CH_3$ ethylbenzene \rightarrow styrene			V_2O_5-MgO	773-873 K	[95] [96] [97]
$CH_3-OH \rightarrow H_2C=O$ $CH_3-CH_2-OH \rightarrow CH_3-CHO$		$V_2O_5-TiO_2$		473-673 K	[98] [99]
$NO_x + NH_3 \rightarrow N_2$ $CO \rightarrow CO_2$				473 K	[91,100] [91,101]
$H_2 \rightarrow H_2O$	600-800 K		[91]		
$SO_2 \rightarrow SO_3$	$V_2O_5-K_2S_2O_7$		773 K	[102]	

- 1. Wacker oxidation -

of the sedentary tunicates [87], and in the fungus *Amanita muscaria* [88]. Vanadium is supposed to play a part in biological redox reactions and in nitrogen fixation.

Industrially, V_2O_5 , usually supported on or mixed with other oxides, can be applied as an oxidation catalyst in a wide range of reactions (Table V and references therein). The well-known preparation of maleic anhydride, starting from C_4H_X , furan or benzene, and that of phthalic anhydride from o-xylene or naphthalene, generally run over $V_2O_5-P_2O_5$ and $V_2O_5-TiO_2(a)$ catalysts, respectively. The reaction temperatures range from 583 to 753 K.

As can be seen from Table V, oxidative dehydrogenation of alkanes to the corresponding alkenes is performed over V_2O_5-MgO type catalysts. At temperatures as high as 773 - 873 K propane and butane can be converted to propylene and 1-butene respectively, and ethylbenzene can be dehydrogenated to styrene. Aldehydes can be produced over TiO_2 -supported V_2O_5 catalysts by dehydrogenation of the corresponding alcohols. The reaction temperatures are relatively low: 373 - 673 K.

TiO_2 -supported V_2O_5 catalysts are also applied in the selective reduction of NO_x by NH_3 at about 473 K, whereas at higher temperatures CO and H_2 can be oxidized to CO_2 and H_2O respectively. A well-known reaction over $V_2O_5-K_2S_2O_7$ catalysts is the oxidation of SO_2 to SO_3 , applied in the preparation of sulphuric acid. High temperatures, roughly about 773 K, are used here.

In view of these very different ranges of reaction temperatures, different mechanisms are likely to be involved in the reactions mentioned. However, generally speaking, most of these mechanisms are variants of the Mars - van Krevelen mechanism [103]; when V_2O_5 catalysts are applied, according to this mechanism, the lattice oxygen, and not the adsorbed dioxygen, is reactive and the catalysts are partly reduced. Dioxygen is needed to regenerate the catalyst *in situ*. It is outside the scope of this introduction to go further into the different reaction mechanisms (for details see [104] and references therein).

The remarkably low reaction temperatures (353 - 393 K) at which the heterogeneous Wacker oxidation over $PdCl_2/V_2O_5$, like the homogeneous Wacker oxidation, runs at measurable rates [78-80,82], point to a mechanism

deviating from the known variants of the Mars - van Krevelen mechanism. This will be discussed further in the Chapters 8, 9 and 10.

Preparation of supported vanadate catalysts

In general a more efficient use of a catalytic compound is reached if more catalytic centres are accessible to the reactants. Therefore, when solid catalysts are used, high surface areas per gram of catalyst are to be preferred. In the case of vanadium oxide high surface area self supporting particles cannot be prepared [105]. However, high surface area vanadium oxide catalysts result when the vanadium oxide is mounted on the surface of high surface area support materials, like alumina, titania, magnesia or silica.

Supported vanadate differs from crystalline vanadium oxide not only with respect to dispersion but also with respect to chemical and catalytic properties. This is due to differences in chemical structure between supported vanadate and crystalline V_2O_5 , caused by chemical interaction between vanadate and the support. Examples of differences in catalytic properties have already been given in the preceding section.

For the preparation of supported vanadium catalysts, several methods have been known, generally based on adsorption of a vanadium compound on a support until equilibrium is reached, or on mixing of the two compounds in the liquid and/or solid state followed by drying and calcination. Every composition between 0 and 100 % V_2O_5 can be realized when the mixing method is used. However, at high vanadium oxide loadings crystalline V_2O_5 will be present too and the original surface area of the support will be lowered due to filling of the pores with crystalline vanadium oxide. When the first-mentioned method, adsorption, is used, a maximum interaction between vanadium oxide and the surface of the support is reached and therefore a maximum influence of the support on the chemical and catalytic properties of the vanadium oxide is to be expected. In general, a high vanadate dispersion is arrived at and the coverage will not go beyond the monolayer. Furthermore, no strong influence on the surface area, when calculated per gram of support, is to be expected.

A very easy method of preparing a V_2O_5 catalyst comprises mechanical mixing of the oxide with a support, usually $TiO_2(a)$ or SiO_2 , followed by calcination at 773 - 923 K [106,107] or at 1423 K [108]. Interestingly, as demonstrated by Haber [107], $TiO_2(\text{anatase})$ is wetted by solid V_2O_5 at 823-923 K, but $TiO_2(\text{rutile})$ does not show any interaction with V_2O_5 at these temperatures.

Also liquid precursors like solutions of aluminium propoxide or titanium oxalate can be mixed with a solution of vanadyl oxalate. After drying and calcination at 723 - 823 K, this leads to mixed oxide catalysts [109].

Another non-equilibrium method comprises wet impregnation of a support with vanadium containing solutions, such as solutions of NH_4VO_3 , vanadyl oxalate, vanadyl sulfate, vanadyl chloride and others, usually followed by evaporation of the solvent, drying at 383 K and calcination at 723-773 K. In most cases $\gamma-Al_2O_3$, silicagel, titanium oxide (anatase and/or rutile) magnesium oxide, and, to a lesser extent, zirconium oxide, cerium oxide, and silica covered by TiO_2 , have been used as a support material [91,110].

Impregnation to incipient wetness is limited by the low solubility of vanadium compounds in most solvents and therefore it is not widely applied [111].

Preparation of catalysts utilizing equilibrium methods can be divided into batch and continuous processes. A batch process comprises wet impregnation of a support with a vanadium containing solution followed by standing still until adsorption equilibrium is reached. Afterwards the solution is decanted and the product is washed with a suitable solvent, dried and calcined at 723-773 K [112].

A vanadium oxide monolayer catalyst is prepared by continuous adsorption. To this end, a dissolved vanadate compound, e.g. NH_4VO_3 or $VO(\text{acac})_2$ [113], or gaseous $VOCl_3$ [114], is led over a support, until equilibrium is reached. In case of $VOCl_3$ the adsorption is followed by hydrolysis.

An advanced preparation technique has been developed by Vogt et al. [115], involving electrochemical reduction of an aqueous solution of NH_4VO_3 to the V(III) valence state. The V(III) is adsorbed on the support (silicagel or silicagel covered by a TiO_2 monolayer).

The structure of vanadate monolayers

It is an intricate task to discuss the structure of vanadate monolayers on a support. It is to be expected that the vanadate layer structure strongly depends on the structure of the surface planes of the supports [116], on the vanadate coverage and, to a lesser extent, on the preparation technique used [116,117]. Furthermore, several different vanadate structures can exist next to each other, and less common oxygen coordinations may be stabilized by

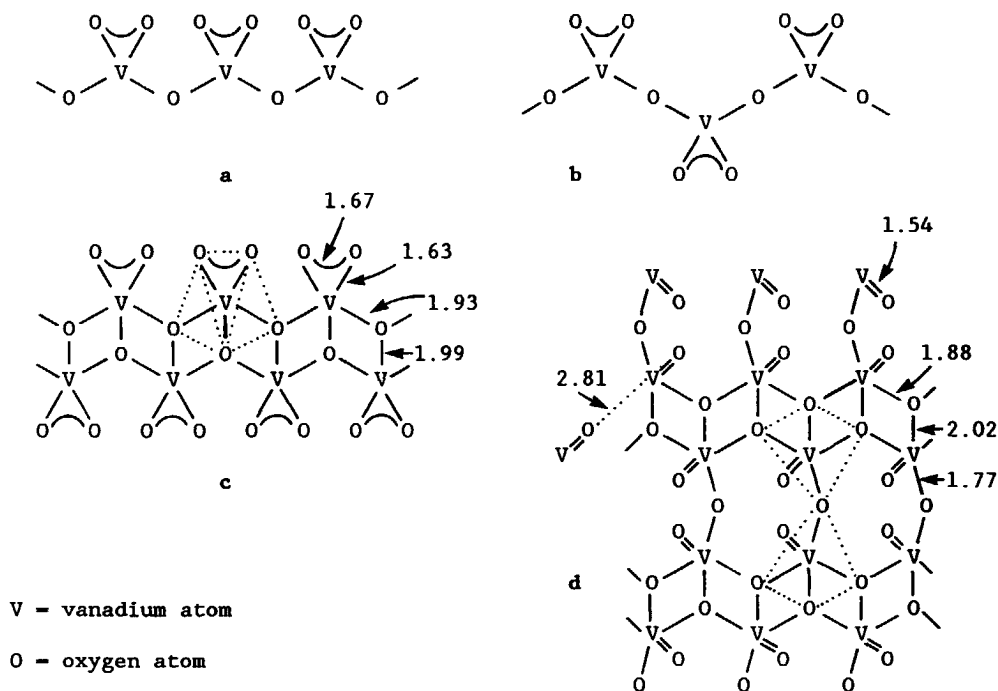


Figure 19. V(V) structures [118]. a: $(VO_3^-)_n$ chains (hypothetical); b: $NaVO_3$; c: $KVO_3 \cdot H_2O$; d: V_2O_5 . Distances are given in Å.

strong interaction with the support. Therefore it is sensible to pay attention first to three dimensional vanadium oxide crystal structures before discussing the monolayer structures.

- 1. Wacker oxidation -

Several coordinations of V(V) by oxygen are known (Fig. 19). A distorted tetrahedral coordination of vanadium is found in the metavanadates, e.g. in NaVO_3 [118,119], involving two single V-O bonds and two V-O bonds of the order 1.5 (Fig. 19, a and b). The chains of corner-sharing tetrahedra are interconnected by the cations. When two chains are linked together, the structure of $\text{KVO}_3 \cdot \text{H}_2\text{O}$ is obtained (Fig. 19, c) [120], in which a distorted trigonal bipyramidal coordination of oxygen around vanadium is present. Again, two V-O bonds of the order 1.5 are available, but all other oxygens now interact with three vanadium atoms. K^+ and H_2O are situated in between the chains and interconnect them.

The structure of V_2O_5 may be interpreted as a layered packing of distorted square pyramids, sharing edges and corners [121]. This structure is formed when the double chains of $\text{KVO}_3 \cdot \text{H}_2\text{O}$ are connected in the way given in Fig. 19, d. The two V-O bonds of the order 1.5 have been changed into one single and one double bond, whereas the other oxygens still interact with three vanadium atoms. The layers are interconnected via the V=O oxygen atoms: the bond distance of these oxygens to the vanadium atoms in the next

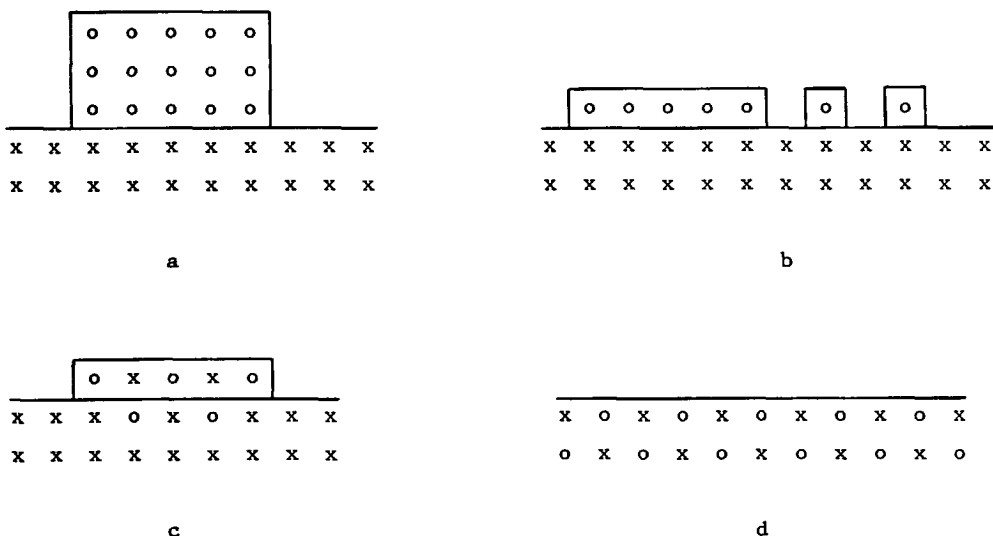


Figure 20. Structure of supported vanadate, according to Roozeboom et al. [122].

layer is 2.81 Å. Therefore the vanadium coordination can also be looked upon as distorted octahedral. The length of a single V-O bond is in between 1.77 and 2.02 Å, whereas the V-O bonds of the order 1.5 and 2 are 1.63 - 1.67 Å and 1.54 Å in length, respectively.

The interaction of the surface of a support with V_2O_5 strongly influences the vanadate structure. Following Roozeboom, four kinds of interaction may be distinguished ([122], see also [116]). Bulk V_2O_5 is easily formed on the surfaces of relatively inert supports (Fig. 20, a), e.g. on $\alpha-Al_2O_3$, $TiO_2(r)$ or SiO_2 . Monolayer catalysts can be prepared when the vanadate precursor reacts with the surface hydroxyl groups. Vanadate monolayers are formed on $\gamma-Al_2O_3$ or $TiO_2(a)$ (Fig. 20, b). When the latter is used as a support, two-dimensional salt formation may occur [109,117], whereas MgO reacts with V_2O_5 to form a crystalline phase (Fig 20, c and d respectively). It should be noted that there exists no absolute demarcation between the distinct structures, but only a gradual transition.

We now have to specify the concept 'monolayer'. The theoretical maximum coverage of a surface by V_2O_5 can be calculated from $\rho(V_2O_5)$ (3.357 g.cm^{-3}) and the mol weight ($181.88 \text{ g.mol}^{-1}$). When the $VO_{2.5}$ unit is assumed to be a cube, a maximal coverage of $7.9 \text{ V-atoms.nm}^{-2}$ is arrived at [122]. From the unit cell dimensions of V_2O_5 [121], the maximal coverage is calculated to range from $6.3 \text{ V-atoms.nm}^{-2}$ (from the (100) plane) to $9.8 \text{ V-atoms.nm}^{-2}$ (from the (010) plane). Hence, no precise value for monolayer coverage can be established.

One should expect that after adsorption to equilibrium of a vanadium compound on a support, at room temperature and at a high concentration, monolayer coverage will result. However, coverages ranging from 0.26 to $13.2 \text{ V atoms.nm}^{-2}$ are reported in literature, without any indication of the formation of crystalline V_2O_5 [112]. It can be concluded that after equilibration layer(s) of the adsorbed vanadate form an ill-defined two-dimensional structure deviating from the structure of crystalline V_2O_5 . This ill-defined vanadate is generally called 'monolayer'. Concluding, the number of $VO_{2.5}$ units corresponding with full coverage appears to be a variable quantity. We shall focus now on monolayer formation both on $\gamma-Al_2O_3$ and on $TiO_2(a)$.

The structure of a vanadate layer on $\gamma-Al_2O_3$ has been characterized by

Roozeboom *et al.* by means of Raman spectroscopy [123]. Indications are found of the existence of three different vanadate structures. Far below monolayer coverage, which was found to correspond to 4.5 V atoms.nm⁻², a broad band is measured at 970 - 1000 cm⁻¹ corresponding to the band of the V₁₀O₂₈⁶⁻ ion in solution. When the V₂O₅ content exceeds 1.5 V atoms.nm⁻², the band at 970 - 1000 cm⁻¹ disappears in favour of a band at 800 - 830 cm⁻¹, which corresponds to the band of VO₃⁻ ion in solution. At loadings above a monolayer crystalline V₂O₅ is formed next to the monolayer structures. The Raman spectra led Roozeboom to conclude that, at loadings far below a monolayer, V₁₀O₂₈⁶⁻ complexes are chemisorbed on the surface of γ-Al₂O₃, followed by formation of a monomeric tetrahedral structure at loadings up to monolayer coverage. In our opinion, however, the formation of monomeric units from oligomeric complexes at increasing loading is quite improbable. Rather the reverse will be true, in which case first monomeric particles are present, analogous to the monomeric units in V₁₀O₂₈⁶⁻, whereas at higher loadings larger complexes consisting of tetrahedral oxygen-coordinated vanadium centres are formed.

This last view is in accordance with Yoshida *et al.* [124], who, by means of ESR, decided on the presence of three different vanadate structures: at low loadings molecularly dispersed vanadate units are present, whereas at increasing loadings an ill-defined vanadate layer is formed. On top of this layer further deposition of crystalline V₂O₅ was detected. It should be remarked, however, that in ESR only V(IV) is detectable.

Burgerett *et al.* [125] studied a V₂O₅ monolayer catalyst on γ-Al₂O₃, (4.0 V atoms.nm⁻²) by means of radial electron distribution (RED). The V-V distances, measured by RED, were found to be larger than in V₂O₅. The presence of tetrahedral corner-sharing VO₄ units, with a flexible two-dimensional structure, was proposed.

A study by Yoshida *et al.* [126] points to the presence of a tetrahedral vanadium oxide structure on γ-Al₂O₃. Water can coordinate to this structure without changing the tetrahedral coordination.

Haber *et al.* [127], applying EXAFS, could only detect dimeric vanadate species on γ-Al₂O₃ at monolayer coverage, as depicted in Fig. 21.

The structure of vanadate monolayers on TiO₂(a) (S(BET) = 117 m².g⁻¹) has been characterized by Busca *et al.* [128] by means of FT-IR. In this case

- 1. Wacker oxidation -

The structure of vanadate monolayers on $\text{TiO}_2(\text{a})$ ($\text{S(BET)} = 117 \text{ m}^2.\text{g}^{-1}$) has been characterized by Busca *et al.* [128] by means of FT-IR. In this case three vanadate phases could be detected as well. At low coverage, far below a monolayer, a band at 980 cm^{-1} was detected which was ascribed to isolated vanadyl species. Supplementary measuring techniques, like ESR, XRD and UV-vis diffuse reflectance spectroscopy, indicate that two kinds of monomeric species are present. The first type is coordinatively saturated, whereas the second form can capture a water molecule. By means of ESR a large portion of the monomeric species was found to be present in the V(IV) valence state. At higher coverages, bands at 890 and 940 cm^{-1} arise which could be ascribed to a bidimensional vanadate layer. At high coverage almost all of the vanadate is present as V(V). No evidence of the formation of crystalline V_2O_5 is found up to monolayer coverage, defined as $5.1 \text{ V atoms.nm}^{-2}$, but at higher loadings characteristic bands at 1019 and 985 cm^{-1} point to the formation of crystalline V_2O_5 . This last result was confirmed by XRD analysis.

Raman spectroscopy also confirms the presence of three vanadate phases on $\text{TiO}_2(\text{a})$ [129]. In a recent Raman study by Bond *et al.* [130], a structure of the monomeric vanadate species was postulated. A tetrahedral coordination

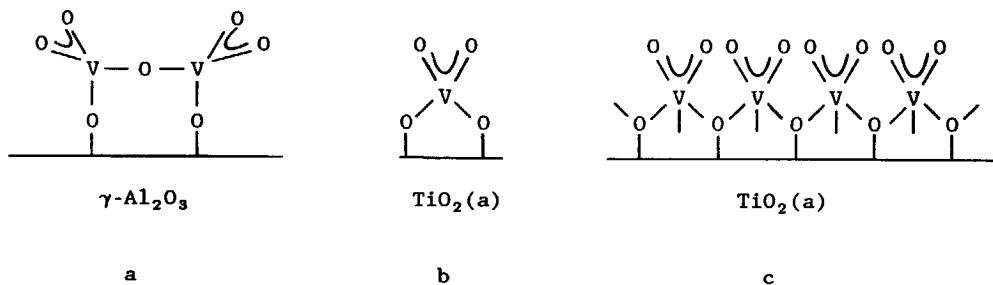


Figure 21. Structure of vanadate; a: on $\gamma\text{-Al}_2\text{O}_3$ and b: on $\text{TiO}_2(\text{a})$, as determined by EXAFS [131,132]; c: on $\text{TiO}_2(\text{a})$ [130] as determined by RAMAN.

of vanadium by oxygen is supposed, comparable to the metavanadate structure depicted in Fig. 21, in which vanadium has two bonding and two terminal oxygen atoms with a bonding order of 1.5. At higher loadings chain formation can occur, as drawn in Fig. 21 [132], forming an ill-defined two-dimensional structure.

For the time being, EXAFS has to be considered as the most powerful technique to determine surface structures. The structure of vanadate on $\text{TiO}_2(\text{a})$ was determined by Kozlovsky *et al.* [131]. Up to monolayer coverage only monomeric vanadate species could be detected. At monolayer coverage the vanadate unit is characterized as a species with two terminal and two bridging oxygens. No well-defined V-V distance could be measured and therefore the monolayer on $\text{TiO}_2(\text{a})$ is proposed to be an ill-defined network of vanadate tetrahedra.

Other authors came to deviating conclusions. The lattice structures of $\text{TiO}_2(\text{a})$ and of V_2O_5 were intercompared by Vejux and Courtine [133], who found a remarkable fit of the crystallographic V_2O_5 (010) plane and the $\text{TiO}_2(\text{a})$ (001) and (010) planes. They conclude that crystalline V_2O_5 can grow epitaxially on the surface of $\text{TiO}_2(\text{a})$. This proposal was confirmed by Kang and Bao [134], who applied high resolution electron microscopy (HREM) to determine the vanadate monolayer structure on $\text{TiO}_2(\text{a})$. They photographed a $\text{TiO}_2(\text{a})$ catalyst with $14.7 \text{ V atoms.nm}^{-2}$ and observed the presence of mainly small crystalline V_2O_5 pyramids, grown by epitaxy. At loadings as high as $73 \text{ V atoms.nm}^{-2}$ both crystalline and amorphous V_2O_5 are present. It should be noted that $14.7 \text{ V atoms.nm}^{-2}$ is already above monolayer coverage. As far as we know no HREM studies of V_2O_5 on $\gamma\text{-Al}_2\text{O}_3$ have been published.

However, it remains to be seen whether epitaxial growth of V_2O_5 on $\text{TiO}_2(\text{a})$ can occur. The V_2O_5 (010) crystal plane, in which $\text{V}=\text{O}$ bonds are exposed, is supposed to interact with the support surface, but in V_2O_5 the $\text{V}=\text{O}$ groups are directed upward and downward as can be seen from Fig. 19. For steric reasons, the $\text{V}=\text{O}$ group can only be directed outwards, when mounted on the TiO_2 surface. No literature dealing with the possibility of the occurrence of such vanadate structures is known to us. In the $\text{V}_{10}\text{O}_{28}^{6-}$ ion two neighbouring $\text{V}=\text{O}$ groups, both directed outwards, are present [135].

By different characterization methods different monolayer structures were found and, for the time being, no definite monolayer structure can be

indicated. In conclusion, at a low vanadate coverage on $\gamma\text{-Al}_2\text{O}_3$ or $\text{TiO}_2(\text{a})$, far below a monolayer, isolated vanadate species are present, probably with the EXAFS structures depicted in Fig. 21. At higher coverages, up to a monolayer, a second structure emerges at the expense of the isolated species. By HREM, it is found that on $\text{TiO}_2(\text{a})$ this structure consists of small crystallites, but by spectroscopic techniques it is found to be an amorphous bidimensional vanadate layer, which is generally called the monolayer structure. The number of layers in what is called a 'monolayer' can be higher than one. No relation between monolayer structures and surface lattice structures is known in literature. At higher loadings, next to the monolayer structure, the presence of crystalline V_2O_5 is observed,

Scope of the thesis

Recently a heterogeneous Wacker catalyst has been introduced by van der Steen *et al.* [85,86]. As mentioned already, it consists of a porous support, γ -alumina, covered by a vanadate monolayer. This monolayer, in turn, is covered by a sub-monolayer of a palladium compound (Fig. 18). In an exploring experiment by van der Steen *et al.* a gas mixture of ethylene, water and air was led over the catalyst. Acetaldehyde formation at a stable rate and with a high selectivity was observed. Further development of this catalyst seemed attractive for both scientific and technological reasons.

In the past, the mechanism of the homogeneous Wacker oxidation of ethylene was thoroughly studied and therefore it is interesting to compare the homogeneous and the heterogeneous oxidation mechanisms. A new variable in the heterogeneous case is the influence of water on the reaction rate. The kinetics, with respect to the relevant variables, are described for the case of ethylene oxidation (Chapter 4), 1-butene oxidation (Chapter 5) and styrene oxidation (Chapter 7) and compared with the kinetics of the homogeneous reaction.

Zerovalent palladium, formed simultaneously with the reaction products, can be oxidized to Pd(II) by the vanadate monolayer. It is known from the literature that the structure of this monolayer depends on the vanadium oxide loading and on the type of support. This matter will be discussed further in Chapter 3.

The influence of the monolayer structure on the reaction rate is the subject of Chapter 8.

The mechanism of oxidation of zero-valent palladium by the redox system, in particular by the vanadate monolayer, and the simultaneous reduction of the monolayer, are investigated by means of a model reaction: the reduction of the catalyst by hydrogen (Chapter 9). The kinetic results are compared with the kinetics of the heterogeneous Wacker oxidation. The interaction between the palladium compound and the redox system appeared to be more important than generally suggested in the literature. In view of this result, a start was made with the development of a homogeneous Wacker catalyst, in which a palladium ion is bound directly to the redox compound.

From a technological point of view the one-step oxidation of the alkenes to ketones or aldehydes is attractive. Acetaldehyde (a crude material in acetic acid production) is produced industrially, using the homogeneous Wacker catalyst. It will be shown in Chapter 4 that the heterogeneous oxidation is possible as well and that this mode of operation offers a number of technological advantages.

At present methyl ethyl ketone (MEK) is produced via hydration of butene followed by dehydrogenation, but on the basis of our study a one-stage process can be developed, applying heterogeneous Wacker oxidation, as described in Chapter 5.

Partial hydrogenation of benzene to cyclohexene followed by oxidation to cyclohexanone might play a role in a new route from benzene to caprolactam, the crude material for the production of the important product Nylon-6. The oxidation of cyclohexene to cyclohexanone can in principle be performed by heterogeneous Wacker oxidation. The performance of our new catalyst in cyclohexene oxidation is explained in Chapter 6.

Finally, the valuable fine-chemical phenylacetaldehyde can be prepared, next to acetophenone, by homogeneous Wacker oxidation of styrene. The performance of the heterogeneous catalyst in the oxidation of styrene is described in Chapter 7.

References

1. F.C. Phillips, *Am. Chem. J.*, **16** (1894) 255.
2. J. Smidt, W. Hafner, R. Jira, J. Sedlmeier, R. Sieber, R. Ruttinger and

- H. Kojer, *Angew. Chem.*, 71 (1959) 176.
3. Y. Moro-Oka, S. Tan and A. Oraki, *J. Catal.*, 17 (1970) 125; A.L. Farragher and G.W.J. Heimerikx, *Proc. 4th Int. Conf. Chem. Uses Molybdenum*, (1982), Amsterdam, 432.
 4. H.J. Kabbe and R. Jira in: *Methoden der Organischen Chemie (Houben-Weyl)*, O. Bayer, H. Meerwein and K. Ziegler (eds.), Müller, Tübingen, 7/2a, (1973) 781.
 5. Kirk Othmer *Encyclopedia of Chemical Technology*, 3rd ed., Vol 1, Wiley, New York, (1981), 97.
 6. A. Aguilo, *Adv. Organometal. Chem.*, 5 (1967) 321, and references therein.
 7. Winnacher-Kuchler *Chemische Technology*, 4th ed., Carl Hauser, München, (1982) 67.
 8. A.J. Pearson: *Metallo-organic Chemistry*, Wiley, New York, (1985) 58.
 9. J. Smidt and H. Krekeler, *Erdöl und Kohle Erdgas Petrochemie*, 16 (1963) 560; J. Smidt and H. Krekeler, *Chem. Eng. News*, (1963) 50; J. Smidt and H. Krekeler, *Hydrocarbon Proc. Petr. Refiner*, 42 (1963) 149.
 10. R.N. Pandey and P.M. Henry, *Can. J. Chem.*, 57 (1979) 982, and references therein.
 11. P.M. Henry, *J. Am. Chem. Soc.*, 86 (1964) 3246; P.M. Henry, *J. Am. Chem. Soc.*, 88 (1966) 1595; P.M. Henry, *J. Org. Chem.*, 38 (1973) 2415; I.I. Moiseev, O.G. Levanda and M.N. Vargaftik, *J. Am. Chem. Soc.*, 96 (1974) 1003.
 12. I.I. Moiseev, M.N. Vargaftik and Y.K. Syrkin, *Izv. Akad. Nauk. Otd. Khim. Nauk. S.S.S.R.*, (1963) 1144.
 13. M. Kosaki, M. Isemura, K. Kiraura, S. Shinoda and Y. Saito, *J. Mol. Catal.*, 2 (1977) 351.
 14. J. Smidt, W. Hafner, R. Jira, R. Sieber, J. Sedlmeier and A. Sabel, *Angew. Chem.*, 74 (1962) 93; W. Hafner, R. Jira and J. Smidt, *Chem. Ber.*, 95 (1962) 1575.
 15. P.M. Henry: *Palladium Catalyzed Oxidation of Hydrocarbons*, Reidel, Dordrecht, (1980).
 16. E.W. Stern, *Catal. Rev.*, 1 (1967) 73.
 17. D.H. Templeton, G.W. Watt and C.S. Garner, *J. Am. Chem. Soc.*, 65 (1973) 1608.
 18. A. Yamamoto: *Organo Transition Metal Chemistry*, Wiley, New York, (1986).
 19. L.L. Wright, R.M. Wing, M.F. Rettig and G.T. Wiger, *J. Am. Chem. Soc.*, 102 (1980) 5949.
 20. T.A. Albright, R. Hoffmann, J.C. Thibeault and D.L. Thorn, *J. Am. Chem. Soc.*, 101 (1979) 3801.
 21. J.S. Anderson, *J. Chem. Soc.*, (1934) 971.
 22. M.J.S. Dewar, *Bull. Soc. Chim. France*, 18 (1951) C71; J. Chatt, L.A. Duncanson, *J. Chem. Soc.*, (1953) 2939.
 23. S.J. Lokken and D.S. Martin, *Inorg. Chem.*, 2 (1963) 562.
 24. J.K. Stille and D.E. James, *J. Am. Chem. Soc.*, 97 (1975) 674; J.K. Stille and D.E. James, *J. Organometal. Chem.*, 108 (1976) 401.
 25. J.K. Stille and R. Divakaruni, *J. Am. Chem. Soc.*, 100 (1978) 1303; J.K. Stille and R. Divakaruni, *J. Organometal. Chem.*, 169 (1979) 239.
 26. J.E. Bäckvall, B. Åkermark and S.O. Ljunggren, *J. Chem. Soc., Chem. Commun.*, (1977) 264; J.E. Bäckvall, B. Åkermark and S.O. Ljunggren, *J. Am. Chem. Soc.*, 101 (1979) 2411.
 27. N. Gragor and P.M. Henry, *J. Am. Chem. Soc.*, 103 (1981) 681.
 28. C. Burgess, F.R. Hartley and G.W. Searle, *J. Organometal. Chem.*, 76 (1974) 247.
 29. W.K. Wan, K. Zaw and P.M. Henry, *J. Molec. Catal.*, 16 (1982) 81.
 30. Y. Saito and S. Shinoda, *J. Molec. Catal.*, 9 (1980) 461.

31. O.N. Shumilo, N.N. Bulgakov and V.A. Likholobov, *React. Kinet. Catal. Lett.*, 23 (1983) 87.
32. R.C. Weast and M.H. Astle (eds.), *CRC Handbook of Chemistry and Physics*, CRC press, Florida, 1979.
33. K.I. Matveev, *Kinet. Katal.*, 18 (1977) 862.
34. K. Fujimoto, Y. Negami, T. Takahashi and T. Kunugi, *Ind. Eng. Chem. Prod. Res. Develop.*, 11 (1972) 303.
35. P.M. Henry, *J. Org. Chem.*, 39 (1974) 3871.
36. H. Mimoun, M. Mercedes and I.S. de Roch, *J. Am. Chem. Soc.*, 100 (1978) 5437.
37. Dow Chemical Co. (J.T. Kummer) US 3,202,715, 24 aug 1965; *Chem. Abstr.*, 63 14708d (1965).
38. F. Chauvet, A. Heumann and B. Waegell, *J. Org. Chem.*, 52 (1987) 1916; B.S. Tovrog, F. Mares and S.E. Diamond, *J. Am. Chem. Soc.*, 102 (1980) 6616; I.E. Beck, E.V. Gusevskaya, A.G. Stepanov, V.A. Likholobov, V.M. Nekipelov, Y.I. Yermakov and K.I. Zamaraev, *J. Molec. Catal.*, 50 (1989) 167; M.A. Andrews and K.P. Kelly, *J. Am. Chem. Soc.*, 103 (1981) 2894; M. Tamura and A. Yasui, *Kogyo Kagaku Zasshi*, 72 (1969) 528 (reference from [34]).
39. K. Fujimoto and T. Kunugi, *Catal.*, *Proc. Int. Congr.*, 5th, (Miami Beach), 1 (1972) 303; K. Fujimoto, H. Takeda and T. Kunugi, *Ind. Eng. Chem. Prod. Res. Develop.*, 13 (1974) 237; K. Fujimoto, O. Kuchi-ishi and T. Kunugi, *Ind. Eng. Chem. Prod. Res. Develop.*, 15 (1976) 259; K. Hwai-DerLiu, K. Fujimoto and T. Kunugi, *Ind. Eng. Chem. Prod. Res. Develop.*, 16 (1977) 223.
40. J. Tsuji, *Synthesis* (1984) 369.
41. S.B. Ziemecki, *Proc. 9th Int. Congr. Catal.*, (Calgary), (1988) 1789; H. Ogawa, H. Fujinami and K. Taya, *J. Chem. Soc., Dalton Trans.*, (1984) 1223; *Catalytica Associates (USA)*, WO 87/01615, March 26, 1987; K.I. Matveev, E.G. Zhishina, N.B. Shitova and L.I. Kuznetsova, *Kinet. Katal.*, 18 (1977) 380.
42. P. François, *Ann. Chim. (Paris)*, 4 (1969) 371.
43. N.G. Satsko, A.P. Belov and K.I. Matveev, *Kinet. Katal.*, 13 (1972) 892.
44. N.B. Shitova, L.I. Kuznetsova and K.I. Matveev, *Kinet. Katal.*, 15 (1974) 72.
45. T. Hosokawa, T. Uno, S. Tuuni and S.I. Murahashi, *J. Am. Chem. Soc.*, 103 (1981) 2318.
46. R. Roffia, F. Conti, G. Gregorio, G.F. Pregaglia and R. Ugo, *J. Organometal. Chem.*, 54 (1973) 357.
47. H. Arai and M. Yashiro, *J. Molec. Catal.*, 3 (1977/1978) 427.
48. R.A. Sheldon and J.K. Kochi: *Metal-Catalysed Oxidations of Organic Compounds*, Acad. Press, New York, (1981) 73.
49. A.F. Wells: *Structural Inorganic Chemistry*, 4th ed., Clarendon press, Oxford, (1975) 417.
50. K.D. Karlin, M.S. Haka, R.W. Cruse, G.J. Meyer, A. Farooq, Y. Gultneh, J.C. Hayes and J. Zubieta, *J. Am. Chem. Soc.*, 110 (1988) 1196.
51. M.M. Rogic and T.R. Demmin, *J. Am. Chem. Soc.*, 100 (1978) 5472 and references therein.
52. F.A. Cotton and G. Wilkinson: *Advanced Inorganic Chemistry*, 4th ed. Wiley, New York, (1980) 800.
53. W.G. Lloyd and B.J. Luberoft, *J. Org. Chem.*, 34 (1969) 3949.
54. R. Jira, *Tetrahedron Lett.*, 17 (1971) 1225.
55. H. Okada, T. Noma, Y. Katzuyama and H. Hashimoto, *Bull. Chem. Soc. Jpn.*, 41 (1968) 1395.
56. N.T. Byrom, R. Grigg and B. Kongkathip, *J. Chem. Soc., Chem. Commun.*, (1976) 216.
57. M. Kolb, E. Bratz and K. Dialer, *J. Molec. Catal.*, 2 (1977) 399. Compare

- also: R.J. Theissen, *J. Org. Chem.*, 36 (1971) 752.
58. W.G. Lloyd, *Fr.* 1,514,031; *Chem. Abstr.*, 71 49551k (1969).
59. A. Kasahara, T. Izumi, K. Sato, M. Maemura and T. Hayasaka, *Bull. Chem. Soc. Jpn.*, 50 (1977) 1899.
60. W. Hafner, R. Jira, J. Sedlmeier and J. Smidt, *Chem. Ber.*, 95 (1962) 1575.
61. S.B. Chandalia, *Ind. J. Technol.*, 5 (1967) 218; S.B. Chandalia, *Ind. J. Technol.*, 6 (1968) 249.
62. M. Hrusovsky, J. Vojtko and M. Cihova, *Hung. J. Ind. Chem.*, 2 (1974) 137.
63. E. Bratz, G. Pranser and K. Dialer, *Chem. Ing. Technol.*, 46 (1974) 161.
64. Y. Moro-oka, T. Okhata, Y. Takita and A. Ozaki, *Bull. Chem. Soc. Jpn.*, 46 (1973) 681; T. Seiyama, M. Yamazoe, J. Hojo and M. Hayakawa, *J. Catal.*, 24 (1972) 173; T. Kubota, F. Kumada, H. Tominaga and T. Kunugi, *Int. Chem. Eng.*, 13 (1973) 539; K. Eguchi, T. Tokiai and H. Arai, *Proc. 9th Int. Congr. Catal. (Calgary)*, 1 (1988) 429.
65. R. Hüttel, J. Kratzer and M. Bechter, *Ann. Chem.*, 94 (1961) 766; R. Hüttel, H. Dietl and H. Christ, *Ann. Chem.*, 97 (1964) 2037.
66. R. Hüttel and M. McNiff, *Chem. Ber.*, 106 (1973) 1789.
67. A. Kaszonyi, J. Vojtko and M. Hrusovsky, *Collection Czechoslovak Chem. Commun.*, 47 (1982) 2128.
68. B. Åkermark and J.E. Bäckvall, *Tetrahedron Lett.*, 10 (1975) 819.
69. W. Hafner, R. Jira, J. Sedlmeier, J. Smidt, P. Fliegel, W. Friedrich and A. Trommet, *Chem. Ber.*, 95 (1962) 1575; *Chem. Abstr.*, 57 (1962) 8411g.
70. K.I. Matveev, *Kinet. Katal.*, 18 (1977) 862, compare also with [9].
71. H. Komiyama and H. Inoue, *J. Chem. Eng. Jpn.*, 8 (1975) 310; P.R. Rony, *Chem. Eng. Science*, 23 (1968) 1021.
72. J. Smidt, W. Hafner, J. Sedlmeier, R. Jira and R. Ruttinger, *Chem. Ind. Genie Chem.*, 101 (1969) 291.
73. T. Kubota, F. Kumada, H. Tominaga and T. Kunugi, *Int. Chem. Eng.*, 13 (1973) 539; H. Arai, T. Yamashiro, T. Kubo and H. Tominaga, *Bull. Jpn. Petr. Inst.*, 18 (1976) 39.
74. M.N. Desai, J.B. Butt and J.S. Dranoff, *J. Catal.*, 79 (1983) 95.
75. A.M. Gaffney, J.J. Leonard, J.A. Sofranko and H.N. Sun, *J. Catal.*, 90 (1984) 261.
76. J.E. Lyons in: J.M. Basset et al. (eds.): *Surface Organometallic Chemistry: Molecular approaches to Surface Catalysis*, Kluwer, Dordrecht, 97 (1988).
77. V. Rao and R. Datta, *J. Catal.*, 114 (1988) 377.
78. L. Forni and G. Terzoni, *Ind. Eng. Chem. Process Des. Dev.*, 16 (1977) 288.
79. A.B. Evnin, J.A. Rabo and P.H. Kasai, *J. Catal.*, 30 (1973) 109.
80. L. Forni and G. Gilardi, *J. Catal.*, 41 (1976) 338; L. Forni, G. Gilardi and G. Terzoni, *Chim. Ind. (Milan)*, 60 (1978) 798.
81. J.L. Seoane, P. Boutry and R. Montarnal, *J. Catal.*, 63 (1980) 191, and references therein.
82. Kirin University, Dep. Chem., Hua Hsueh Tung Pao, 4 (1976) 211 (Ch.); *Chem. Abstr.*, 86 (1976) 43136; Kirin University, Dep. Chem., Chi-lin Ta Hsueh Pao, Tzu Jan K'o Hsueh Pao, 2 (1977) 59 (Ch.); *Chem. Abstr.*, 93 (1977) 226360; Y.-S. Ji, Y.-L. Bi, D.-J. Wang and K.J. Zhen, *Chi-lin Ta Hsueh, Tzu Jan K'o Hsueh Hsueh Pao*, 3 (1980) 114 (Ch.); *Chem. Abstr.*, 94 (1980) 120563; Z.-Y. Wu, H.-C. Guo, M.-X. Li and Z.-Q. Zhao, *Kao Teng Hsueh Hsiao Hua Hsueh Hsueh Pao*, 2 (1981) 225 (Ch.); *Chem. Abstr.*, 95 (1981) 13445; Z. Wu, Gaodeng Xuexiao Huaxue Xuebao, 4 (1983) 392 (Ch.); *Chem. Abstr.*, 99 (1983) 44057.

- 1. Wacker oxidation -

83. P.J. van der Steen, *Thesis*, Delft University Press, (1987).
84. J.J.F. Scholten and P.J. van der Steen, European Patent Specification 0210705, d.d. 22.03.1989.
85. R.L. Robson, R.R. Eady, T.H. Richardson, R.W. Miller, M. Hawkins and J.R. Postgate, *Nature*, 322 (1986) 388.
86. E. de Boer, M.G.M. Tromp, G.E. Kreum and R. Wever, *Biochim. Biophys. Acta*, 872 (1986) 104.
87. N.M. Senozan, *J. Chem. Educ.*, 51 (1974) 503.
88. H. Kneifel and E. Bayer, *Angew. Chem. Int. Ed.*, 12 (1973) 508.
89. M. Ai, *J. Catal.*, 100 (1986) 336; G. Busca, F. Cavani, G. Centi and F. Trifiro, *J. Catal.*, 99 (1986) 400; G. Centi, G. Fornasari and F. Trifiro, *J. Catal.*, 89 (1984) 44; R.M. Contractor, H.E. Gergna, J.S. Horowitz, C.M. Blackstone, B. Malone, C.C. Torardi, B. Griffiths, U. Chowdhry and A.W. Sleight, *Catal. Today*, 1 (1987) 49; F. Garbassi, J.C.F. Bart, R. Tassinari, G. Vlaic and P. Lagarde, *J. Catal.*, 98 (1986) 317; W. Hanke, K. Heise, H.-G. Jerschke, G. Lischke, G. Oehlmann and B. Parlitz, *Z. anorg. allg. Chem.*, 483 (1978) 176.
90. M. Ai, *J. Catal.*, 85 (1984) 324; E. Bordes and P. Courtine, *J. Catal.*, 57 (1979) 236.
91. A. Miyamoto, K. Mori, M. Inomata and Y. Murakami, *Proc. 8th Int. Congr. Catal. (Berlin)*, 4 (1984) 285.
92. M. Akimoto, M. Usami and E. Echigoya, *Bull. Chem. Soc. Jpn.*, 51 (1978) 2195; G.C. Bond, A.J. Sarkany and G.D. Parfitt, *J. Catal.*, 57 (1979) 476; G. Centi and F. Trifiro, *J. Molec. Catal.*, 35 (1986) 255.
93. G.C. Bond and P. König, *J. Catal.*, 77 (1982) 309; C.G. Bond and K. Brückmann, *Faraday Disc.*, 72 (1981) 235; G.K. Borekov, A.A. Ivanov, O.M. Ilyinich and V.G. Ponomareva, *React. Kinet. Katal. Lett.*, 3 (1975) 1; M. Gasior and T. Machej, *J. Catal.*, 83 (1983) 472; K. Hauffe, H. Raveling, *Ber. Bunsenges. Phys. Chem.*, 84 (1980) 912. A.J. van Hengstum, J.G. van Ommen, H. Bosch and P.J. Gellings, *Proc. 8th Int. Congr. Catal. (Berlin)*, 4 (1984) 297; J. Papachryssanthou, E. Bordes, A. Vejux, P. Courtine, R. Marchand and M. Tournaux, *Catal. Today*, 1 (1987) 219.
94. E.I. Andreikov, *React. Kinet. Katal. Lett.*, 22 (1983) 351.
95. M.A. Chaar, D. Patel and H.H. Kung, *J. Catal.*, 109 (1988) 463.
96. M.A. Chaar, D. Patel, M.C. Kung and H.H. Kung, *J. Catal.*, 105 (1987) 483.
97. M. DelArco, M.J. Holgado, C. Martin and V. Rives, *J. Mater. Sci. Lett.*, 6 (1987) 616.
98. A. Baiker and D. Monti, *J. Catal.*, 91 (1985) 361; A.J. van Hengstum, J.G. van Ommen, H. Bosch and P.J. Gellings, *Proc. 8th Int. Congr. Catal. (Berlin)*, 4 (1984) 297; J. Kijenski, A. Baiker, M. Glinski, P. Dollenmeyer and A. Wokaun, *J. Catal.*, 101 (1986) 1; L.N. Kurina and G.I. Sterligova, *Kinet. Katal.*, 13 (1972) 942; F. Roozeboom, P.D. Cordingley and P.J. Gellings, *J. Catal.*, 68 (1981) 464.
99. W. Hanke, K. Heise, H.-G. Jerschke, G. Lischke, G. Oehlmann and B. Parlitz, *Z. anorg. allg. Chem.*, 483 (1978) 176; Y. Nakagawa, T. Ono, H. Miyata and Y. Kubokawa, *J. Chem. Soc., Faraday Trans. I*, 79 (1983) 2929.
100. C.M. van den Bleek and P.J. van den Berg, *J. Chem. Tech. Biotechnol.*, 30 (1980) 467; E.T.C. Vogt, A. Boot, A.J. van Dillen, J.W. Geus, F.J.J.G. Janssen and F.M.G. van den Kerckhof, *J. Catal.*, 114 (1988) 313; M. Inomata, A. Miyamoto and Y. Murakami, *J. Catal.*, 62 (1980) 140; G.L. Baurle, S.C. Wu and K. Nobe, *Ind. Eng. Chem. Prod. Proc. Res. Dev.*, 14 (1975) 268.
101. M.R. Goldwasser, D.L. Trimm, *Ind. Eng. Chem. Prod. Res. Dev.*, 18 (1979)

- 27; F. Roozeboom, A.J. van Dillen, J.W. Geus and P.J. Gellings, *Ind. Eng. Chem. Prod. Res. Dev.*, 20 (1981) 304.
102. V.M. Mastikhin, O.B. Lapina, B.S. Balzhinimaev, L.G. Simonova, L.M. Karnatovskaya and A.A. Ivanov, *J. Catal.*, 103 (1987) 160; D.B. Dabydurjor, S.S. Jewur and E. Ruckenstein, *Catal. Rev.*, 19 (1979) 293.
103. P. Mars and D.W. van Krevelen, *Chem. Eng. Sci. (Special suppl.)*, 3 (1954) 41.
104. P.J. Gellings, *Catal.*, 7 (1985) 105.
105. G. Busca, G. Ramis and V. Lormselli, *J. Molec. Catal.*, 50 (1989) 231.
106. A.M. Gritskov, V.A. Shvets and V.B. Kazanskii, *Kinet. Katal.*, 14 (1973) 1062. V.M. Mastikhin, O.B. Lapina, B.S. Balzhinimaev, L.G. Simonova, L.M. Karnatovskaya and A.A. Ivanov, *J. Catal.*, 103 (1987) 160; D.Kh. Sembaev, B.V. Suvorov, L.I. Saurambaeva and A.E. Shalamov, *Kinet. Katal.*, 15 (1974) 252..
107. J. Haber, T. Machej and T. Czeppe, *Surf. Sci.*, 151 (1985) 301.
108. A. Andersson, *J. Catal.*, 76 (1982) 144.
109. K. Nowinska, *Bull. Acad. Pol. Sci., Ser. Sci. Chim.*, 28 (1980) 741; A. Uano, H. Suzuki and Y. Katera, *J. Chem. Soc., Faraday Trans. I*, 79 (1983) 127.
110. M. DeArco, M.J. Holgado, C. Martin and V. Rives, *J. Catal.*, 99 (1986) 19; G. Bergerett, P. Gallezot, K.V.R. Chary, B.R. Rao and V.S. Subrahmanyam, *Appl. Catal.*, 40 (1988) 191; V.M. Fenin, V.A. Shvets and V.B. Kazanskii, *Kinet. Katal.*, 16 (1975) 1046; D.J. Hucknall and C.F. Cullis, *J. Thermal Anal.*, 13 (1978) 15; Z.C. Kang and Q.X. Bao, *Appl. Catal.*, 26 (1986) 251; R. Koslowski, R.F. Pettifer and J.M. Thomas, *J. Phys. Chem.*, 87 (1983) 5176; N.K. Nag, K.V.R. Chary, M. Reddy, B.R. Rao and V.S. Subrahmanyam, *Appl. Catal.*, 9 (1984) 225; M. Niwa, Y. Matzuoka and Y. Murakami, *J. Phys. Chem.*, 91 (1987) 4519; H. Praliaud and M.-V. Mathieu, *J. Chim. Phys.*, 73 (1976) 689; L.L. van Reyen and P. Cosse, *Disc. Faraday Soc.*, 41 (1966) 277; A. Vejux and P. Courtine, *J. Solid State*, 23 (1978) 93; L.N. Vorob'ev, I.K. Badalova, K. Kh. Razikov, *Kinet. Katal.*, 23 (1982) 119; I.E. Wachs, S.S. Chan, R.Y. Saleh, *J. Catal.*, 91 (1985) 366; I.E. Wachs, R.Y. Saleh, S.S. Chan and C.C. Chersich, *Appl. Catal.*, 15 (1985) 339; V.M. Vorotyntzev, V.A. Shvets and V.B. Kazanskii, *Kinet. Katal.*, 12 (1971) 678; S. Yoshida, T. Iguchi, S. Ishida and K. Tarama, *Bull. Chem. Soc. Jpn.*, 45 (1972) 376; S. Yoshida, T. Matsuzaki, T. Kashiwazaki, K. Mori and K. Tarama, *Bull. Chem. Soc. Jpn.*, 47 (1974) 1564.
111. G.C. Bond, A.J. Sarkany and G.D. Parfitt, *J. Catal.*, 57 (1979) 476; J.L.G. Fierro, L.A. Gambaro, T.A. Cooper and G. Kremenec, *Appl. Catal.*, 6 (1983) 363.
112. G.C. Bond, J.P. Zurita, S. Flamerz, P.J. Gellings, H. Bosch, J.G. van Ommen and B.J. Kip, *Appl. Catal.*, 22 (1986) 361; G. Busca, L. Marchetti, *J. Chem. Soc., Faraday Trans. I*, 81 (1985) 1003; S.S. Chan, I.E. Wachs, L.L. Murell, L. Wang and W.K. Hall, *J. Phys. Chem.*, 88 (1984) 5831; J. Haber, A. Kozlovska and R. Kozlovsky, *Proc. 9th Int. Congr. Catal. (Calgary)*, (1988) 1481; A.J. van Hengstum, J.G. van Ommen, H. Bosch and P.J. Gellings, *Appl. Catal.*, 5 (1983) 207; B. Horvath, J. Geyer and J.L. Krauss, *Z. anorg. allg. Chem.*, 426 (1976) 141; S.I. Kol'tsov, A.A. Malygin, A.N. Volkova and V.B. Aleskovskii, *Russ. J. Phys. Chem.*, 47 (1973) 558; R. Koslowski, R.F. Pettifer and J.M. Thomas, *J. Chem. Soc., Chem. Commun.*, (1983) 438; J.G. van Ommen, K. Hoving, H. Bosch, A.J. van Hengstum and P.J. Gellings, *Z. Phys. Chem. Neue Folge*, 134 (1983) 99; J.G. van Ommen, H. Bosch, P.J.

- Gellings and J.R.H. Ross, in: Preparation of Catalysts IV, B. Delmon, P. Grange, P.A. Jacobs and G. Poncelet (eds.), Elsevier, Amsterdam, (1987) 151; V.N. Pak, J. Phys. Chem. U.S.S.R., 50 (1976) 850.
113. A.J. van Hengstum, J. Pranger, J.G. van Ommen, H. Bosch and P.J. Gellings, Appl. Catal., 11 (1984) 317; A.J. van Hengstum, J.G. van Ommen, H. Bosch and P.J. Gellings, Appl. Catal., 8 (1983) 369; G. Meunier, B. Mocaer, S. Kastelan, L.R. le Coustumer, J. Brimblot and J.P. Bonnelle, Appl. Catal., 21 (1986) 329; F. Roozeboom, M.C. Mittelmeyer-Hazeleger, J.A. Moulijn, J. Medema and V.H.J. de Beer, J. Phys. Chem., 84 (1980) 2783.
114. J.L.G. Fierro, L.A. Gambaro, T.A. Cooper and G. Kremenec, Appl. Catal., 6 (1983) 363; W. Hanke, R. Bienert and H.-G. Jerschke, Z. anorg. allg. Chem., 414 (1975) 109; C. Martin and V. Rives, Ads. Sci. & Techn., 2 (1985) 241.
115. E.T.C. Vogt, A. Boot, A.J. van Dillen, J.W. Geus, F.J.J.G. Janssen and F.M.G. van den Kerkhof, J. Catal., 114 (1988) 313.
116. Y. Murakami, M. Inomata, K. Mori, T. Ui, K. Suzuki, A. Miyamoto and T. Hattori in: Preparation of Catalysts III, G. Poncelet, P. Grange and P.A. Jacobs (eds.), Elsevier, Amsterdam, (1983).
117. G. Busca, G. Centi, L. Marchetti and F. Trifiro, Langmuir, 2 (1986) 568; R.Y. Saleh, I.E. Wachs, S.S. Chan and C.C. Chersich, J. Catal., 98 (1986) 102.
118. A.F. Wells: Structural Inorganic Chemistry, 4th ed., Clarendon, Oxford, (1975) 467.
119. H.T. Evans and S. Block, Inorg. Chem., 5 (1966) 1808.
120. C.L. Christ, J.R. Clark and H.T. Evans, Acta Cryst., 7 (1954) 801.
121. H.G. Bachmann, F.R. Ahmed and W.H. Barnes, Z. Kristallog., 115 (1961) 110.
122. F. Roozeboom, T. Fransen, P. Mars and P.J. Gellings, Z. anorg. allg. Chem., 449 (1979) 25.
123. F. Roozeboom, J. Medema and P.J. Gellings, Z. Phys. Chem., Neue Folge, 111 (1978) 215.
124. S. Yoshida, T. Iguchi, S. Ishida and K. Tarama, Bull. Chem. Soc. Jpn., 45 (1972) 376.
125. G. Bergerett, P. Gallezot, K.V.R. Chary, B.R. Rao and V.S. Subrahmanyam, Appl. Catal., 40 (1988) 191.
126. S. Yoshida, T. Tanaka, Y. Nishimura, H. Mizutani and T. Funabiki, Proc. 9th Int. Congr. Catal. (Calgary), (1988) 1473.
127. J. Haber, A. Kozlovska and R. Kozlovsky, J. Catal., 102 (1986) 52.
128. G. Busca, Langmuir, 2 (1986) 577.
129. S.S. Chan, I.E. Wachs, L.L. Murell, L. Wang and W.K. Hall, J. Phys. Chem., 88 (1984) 5831; F. Roozeboom, M.C. Mittelmeyer-Hazeleger, J.A. Moulijn, J. Medema and V.H.J. de Beer, J. Phys. Chem., 84 (1980) 2783.
130. G.C. Bond, J.P. Zurita, S. Flamerz, P.J. Gellings, H. Bosch, J.G. van Ommen and B.J. Kip, Appl. Catal., 22 (1986) 361.
131. R. Koslowski, R.F. Pettifer and J.M. Thomas, J. Chem. Soc., Chem. Commun., (1983) 438; R. Koslowski, R.F. Pettifer and J.M. Thomas, J. Phys. Chem., 87 (1983) 5172; R. Koslowski, R.F. Pettifer and J.M. Thomas, J. Phys. Chem., 87 (1983) 5176.
132. I.E. Wachs, R.Y. Saleh, S.S. Chan and C.C. Chersich, Appl. Catal., 15 (1985) 339.
133. A. Vejux and P. Courtine, J. Solid State, 23 (1978) 93.
134. Z.C. Kang and Q.X. Bao, Appl. Catal., 26 (1986) 251.

2

Some experimental aspects of heterogeneous Wacker oxidation

Catalyst preparation

Heterogeneous Wacker catalysts are composed of a support material, like $\gamma\text{-Al}_2\text{O}_3$ or $\text{TiO}_2(\text{a})$, covered with a vanadate monolayer, which, in turn, is covered by a sub-monolayer of a palladium salt, for instance palladium chloride or palladium sulphate. As mentioned already in Chapter 1, several

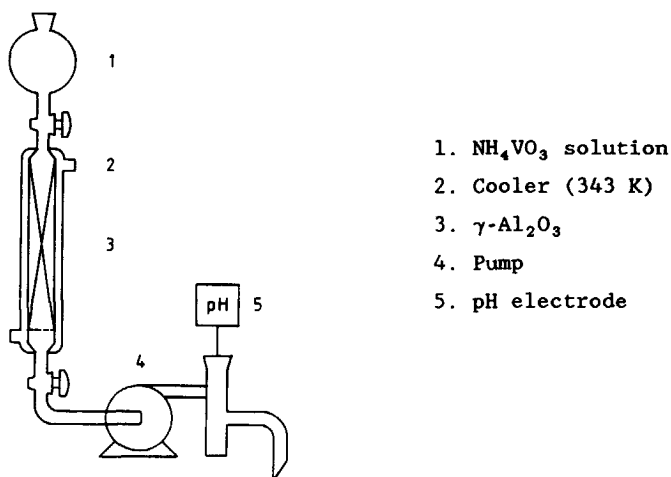


Figure 1. Apparatus used for catalyst preparation.

- 2. Experimental aspects -

methods exist for the fixation of vanadate monolayers. Out of these methods we have chosen the 'gentle method' (Roozeboom et al. [1]), which involves leading an NH_4VO_3 solution through a bed of the support material until equilibrium is reached. The monolayer formation is followed by drying at 353 K and calcination in a stream of air at 673 K. Afterwards, impregnation to incipient wetness with a palladium chloride or palladium sulphate solution is carried out.

Before adsorption of NH_4VO_3 , $\gamma\text{-Al}_2\text{O}_3$ pellets, type 000-3P, $S(\text{BET}) = 250 \text{ m}^2 \cdot \text{g}^{-1}$ (AKZO) or $\text{TiO}_2(\text{a})$ extrudates, type CRS 31 LOT 2, $S(\text{BET}) = 127 \text{ m}^2 \cdot \text{g}^{-1}$ (Rhône Poulenc) were crushed and sieved to particle diameters ranging from 425 to 600 μm . As will be explained later on, any diffusional retardation during catalytic use is thus avoided. A 1 % NH_4VO_3 solution, acidified with sulphuric acid to $\text{pH} = 4$, is led over these particles at 343 K for 24 h. At a pH of 4 the main solute is the decavanadate ion $\text{HV}_{10}\text{O}_{28}^{5-}$ [2]. The solution is relatively stable; it takes more than a week before spontaneous

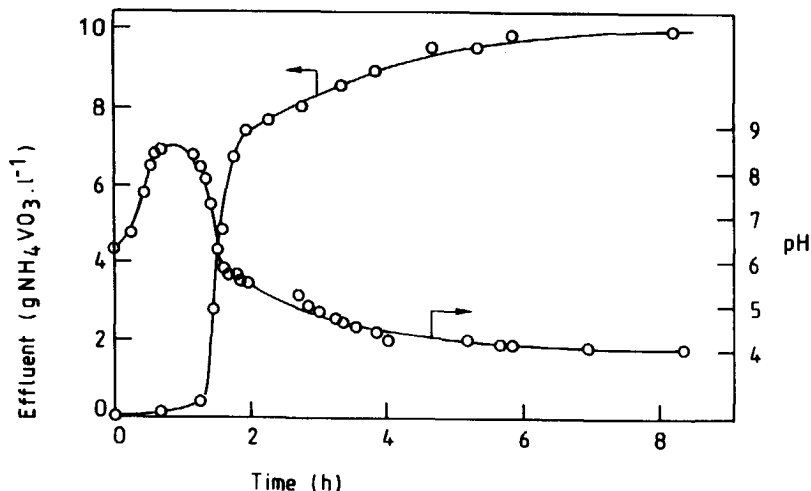


Figure 2. Breakthrough curve observed during catalyst preparation.

V_2O_5 precipitation is observed, but at higher acid concentrations V_2O_5 crystals readily form. At a pH of 4, which is below the isoelectric point (IEP) of the supports, the surface will be positively charged and therefore

- 2. Experimental aspects -

the negatively charged vanadate ions in solution are attracted by the surface.

Increasing the pH of the NH_4VO_3 solution leads to a decrease of the final vanadate coverage of $\gamma\text{-Al}_2\text{O}_3$ [3], probably due to an increasing repulsion of the vanadate ions by the surface. At pH values higher than 7, above the IEP of $\gamma\text{-Al}_2\text{O}_3$, no vanadate is adsorbed anymore.

For the deposition of a vanadate monolayer on $\gamma\text{-Al}_2\text{O}_3$, the apparatus depicted in Fig. 1 has been used. During the course of the reaction the change of the pH and of the effluent vanadate concentration in the effluent could be measured. The results are given in Fig. 2; it is seen that at first a slight increase of the pH occurs; due to the basic properties of the $\gamma\text{-Al}_2\text{O}_3$, protons are taken up and possibly also traces of ammonia are formed. However, NH_4VO_3 is adsorbed without decomposition, otherwise a stronger increase of the pH would have occurred. At the breakthrough point of vanadate, the loading of the support is calculated to correspond to 2.3 V atoms. nm^{-2} (8 wt % V_2O_5). The slow further increase of the effluent concentration is related to a slow further increase of the vanadate loading up to 4.3 V atoms. nm^{-2} (14 wt % V_2O_5) after 24 h adsorption time. From Fig. 2 it appears that the pH of the effluent is indicative of the coverage reached.

The final equilibrium loading (24 h equilibration) appeared to be independent of the NH_4VO_3 concentration (Fig. 3), which points to the

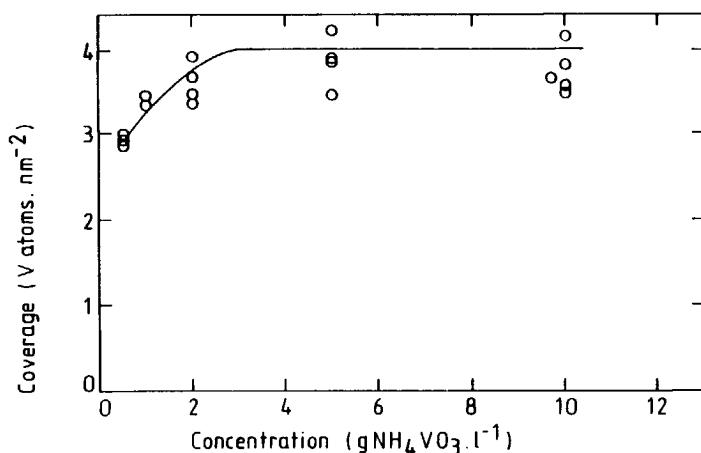


Figure 3. Dependence of the vanadate coverage on the concentration.

- 2. Experimental aspects -

absence of diffusional retardation of the transport of NH_4VO_3 to the surface. However, at concentrations below 0.1 % NH_4VO_3 , a lower equilibrium vanadate coverage is found.

The occurrence of the first of the two adsorption reactions, the fast reaction up to $2.3 \text{ V atoms.nm}^{-2}$, is confirmed by batch experiments, the results of which are presented in Fig. 4. In these experiments, particles smaller than $250 \mu\text{m}$ were added to a magnetically stirred vanadate solution and the vanadate uptake was determined as a function of time. As

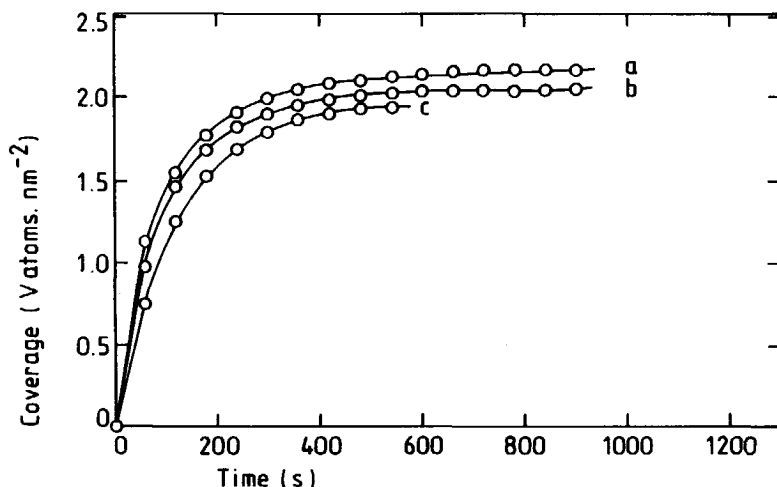


Figure 4. Adsorption of NH_4VO_3 on $\gamma\text{-Al}_2\text{O}_3$ as a function of time. Curve a: $10 \text{ g NH}_4\text{VO}_3 \cdot \text{l}^{-1}$, curve b: $9 \text{ g NH}_4\text{VO}_3 \cdot \text{l}^{-1}$, curve c: $8 \text{ g NH}_4\text{VO}_3 \cdot \text{l}^{-1}$. $\gamma\text{-Al}_2\text{O}_3$, particle diameter $< 250 \mu\text{m}$. The reaction is stopped by addition of distilled water.

seen clearly in Fig. 4, a fast NH_4VO_3 uptake occurs, up to $2.3 \text{ V atoms.nm}^{-2}$, this being the same coverage as found from the breakthrough point during continuous vanadate adsorption. For particle diameters ranging from 250 to $425 \mu\text{m}$ the same curves are found and therefore we are not dealing with diffusional retardation.

The first rapid and strong ammonium vanadate uptake is presumably due to ionic bonding of NH_4^+ and VO_3^- on the acidic and basic sites on the $\gamma\text{-Al}_2\text{O}_3$ surface. This strongly bound layer could be removed completely by leading over of distilled water (pH = 6).

- 2. Experimental aspects -

After drying of the ammonium vanadate-loaded particles at 353 K in air, or after ageing for 1 h at 293 K in the mother liquor, rinsing with water did no longer result in removal of the vanadate. Apparently some surface reaction had now taken place, resulting in a stronger mode of bonding.

The drying procedure was followed by calcination in air at 673 K for 4 h.

In order to get an impression of the thickness of (sub) monolayers, the pore volume distributions were determined from the capillary condensation of nitrogen at 77 K. The distribution was calculated according to the Broekhoff-de Boer method [4]. The results were compared with the pore volume distribution of the non-loaded $\gamma\text{-Al}_2\text{O}_3$ support and also with a pore volume distribution calculated for a theoretical layer thickness of 3 Å.

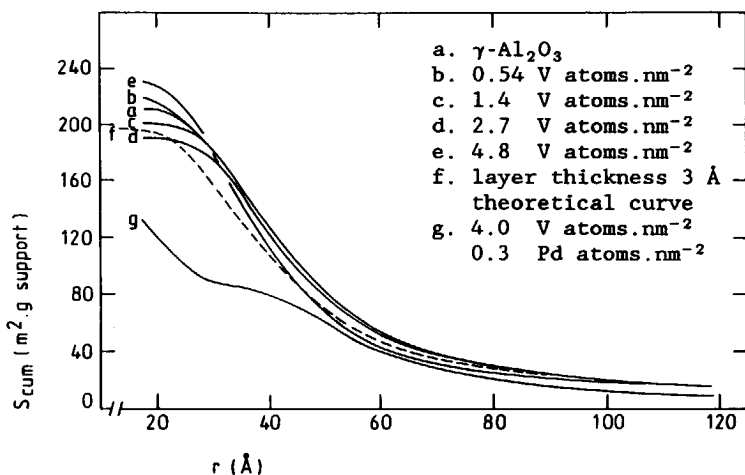


Figure 5. The cumulative surface area, $S(\text{cum})$, as a function of the pore radius at several vanadate coverages. Dashed line: theoretical curve calculated for a layer thickness of 3 Å. Surface areas are given per gram of support material.

As can be concluded from Fig. 5, the vanadate is deposited as a thin layer over the whole range of pore radii. Taking the thickness of one layer to be 3 Å, it can be concluded that after adsorption to equilibrium a thickness of about one layer is formed.

In summary, on $\gamma\text{-Al}_2\text{O}_3$ NH_4VO_3 adsorbs without decomposition. The adsorption process is built up of at least two steps: first a fast vanadate uptake to about 2.3 V atoms.nm⁻² takes place, followed by a slow

transformation to another chemically bound form. Simultaneously a slow adsorption reaction appeared up to $4.3 \text{ V atoms.nm}^{-2}$. After calcination, a monolayer coverage is found from a study of pore surface distributions.

The catalytic performance

For determining the performance of the catalysts, a continuous flow stainless-steel equipment (see Fig. 6) has been used, operating in the pressure range from 0.1 to 0.6 MPa pressure. The gases were dried over activated zeolites and the composition of the feed was regulated by means of mass-flow controllers (Inacom, The Netherlands). Water was distilled twice and dosed to the feed by leading finely divided bubbles of nitrogen through

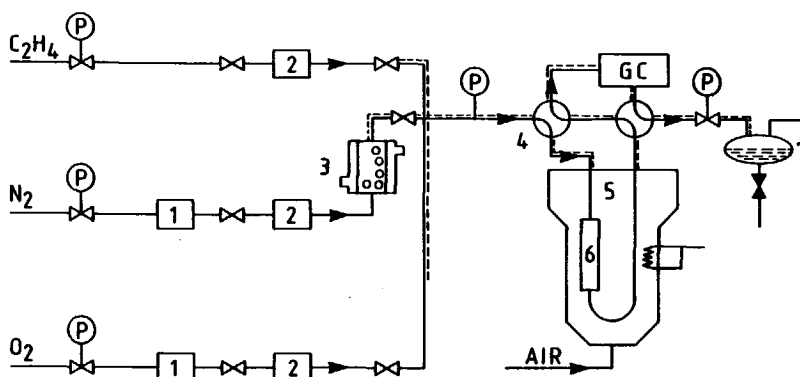


Figure 6. Micro-scale oxidation unit. 1: Zeolite, type 3A; 2: Mass flow controller; 3: Water evaporator; 4: Four-way valve; 5: Fluidized bed heater; 6: Reactor; 7: Condensor.

a thermostatted flask filled with water. Up to 320 K, the nitrogen is completely saturated with water, but at higher temperatures a non-ideal behaviour of the water evaporation occurs. The composition of the feed was corrected for this effect. Liquid alkenes like cyclohexene and styrene were also dosed by evaporation. In most cases the total gas stream was adjusted to 100 ml (STP) of gas per minute and the total pressure was kept constant at 0.11 MPa.

- 2. Experimental aspects -

The reactor, a continuous-flow fixed-bed stainless-steel tube, internal diameter 1 cm and length 10 cm, was heated by means of a fluidized bed oven, connected and temperature-regulated by a Eurotherm thyristor. The catalyst bed temperature appeared to be constant over the whole length of the reactor within 1 K. Temperatures could be measured inside and outside the fixed bed and these temperatures appeared to be equal within 2 K. In most experiments 0.5 to 3 g of catalyst were used.

Product gas analysis was performed by means of a gas chromatograph equipped with a hot sampling valve and a FID detector and peak areas were recorded and integrated by a microcomputer (Digital LCI 11/03, USA). Response factors of the different products relative to the alkene peaks were determined in separate experiments. By means of two four-way valves both the feed and the product stream could be analysed. The product stream was cooled down to about 293 K and collected in a condenser and the liquid was subjected to further analysis. On the basis of the carbon material balance the oxidation selectivity to CO and CO₂ was shown to be below 5 % in all cases.

Intra-particle mass transfer of ethylene may influence the reaction rate and therefore the experimental Thiele modulus Φ_{exp} (eq. (1)) [5] was calculated for the reaction conditions given in the legend of Fig. 7.

$$\Phi_{\text{exp}} = \frac{(-r_{\text{exp}}) \cdot (n+1) \cdot (V_p)^2}{c \cdot (1-\epsilon_b) \cdot 2 \cdot D_e \cdot (A_p)^2} \quad (1)$$

where:

$(-r)_{\text{exp}}$	the observed reaction rate	$(6.3 \cdot 10^{-2} \text{ mol} \cdot \text{m}^{-3} \cdot \text{reactor} \cdot \text{s}^{-1})$
n	(the highest activity of Fig. 7 is taken) the over-all order of reaction	(1)
V_p	the particle volume	$(4.8 \cdot 10^{-11} \text{ m}^3)$
c	the inlet alkene concentration	$(0.44 \text{ mol} \cdot \text{m}^{-3})$
ϵ_b	the porosity of the catalyst bed	(0.5)
D_e	the effective diffusion coefficient	$(1.5 \cdot 10^{-7} \text{ m}^2 \cdot \text{s}^{-1})$
	(calculated from both gas and Knudsen diffusion and corrected for particle porosity and tortuosity of the particles, resp. 0.69 and 3)	
A_p	the mean external particle surface area	$(6.4 \cdot 10^{-7} \text{ m}^2)$

- 2. Experimental aspects -

From Φ_{exp} the (theoretical) Thiele modulus Φ_p and the efficiency factor E can be calculated (eq. (2)):

$$E = \frac{\text{tgh}(\Phi_p)}{\Phi_p} \quad \text{and} \quad \Phi_{\text{exp}} = \Phi_p \cdot \text{tgh}(\Phi_p) \quad (2)$$

An E value of 0.996 was found, which indicates that no pore diffusion limitations are to be expected. Experiments carried out with varying particle diameters (V_p/A_p) confirm this expectation; no influence of the

Table I. Influence of particle diameter and space time on the catalyst activity.

<u>Particle diameters</u>	<u>conversion</u> ¹
425 - 500 μm	10.5 %
750 - 825 μm	10.3 %

¹ Catalyst and conditions as mentioned in the legend of Fig. 7. Total gas flow: 1.66 ml STP.s⁻¹.

$$c = \frac{E_a \cdot (-r)_{\text{exp}} \cdot V_p \cdot (-\Delta H_r) \cdot (n+1)}{R \cdot T \cdot (1 - \epsilon_b) \cdot A_p \cdot h \cdot T \cdot 2} \quad (3)$$

where:

E_a	the apparent activation energy	(36 kJ.mol ⁻¹)
$(-r)_{\text{exp}}$	the observed reaction rate	(6.3 · 10 ⁻² mol.m ⁻³ .s ⁻¹)
V_p	the particle volume	(4.8 · 10 ⁻¹¹ m ³)
(ΔH_r)	the reaction enthalpy	(- 214 kJ.mol ⁻¹)
n	the over-all order of reaction	(1)
R	the gas constant	(8.314 J.mol ⁻¹ .K ⁻¹)
T	the gas- and particle temperature	(373 K)
ϵ_b	the porosity of the catalyst bed	(0.5)
A_p	the external particle surface area	(6.4 · 10 ⁻⁷ m ²)
h	the heat transfer constant	(42 J.m ⁻² .K ⁻¹ .s ⁻¹)
	(calculated with the properties of flowing air)	

- 2. Experimental aspects -

particle size on the activity has been found (Table I).

Also non-isothermal conditions due to heat transfer limitations may influence the reaction rate. In the heat transfer steps from inside to outside the particle, the most critical step is transfer of heat from the particle surface to the gas phase. To verify whether film heat transfer limitation occurred eq. (3) has been applied [6].

In the absence of heat transfer limitation c is below 0.1. It appeared to be $1.5 \cdot 10^{-3}$, which indicates that no heat transfer limitation over the film around the particle was present. Measurements in which the space time was varied at low conversions showed a linear relationship between space time and conversion, which also points to the absence of heat transfer limitations (Fig. 7).

Space time and conversion were reduced by mixing the catalyst particles

$$\frac{b \cdot d_p}{L_r \cdot I} \leq 4 \cdot 10^{-3} \quad (4)$$

where:

b	the fraction of inert material	(0.8)
d_p	the particle diameter	$(4.5 \cdot 10^{-4} \text{ m})$
L_r	the length of the reactor	(0.1 m)
I	the percentual error in the reaction rate.	

with glass spheres with a diameter of 0.5 mm. The ratio of the reactor diameter to the mean particle size was about 20 and the ratio of the length of the reactor to the mean particle size was about 250. These ratios were sufficiently high to make sure that we were dealing with plug flow of the gas in the reactor [6].

When the catalyst particles are diluted by glass spheres, bypassing might influence the reaction rate. A criterion for this is eq. (4) [7]. A maximum error I of 0.8 % is found from eq. 4, which is an acceptably low value.

Finally, the measured reaction rate can be influenced by integral behaviour of the reactor. As shown in Fig. 7, below 10 % conversion the difference between differential and integral behaviour can be neglected in our case, as we are dealing with a reaction which is first order with

- 2. Experimental aspects -

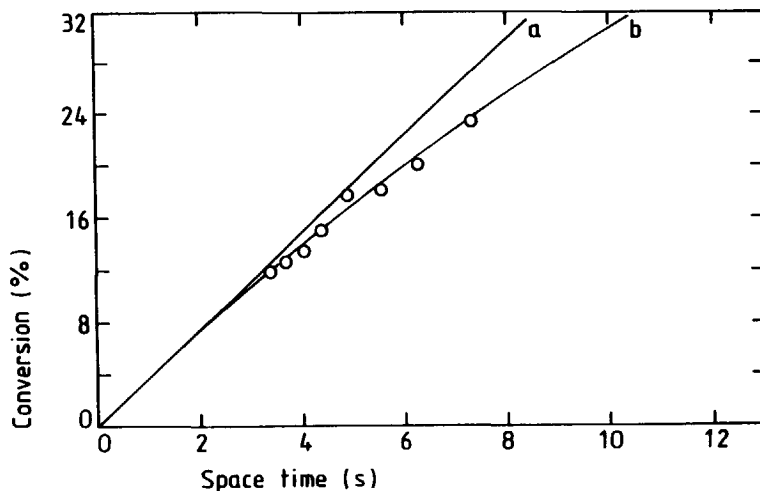


Figure 7. Measured and calculated conversions (ξ) versus space time (τ) for the oxidation of ethylene. For a first order reaction: curve a: $\xi = 100 \cdot k \cdot \tau$ (differential behaviour); curve b: $\xi = 100 \cdot (1 - e^{-k \cdot \tau})$ (integral behaviour). Catalyst: 83.6 mol % Al_2O_3 ; 7.95 mol % V_2O_5 ; 1.403 mol % PdCl_2 , 7.014 mol % HCl , 1 g of catalyst. Feed composition: 0.5 mol % C_2H_4 ; 6.5 mol % H_2O , 93 mol % air. Total pressure: 0.11 MPa. Reactor volume: 7.85 cm^3 .

respect to ethylene. At 10 % conversion the theoretical error in the reaction rate is 4.8 %. In the experiments reported in this thesis the conversion was practically always below 10 % and hence no correction for non-differential behaviour has to be applied. Only when TiO_2 (a) supported catalysts were used (Chapter 8) conversions up to 20 % were arrived at. In this case the reaction rates were recalculated to their differential values.

References

1. F. Roozeboom, T. Fransen, P. Mars and P.J. Gellings, *Z. Anorg. Allg. Chem.*, **449** (1979) 25.
2. M.T. Pope and B.W. Dale, *Quart. Rev.*, **22** (1968) 527.
3. L. Wang and W.K. Hall, *J. Catal.*, **77** (1982) 232.
4. J.C.P. Broekhoff, *Thesis*, Delft University of Technology, (1969); J.B. Parra Soto and C. Otera Arean, *Comp. Chem.*, **10** (1986) 27.
5. H. Scott Fogler, *Elements of Chemical Reaction Engineering*, Prentice Hall, New Jersey, (1986).
6. D.E. Mears, *Ind. Eng. Chem. Process Des. Dev.*, **10** (1971) 541.
7. C.M. van den Bleek, K. van der Wiele and P.J. van den Berg, *Chem. Eng. Sci.*, **24** (1969) 681.

Solid-state ^{51}V NMR and DRIFT structural studies of vanadate monolayers on $\gamma\text{-Al}_2\text{O}_3$

Abstract

^{51}V NMR and Diffuse Reflectance Infrared Fourier Transform spectroscopy (DRIFT) have been applied in a study on the structure of vanadate supported on $\gamma\text{-Al}_2\text{O}_3$. At coverages far below a monolayer isolated (probably monomeric or dimeric) tetrahedrally surrounded vanadate species were present. During dehydration the tetrahedral structure disappeared, a non-symmetrical vanadate environment being formed. At increasing coverage, a tetrahedrally coordinated but water-insensitive vanadate structure appeared, simultaneously with an increase of the number of vanadyl ($\text{V}=\text{O}$) groups. This could be ascribed to the formation of one- or two-dimensional vanadate structures. At these coverages the number of $\text{V}=\text{O}$ groups also increased with decreasing water coverage, without significant changes in the coordination of vanadium. Up to monolayer coverage (estimated to be $4.8 \text{ V atoms.nm}^{-2}$) no crystalline V_2O_5 could be detected.

Introduction

In many catalytic reactions the use of vanadate monolayer catalysts is preferred over the application of crystalline vanadium oxide. Monolayer vanadate catalysts differ from crystalline vanadium oxide not only with respect to the vanadium oxide dispersion, but also with regard to the chemical and catalytic properties. Typical reactions, reviewed by Gellings [1], include: selective oxidation [2], selective NO_x reduction in the presence of oxygen [3] and oxidative dehydrogenation [4]. Quite recently heterogeneous Wacker oxidation has also been performed over vanadate monolayer catalysts. In this case the monolayer was covered with a second sub-monolayer of palladium chloride or palladium sulphate [5].

Many recent studies deal with spectroscopic investigations into the precise structure of the monolayer. Such structures were found to depend on the vanadate coverage and on the type of support used, and, to a lesser extent, on the preparation method. The two-dimensional vanadate structure strongly deviates from the structure of crystalline vanadium oxide.

RAMAN spectroscopy, applied by Roozeboom *et al.* [6], revealed the existence of two distinct vanadate structures, their relative abundances being dependent on the vanadate coverage. Burgerett *et al.* [7] studied a vanadate monolayer on $\gamma\text{-Al}_2\text{O}_3$ by means of radial electron distribution and they concluded that tetrahedral corner-sharing VO_4 units were present, with a flexible two-dimensional structure. A study by Yoshida *et al.* [8] points to the presence of a tetrahedral vanadate structure on $\gamma\text{-Al}_2\text{O}_3$. Water can coordinate to this structure without any change in the tetrahedral coordination. Haber *et al.* [9], applying EXAFS, only detected dimeric tetrahedral vanadate species on $\gamma\text{-Al}_2\text{O}_3$ at monolayer coverage.

The vanadate structure on $\text{TiO}_2(\text{a})$ has been characterized by Busca *et al.* [10] by means of FT-IR. Three distinct vanadate phases could be detected. Far below monolayer coverage, two kinds of isolated vanadyl species are present. The first type is coordinatively saturated, whereas the second form can capture a water molecule. At higher coverages a two-dimensional structure is formed. On the basis of RAMAN [11] and EXAFS [9] studies a tetrahedral coordination of vanadium by oxygen is supposed to be present, comparable to the coordination in the metavanadate structure.

Solid state ^{51}V NMR appeared to be a powerful method to study vanadate monolayers. The structure of vanadate on $\gamma\text{-Al}_2\text{O}_3$ at low coverage, studied by Eckert and Wachs [12], corresponds to the structure of (polymeric) metavanadate. At increasing coverage, ranging from 3 to 7 V atoms.nm $^{-2}$, a distorted octahedral vanadate surface structure differing from crystalline vanadium oxide emerges. This distorted octahedral vanadate structure is present in a wide range of coverages on $\text{TiO}_2(\text{a})$ as well [12].

In this chapter we now report on the structure of vanadate layers supported on $\gamma\text{-Al}_2\text{O}_3$, studied by combining ^{51}V NMR and DRIFT analysis.

Experimental

Chemicals

$\gamma\text{-Al}_2\text{O}_3$, type 000-3P, S(BET) = 250 m 2 .g $^{-1}$, was supplied by Akzo (The Netherlands). NH_4VO_3 , analytical grade, was purchased from Merck (F.R.G.) and H_2SO_4 , analytical grade, was purchased from Baker (The Netherlands). Water was distilled before use.

Catalyst preparation

The $\gamma\text{-Al}_2\text{O}_3$ pellets were crushed and sieved to particle diameters from 425 to 500 μm . By leading an NH_4VO_3 solution of pH = 4 over these particles, following the method described by Roozeboom [13], the surface was covered with a vanadate monolayer. Sub-monolayer catalysts were prepared by equilibration of $\gamma\text{-Al}_2\text{O}_3$ particles at 293 K in diluted solutions of NH_4VO_3 . The pH was adjusted to 4 by addition of diluted H_2SO_4 to the solutions. After standing for 24 h, the mother liquor was decanted.

In all cases the particles were dried at 353 K for 16 h and calcined at 673 K in a stream of dry air. Finally, the vanadium coverage was determined by titration with Fe(II). A vanadium coverage of 4.8 V atoms.nm $^{-2}$ (15.3 wt % V_2O_5) was estimated to correspond to a monolayer.

^{51}V NMR

$\gamma\text{-Al}_2\text{O}_3$ supported catalysts were measured without pretreatment. Also samples dried at 423 K for 16 h at 133 Pa pressure were measured. The ^{51}V NMR experiments were performed on a Bruker AM 500, working at 157.728 MHz. All

experiments were performed on static (non-spinning) samples. No strong influence on the spectra was found when MAS was applied. Spectra are given relative to V_2O_5 .

DRIFT

Diffuse Reflectance Infrared Fourier Transform spectroscopy (DRIFT) was performed on a Nicolet FTIR SXB 20 apparatus, working in the range of 400 cm^{-1} to 4000 cm^{-1} and equipped with a Barnes diffuse reflectance cell. In all cases 0.03 g of catalyst was diluted with 0.15 g of diamond powder and measured.

Results

^{51}V NMR

Since the ^{51}V isotope has a nuclear magnetic spin $7/2$, and therefore a large nuclear electric quadrupole moment, wide-line ^{51}V NMR spectra can be quite complex. As clearly shown in Fig. 1, the wide-line ^{51}V NMR signals of adsorbed vanadate at different coverages on $\gamma\text{-Al}_2\text{O}_3$ are shifted to high-field, relative to V_2O_5 . This points to the coordination number of the vanadate being lower than in V_2O_5 , probably corresponding to tetrahedral coordination.

On varying the coverage of vanadate on $\gamma\text{-Al}_2\text{O}_3$ a multiplet is seen at 2 wt % V_2O_5 , which can be ascribed to the occurrence of one or two distinct vanadate structures only.

At 3.6 wt % V_2O_5 a broad signal is found, which indicates that now a more complicated vanadate structure is formed on the $\gamma\text{-Al}_2\text{O}_3$ surface. With increasing coverage up to a monolayer, corresponding to 15.3 wt % V_2O_5 ($4.8\text{ V atoms.nm}^{-2}$), the signal further broadens and its maximum is gradually shifted down-field, which indicates that the vanadium coordination number increases with increasing coverage. Even at 15.3 wt % V_2O_5 no formation of crystalline V_2O_5 can be detected.

During handling and storage, the samples came into contact with air. A low water uptake from the air appeared to influence the ^{51}V NMR measurements. Therefore the samples were thoroughly dried at 423 K for 24 h in vacuum (100 Pa) and the spectra derived subsequently are depicted in Fig. 2. At 2 and 3.6 wt % V_2O_5 , the ^{51}V NMR signal is extremely broadened or split up into many signals, and noise signals prevail. Apparently, the

- 3. Vanadate monolayers -

bonding geometry has changed from a more symmetrical to a less symmetrical coordination. At coverages of 5 and 6.9 wt % V_2O_5 , the original spectra are strongly influenced by removal of water. The sample with 9.4 wt % V_2O_5 changed its colour into black during evacuation and no NMR signal could be

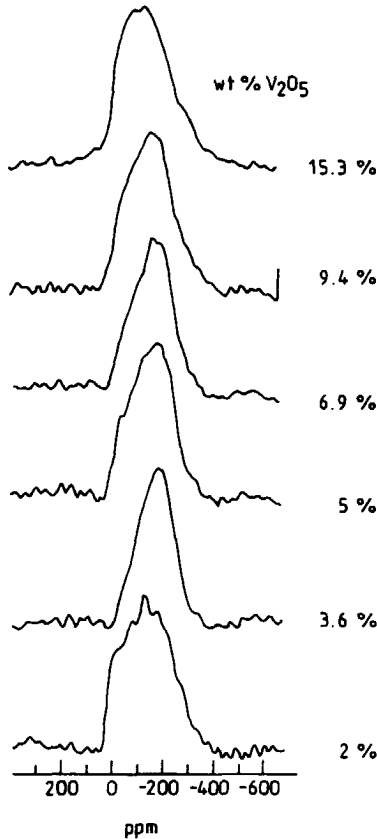


Figure 1. ^{51}V NMR spectra of samples with different vanadate coverages on $\gamma-Al_2O_3$, moistened by contact with air.

detected. Both phenomena are due to reduction of the vanadate to the paramagnetic V(IV) valence state. However, monolayer vanadate (15.3 wt % V_2O_5) appeared to be unaffected by dehydroxylation, which points to the absence of coordination of water in this case.

DRIFT

More information about the vanadate structures was derived from Diffuse Reflectance Infrared Fourier Transform (DRIFT) analysis. The relevant samples, diluted with diamond powder, were dried *in situ* at 573 K in a dry helium-oxygen stream, and subsequently wetted by leading over a helium-oxygen stream, saturated with water at 293 K, at 373 K for 15 min. Longer

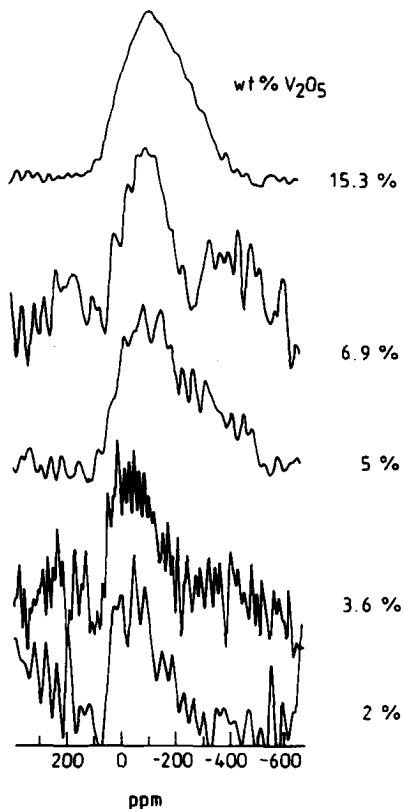


Figure 2. ^{51}V NMR spectra of dried samples with different vanadate coverages on $\gamma\text{-Al}_2\text{O}_3$.

waiting times did not significantly change the spectra. The DRIFT spectra are given in Fig. 3. At 2 wt % V_2O_5 a double band of a low intensity with maxima at 973 cm^{-1} and 1039 cm^{-1} was found. At 5 wt % and 9.4 wt % V_2O_5 , the intensity increases linearly with the vanadate coverage, whereas maxima at

- 3. Vanadate monolayers -

973 cm^{-1} and 999 cm^{-1} are found. At 15.3 wt % V_2O_5 only one broad band shifted to 999 cm^{-1} is present. As is clearly shown in Fig. 4, the DRIFT spectra are influenced by water, a phenomenon found also in the ^{51}V NMR analysis. After drying the samples *in situ* at 573 K in a flow of oxygen and helium, at 2 wt % V_2O_5 a band of low intensity at 1026 cm^{-1} is found. At 5 wt % and 9.4 wt % V_2O_5 a double band with maxima at 959 cm^{-1} and 1019 cm^{-1} is present. The band at 1019 cm^{-1} increases relative to the 959 cm^{-1} band, which results in a band shifted to 1026 cm^{-1} , with a shoulder at 959 cm^{-1} in the 15.3 wt % sample.

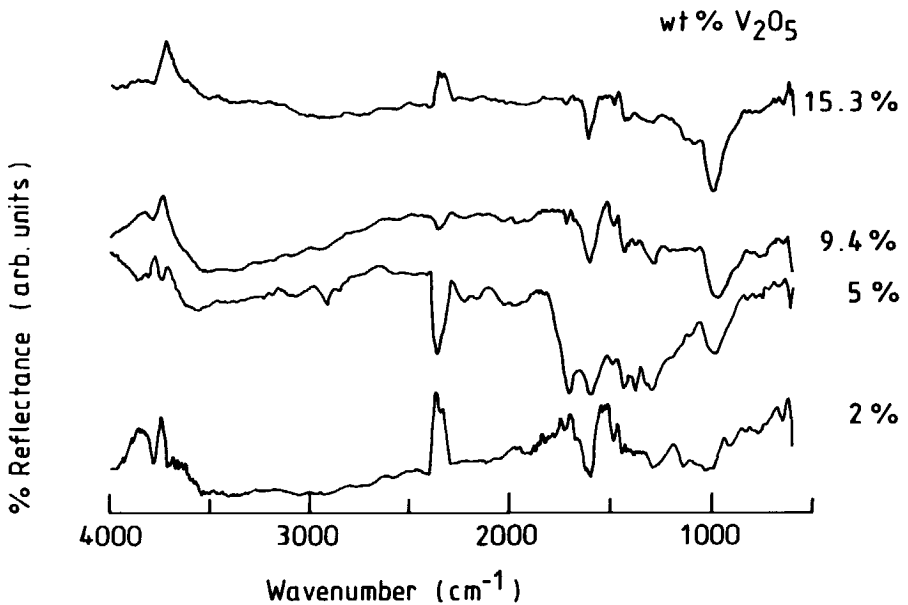


Figure 3. DRIFT spectra of moistened samples with different vanadate coverages on $\gamma\text{-Al}_2\text{O}_3$.

The other signals in the spectra presented in Fig. 3 and 4 can be ascribed to the presence of water ($1200\text{ cm}^{-1} - 1900\text{ cm}^{-1}$ and $3500\text{ cm}^{-1} - 4000\text{ cm}^{-1}$) and to the presence of traces of gaseous CO_2 (2355 cm^{-1}).

The influence of water on the DRIFT spectra is depicted in Fig. 5. In this figure the spectra of dried samples are subtracted from the spectra of

- 3. Vanadate monolayers -

the same but moist samples, and the Kubelka Munk equation is applied to quantify this effect. At 2 wt % and 5 wt % V_2O_5 a small but significant negative band at 1030 cm^{-1} is present. This negative band is more pronounced in the spectrum of 9.4 wt % at 1032 cm^{-1} , whereas at 15.3 wt % the negative signal is shifted to 1034 cm^{-1} . The band position points to the presence of an extremely short $V=O$ bond length in dry samples. The band disappears upon reaction with water. This reaction was found to be reversible.

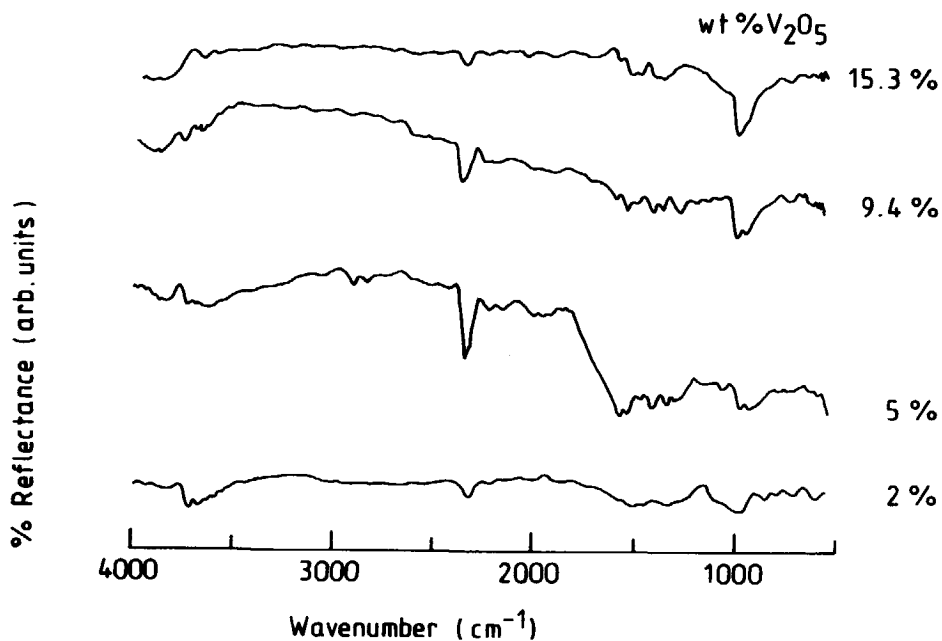


Figure 4. DRIFT spectra of dried samples with different vanadate coverages on $\gamma\text{-Al}_2\text{O}_3$.

The bands in the range from 1500 cm^{-1} to 1800 cm^{-1} are ascribed to the presence of adsorbed water, apparently increasing at increasing vanadate coverage.

Discussion

At all vanadate coverages, the ^{51}V NMR spectra point to the presence of low-coordinated, probably tetrahedrally surrounded, vanadate structures. EXAFS measurements, performed by Haber *et al.* [9], confirm tetrahedral

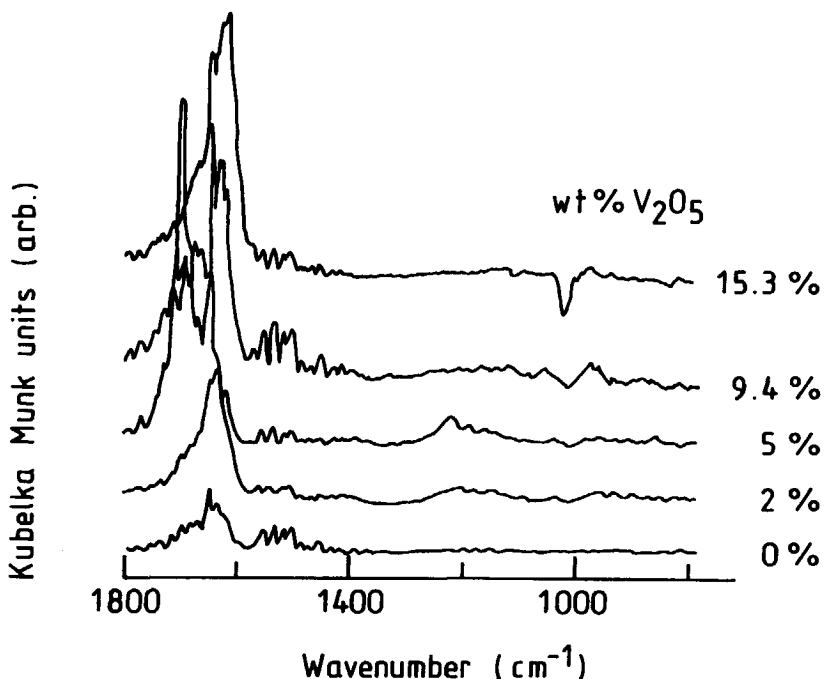


Figure 5. DRIFT spectra of moisted samples with different vanadate coverages on $\gamma\text{-Al}_2\text{O}_3$; the spectra of dried samples were subtracted.

coordination. At monolayer coverage, a dimeric, distorted, tetrahedrally surrounded vanadate structure on $\gamma\text{-Al}_2\text{O}_3$ is proposed, whereas on $\text{TiO}_2(\text{a})$ an analogous but monomeric unit is present (Fig. 6, a). Also a ^{51}V NMR study by Eckert and Wachs [12] points to the presence of tetrahedrally coordinated vanadate. They proposed the presence of chains of polymeric metavanadate.

As is confirmed by ^{51}V NMR, at 2 wt % V_2O_5 , the tetrahedrally coordinated vanadate compound is extremely sensitive to dehydration, and without water an asymmetrical structure results. Dehydration appeared to be

- 3. Vanadate monolayers -

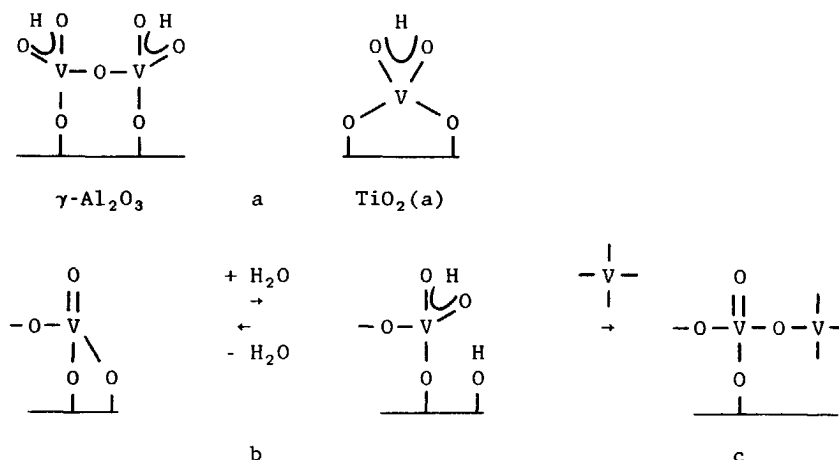


Figure 6. Structures of supported vanadate. a: according to Haber (EXAFS) [9]; b: proposed reaction of a vanadyl group with water; c: proposed vanadate structures formed at increasing coverages, up to monolayer.

reversible.

At increasing coverages the sensitivity to the removal of water decreases. The V-O-H site on vanadium, formed after coordination with water, is probably occupied by a V-O-V unit at higher coverages. In that case the reaction sketched in Fig. 6, b, may occur. This means that isolated (monomeric or dimeric) units, which are present at a low coverage and are sensitive to coordination by water, become interconnected by addition of vanadate. In this way, one- or two-dimensional vanadate structures are formed on the surface of the alumina, which are no longer able to take up water molecules. The same was described by Eckert and Wachs [12]. The coordination of vanadate at coverages around 3 V atoms.nm⁻², ascribed to a one-dimensional tetrahedrally surrounded metavanadate structure, was reported to be insensitive to hydration.

If the above view is correct, both at increasing coverage and at a decreasing water content an increase of the number of V=O groups is to be expected, as depicted in Fig. 6.

This view is confirmed by DRIFT. The V=O frequency, present at 1019 cm⁻¹ in crystalline V₂O₅, is absent in the spectra of the moistened samples with 5 wt % and 9.4 wt % V₂O₅ (Fig. 3), but the peak maximum shifts to higher

wave numbers at 15.3 wt % V_2O_5 . In the spectra of dried samples, this positive effect of increasing coverage on the intensity of the V=O frequency is more pronounced, as is clearly shown in Fig. 4.

The influence of water on the vanadium environment is shown in Fig. 5. During wetting of thoroughly dried samples, a band, at 1030 cm^{-1} (2 wt % V_2O_5) or at 1034 cm^{-1} (15.3 wt % V_2O_5), disappeared. This is due to the reaction of a V=O group, with an extremely short bonding length, with water, probably accompanied by the formation of two V-O bonds of the order 1.5, as shown in Fig. 6. In the case of $TiO_2(a)$ supported vanadate an extremely short V=O bond, corresponding to a RAMAN band at 1030 cm^{-1} , was found by Wachs *et al.* [14]. The broad DRIFT bands at about 987 cm^{-1} in the spectra of the 9.4 wt % and 15.3 wt % V_2O_5 samples in Fig. 5 and at 973 cm^{-1} in the spectra of 5 wt % and 9.4 wt % in Fig. 3 may be ascribed to the V-O bonds of the order 1.5. However, in Fig. 5 the bonds are weak, probably due to broadening of the band as a result of the occurrence of resonance structures.

Conclusions

Summarizing, in all thoroughly dried $\gamma\text{-Al}_2\text{O}_3$ supported vanadate samples V=O groups with an extremely short bond and with wave numbers of from 1030 cm^{-1} to 1034 cm^{-1} are present. These vanadyl groups react reversibly with water, probably resulting in two V-O bonds of the order 1.5.

At 2 wt % V_2O_5 on $\gamma\text{-Al}_2\text{O}_3$, mainly isolated (monomeric or dimeric), probably tetrahedral vanadate units are present. These units can bind water reversibly, in which process the vanadate coordination is strongly altered.

At increasing vanadate coverage, up to 15.3 wt % V_2O_5 , increasing amounts of one- or two-dimensional, but still low-coordinated (probably tetrahedral) vanadate structures are formed, corresponding to an increase of the number of V=O groups. At coverages above 5.3 wt % V_2O_5 water reacts with the vanadate, but without a significant change in vanadate coordination.

Vanadate structures as depicted in Fig. 6 may account for these observations.

References

1. P.J. Gellings, *Catal.*, 7 (1985) 105.
2. A. Miyamoto, K. Mori, M. Inomata and Y. Murakami, *Proc. 8th Int. Congr. Catal. (Berlin)*, 4 (1984) 285; J. Kijenski, A. Baiker, M. Glinski, P. Dollenmeyer and A. Wokaun, *J. Catal.*, 101 (1986) 1.
3. E.T.C. Vogt, A. Boot, A.J. van Dillen, J.W. Geus, F.J.J.G. Janssen and F.M.G. van den Kerkhof, *J. Catal.*, 114 (1988) 313; M. Inomata, A. Miyamoto and Y. Murakami, *J. Catal.*, 62 (1980) 140.
4. M.A. Chaar, D. Patel, M.C. Kung and H.H. Kung, *J. Catal.*, 105 (1987) 483; M.A. Chaar, D. Patel and H.H. Kung, *J. Catal.*, 109 (1988) 463; M. DelArco, M.J. Holgado, C. Martin and V. Rives, *J. Mater. Sci. Lett.*, 6 (1987) 616.
5. J.J.F. Scholten and P.J. van der Steen, European Patent Specification 0210705, d.d. 22.03.1989; E. van der Heide, M. de Wind, A.W. Gerritsen and J.J.F. Scholten, *Proc. 9th Int. Congr. Catal. (Calgary)*, 4 (1988) 1648; E. van der Heide, J.A.M. Ammerlaan, A.W. Gerritsen and J.J.F. Scholten, *J. Molec. Catal.*, 55 (1989) 320; E. van der Heide, J. Schenk, A.W. Gerritsen and J.J.F. Scholten, *Recl. Trav. Chim. Pays-Bas*, 109 (1990) 93.
6. F. Roozeboom, T. Fransen, P. Mars and P.J. Gellings, *Z. Phys. Chem., Neue Folge*, 111 (1978) 215.
7. G. Bergeret, P. Gallezot, K.V.R. Chary, B.R. Rao and V.S. Subrahmanyam, *Appl. Catal.*, 40 (1988) 191.
8. S. Yoshida, T. Tanaka, Y. Nishimura, H. Mizutani and T. Funabiki, *Proc. 9th Int. Congr. Catal. (Calgary)*, (1988) 1473.
9. J. Haber, A. Kozlovska and R. Kozlovsky, *J. Catal.*, 102 (1986) 52.
10. G. Busca, *Langmuir*, 2 (1986) 577.
11. G.C. Bond, J.P. Zurita, S. Flamerz, P.J. Gellings, H. Bosch, J.G. van Ommen and B.J. Kip, *Appl. Catal.*, 22 (1986) 361.
12. H. Eckert and I.E. Wachs, *J. Phys. Chem.*, 93 (1989) 6796.
13. F. Roozeboom, T. Fransen, P. Mars and P.J. Gellings, *Z. Anorg. Allg. Chem.*, 499 (1979) 25.
14. I.E. Wachs, J.M. Jehng and F.D. Hardcastle, *Solid State Ionics*, 32/33 (1989) 904.

Kinetics and mechanism of the gas phase oxidation of ethylene to acetaldehyde over a new heterogenized surface-vanadate Wacker catalyst

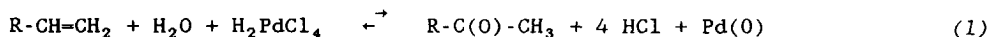
Evert van der Heide, Menno de Wind, Albert W. Gerritsen and Joseph J.F. Scholten.

Abstract

A study has been made of the kinetics and mechanism of the oxidation of C_2H_4 to CH_3CHO over new heterogeneous monolayer-vanadate Wacker catalysts in the temperature range from 348 to 393 K and at 0.11 MPa total pressure. The stability of such catalysts appears to be much higher than that of older types [1,2], consisting of large V_2O_5 particles on an $\alpha-Al_2O_3$ support. The kinetics of the reaction with respect to the dependency of the rate of reaction on the partial pressures of C_2H_4 , O_2 and H_2O as well as on the surface Pd and HCl concentrations is logically related to the kinetics of the homogeneous Wacker process. From XPS/AES analysis of spent catalysts it follows that deactivation is probably caused by the gradual increase of the ratio $Pd(0) / H_2PdCl_4$ on the surface. Besides $\gamma-Al_2O_3$, also ZrO_2 and TiO_2 (rutile and anatase) supported catalysts have been investigated. Anatase-based catalysts appeared to exhibit the highest activity. Replacing HCl by LiCl is possible and leads to a more stable catalyst.

Introduction

In the homogeneous Wacker oxidation alkenes are oxidized to the corresponding aldehydes or ketones by an aqueous solution of H_2PdCl_4 in excess HCl (eq. (1)):



This overall reaction is built up of at least four elementary steps and it has been shown that $\text{PdCl}_3\text{.CH}_2\text{=CH-R}$ is the proper catalyst [3]. Precipitation of Pd(0) in the form of palladium-black is eliminated by continuous oxidation of Pd(0) to Pd(II) by oxygen, making use of the redox couple Cu(I)/Cu(II) [4].

Technical disadvantages of the homogeneous Wacker process are the highly corrosive properties of the excess HCl in combination with oxygen, the unwanted formation of chlorinated byproducts and the difficulty of separation of the products from the aqueous reaction mixture when starting from C_3 or higher alkenes. Attempts to circumvent these difficulties have been undertaken by replacing the Cu(I)/Cu(II) redox couple by $\text{V}_2\text{O}_4/\text{V}_2\text{O}_5$, along with heterogenizing the catalyst by attachment of V_2O_5 crystallites to the surface of porous α -alumina [1,2]. Such catalysts appear to be active indeed, but suffer from deactivation in relatively short periods.

In the present paper we report on the preparation and performance of new stable heterogenized Wacker catalysts [5,6] and discuss the mechanism and kinetics of ethylene oxidation to acetaldehyde.

Experimental

Chemicals.

O_2 , N_2 and C_2H_4 (in cylinders) were obtained from Air Products (U.S.A.). These gases were of high purity except O_2 , which was industrial grade. H_2O was distilled twice. PdCl_2 , analytical grade, was obtained from Drijfhout (The Netherlands). HCl and H_2SO_4 , analytical grade, were purchased from Baker (The Netherlands). NH_4VO_3 , also analytical grade, was purchased from

- 4. Ethylene oxidation -

Merck (F.R.G.). γ -Al₂O₃, type 000-3P, S(BET) = 250 m².g⁻¹, was supplied by Akzo (The Netherlands) and TiO₂ (anatase) type CRS 31 LOT 2, S(BET) = 127 m².g⁻¹, was obtained from Rhône Poulenc (France). α -Al₂O₃, from Rhône Poulenc, type SCS-9, had a BET surface area of 6.2 m².g⁻¹ and ZrO₂, type 0304 T 1/8, S(BET) = 57 m².g⁻¹, was obtained from Harshaw (The Netherlands) and contained 2 % Al₂O₃.

Apparatus.

The catalytic performance has been studied in a continuous-flow fixed-bed stainless-steel reactor, internal diameter 1 cm and length 10 cm, at a total pressure of 0.11 MPa and in the temperature range 348 to 393 K. The composition of the feed was regulated by means of mass-flow controllers (Inacom, The Netherlands) and all gases were dried over molecular sieves. Water was dosed to the feed by leading finely divided bubbles of nitrogen through a thermostatted flask filled with water. Off-gas analysis was performed gas chromatographically, applying a Porapak QS column, length 100 cm, diameter 3 mm, at 423 K. Peak areas were recorded and integrated by a micro computer (Digital LCI 11/03, U.S.A.).

Surface analysis was carried out in a Leybold-Heraeus (F.R.G.) type LHS-10 XPS/AES apparatus. A MgK α excitation source (energy 1253.6 eV) was applied at the operating conditions of 13 kV and 20 mA. Spectral lines were compared with standard values [7,8]. Samples were pretreated in vacuo at 393 K in a preparation chamber connected to the XPS/AES chamber via a valveless UHV lock.

Catalyst preparation.

The γ -Al₂O₃ pellets were crushed and sieved to particle diameters from 425 to 500 μ m. By leading an NH₄VO₃ solution of pH = 4 at 343 K over these particles, following the method described by Roozeboom [9], the surface was covered with a vanadate monolayer. Then the particles were calcined in air at 673 K for 4 h. From titration with Fe(II) the vanadium coverage was found to correspond to 3.9 vanadium atoms per nm². Next, through impregnation to incipient wetness with a solution of H₂PdCl₄, followed by drying at 353 K, the alumino vanadate layer was covered by a sub-monolayer of the Pd compound. The final Pd/V ratio was varied between 0.009 and 0.4. These types of catalyst are coded A.

- 4. Ethylene oxidation -

In preparing TiO₂(anatase)-based catalysts the same procedure was followed as in the case of γ -Al₂O₃, except for the temperature and duration of vanadium monolayer deposition, viz. 293 K and 4 h. A vanadium coverage of 4.7 vanadium atoms per nm² was arrived at.

Rutile, prepared by heating anatase for 5 hrs at 1273 K in air, had a S(BET) of 3.1 m².g⁻¹. The vanadate monolayer and the Pd complex were placed upon the carrier as mentioned for γ -Al₂O₃, a coverage of about 4 V atoms. nm⁻² being arrived at.

A ZrO₂ based catalyst was prepared in the same manner as the γ -Al₂O₃ based types, the final V coverage being 2.3 atoms.nm⁻².

In order to compare its stability with that of our alumino vanadate monolayer catalysts a V₂O₅-on- α -alumina catalyst (catalyst B) was prepared, following the procedure prescribed by Evnin [1], except for the final calcination procedure, which was omitted. No improvement of the stability of these catalysts by calcination was found [6].

Results and discussion

For the homogeneous Wacker oxidation the kinetic equation is as follows (eq. (2)):

$$r = k \cdot \frac{[\text{PdCl}_4^{2-}][\text{C}_2\text{H}_4]}{[\text{H}^+][\text{Cl}^-]^2} \quad (2)$$

Fig. 1 presents an intercomparison between the stabilities and activities of catalyst types A and B in the oxidation of ethylene to acetaldehyde, and clearly shows the comparable initial activities of the catalysts, calculated per Pd atom, and the appreciably higher stability of the surface vanadate types. Replacing HCl by LiCl (catalyst A2) leads to perfect stability; after a 5 days run no sign of deactivation was observed.

The kinetics with respect to the partial pressures of C₂H₄ and of O₂ is summarized in Fig. 2. The observed zeroeth order in O₂ pressure points to a redox equilibrium, presumably $\text{V}_2\text{O}_4 + \frac{1}{2} \text{O}_2 \rightleftharpoons \text{V}_2\text{O}_5$, being shifted strongly to the right and the reoxidation of Pd(0) to Pd(II) not being rate

- 4. Ethylene oxidation -

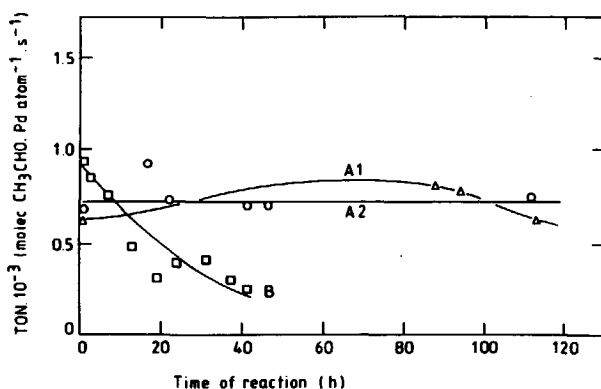


Figure 1. Turnover numbers as a function of time, applying catalyst types A and B. Conditions: Temp. 373 K; total pressure 0.11 MPa; feed composition: 1 % C_2H_4 , 6.6 % H_2O , 18.5 % O_2 , 73.9 % N_2 . Flow rate: $1.67 \text{ cm}^3(\text{STP}) \cdot \text{s}^{-1} \cdot \text{g cat}^{-1}$. Initial C_2H_4 conversion per pass: cat A1: 9.1 % (1 g of catalyst; 86.6 mol% Al_2O_3 , 7.6 mol% V_2O_5 , 1.0 mol% $PdCl_2$, 4.9 mol% HCl), cat A2: 9.4 % (1 g of catalyst; as A1, but HCl replaced by $LiCl$); cat B: 0.8 % (1.6 g of catalyst; 99.5 mol% Al_2O_3 , 0.3 mol% V_2O_5 , 0.02 mol% $PdCl_2$, 0.12 mol% HCl).

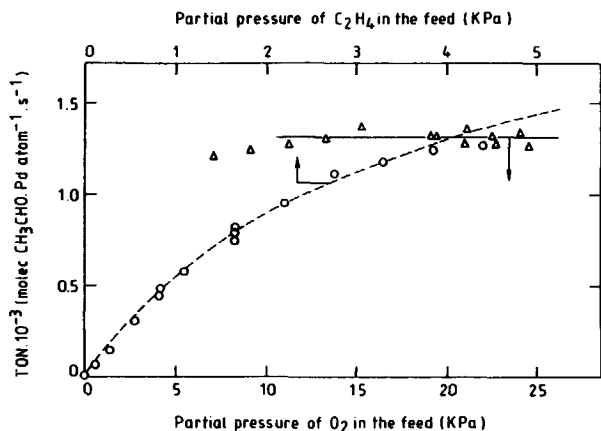


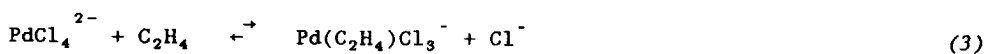
Figure 2. TON as a function of partial pressures of C_2H_4 and of O_2 for catalyst A1. Conditions: 1 g of catalyst; total pressure 0.11 MPa; flow rate $1.67 \text{ cm}^3(\text{STP}) \cdot \text{s}^{-1} \cdot \text{g}^{-1}$. Composition of the feed for C_2H_4 measurement: (temp. 373 K) 6.3 % H_2O , 18.3 % O_2 , 75.2 % gas of variable C_2H_4/N_2 ratio. In the O_2 measurement: (temp. 393 K) 1 % C_2H_4 , 13.5 % H_2O , 85.5 % gas of variable O_2/N_2 ratio. Dashed line: theoretical course of TON as a function of the C_2H_4 pressure, following Langmuir kinetics.

- 4. Ethylene oxidation -

determining. At too low an O₂ pressure a slow irreversible deactivation of the catalyst is found.

As is well known, in the classical homogeneous Wacker process the rate is first order in C₂H₄ pressure, according to eq. (3). Interestingly, in the heterogeneous case we are dealing with here, a Langmuir-type pressure dependency is observed, the rate being initially first order in C₂H₄ pressure and gradually decreasing at higher pressures, indicating an increasing saturation of the surface Pd complexes with C₂H₄.

In Fig. 3 the TON at 373 K is plotted as a function of the H₂O coverage. The relation between the partial pressure of water and $\theta(\text{H}_2\text{O})$ has



been determined in a separate experiment in which the water adsorption isotherm was measured volumetrically at 293 K. The isotherm could be

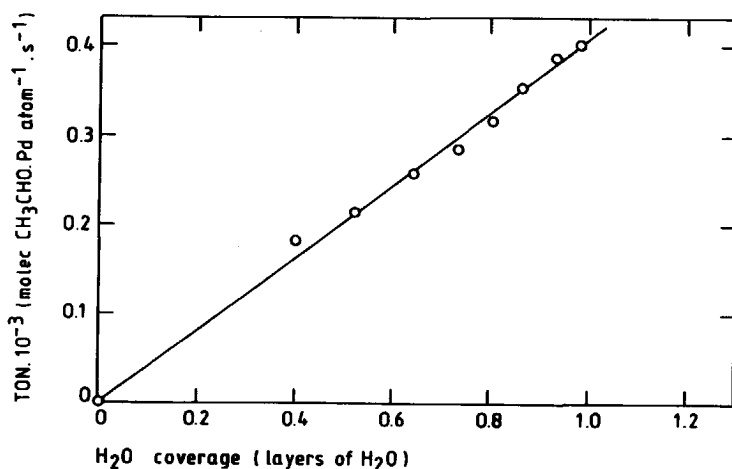
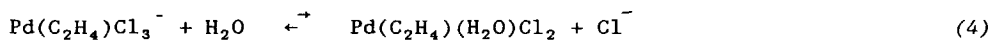


Figure 3. TON as a function of the water surface concentration for catalyst A1. Conditions: 1 g of catalyst; temp. 373 K; pressure 0.11 MPa; flow rate 1.67 cm³(STP) · s⁻¹ · g⁻¹. Composition of the feed: 1 % C₂H₄, 18 % O₂, 81 % gas of variable H₂O/N₂ ratio.

described by the BET equation and a C-value of 12 was found. Being reactant, water plays an important role in the kinetics. In the homogeneous process, H₂O is available in excess and the H₂O concentration dependency is



expected to be zero order. But with heterogeneous operation, as is the case here, a first order relation between TON and $\theta(\text{H}_2\text{O})$ is according to expectation. This means that equilibrium (4) is positioned strongly on the left-hand side and hence shifts to the right proportionally to $\theta(\text{H}_2\text{O})$.

In Fig. 4 the TON is plotted as a function of the surface concentration of the palladium complex for three different surface concentrations of chlorine anions. As was to be expected, a linear relationship is found in all three cases, but as soon as the palladium to chlorine concentration ratio becomes too high a strong deviation from linearity is observed. This

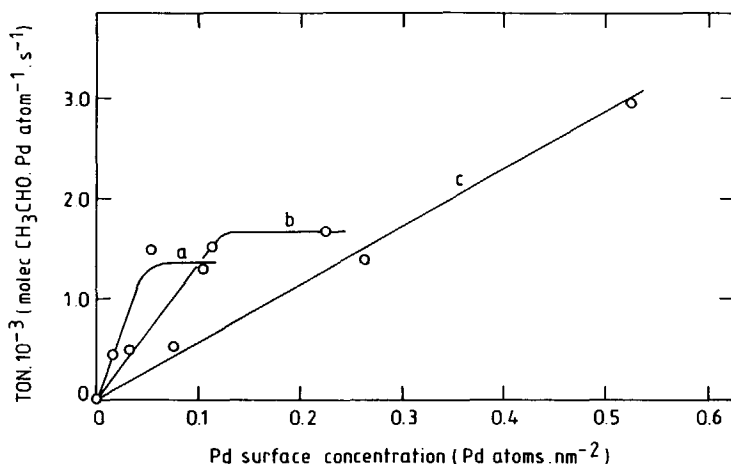


Figure 4. TON as a function of the Pd surface concentration for catalysts of type A. Conditions as indicated in the legend of Fig.1. Surface Cl^- concentration: curve a: $0.31 \text{ Cl}^- \text{ ions} \cdot \text{nm}^{-2}$, curve b: $0.67 \text{ Cl}^- \text{ ions} \cdot \text{nm}^{-2}$, curve c: $1.57 \text{ Cl}^- \text{ ions} \cdot \text{nm}^{-2}$.

is probably due to the influence of the chlorine/palladium ratio on the electric potential of the $\text{Pd}(0)/\text{Pd}(\text{II})$ redox couple. Upon lowering of the amount of chlorine this potential increases and at a certain concentration ratio the $\text{V}(\text{IV})/\text{V}(\text{V})$ redox couple has too low an electric potential to reoxidize $\text{Pd}(0)$.

Fig. 5 presents the TON as a function of the surface chlorine anion concentration at a surface Pd concentration of $0.22 \text{ Pd atoms} \cdot \text{nm}^{-2}$. The H^+

- 4. Ethylene oxidation -

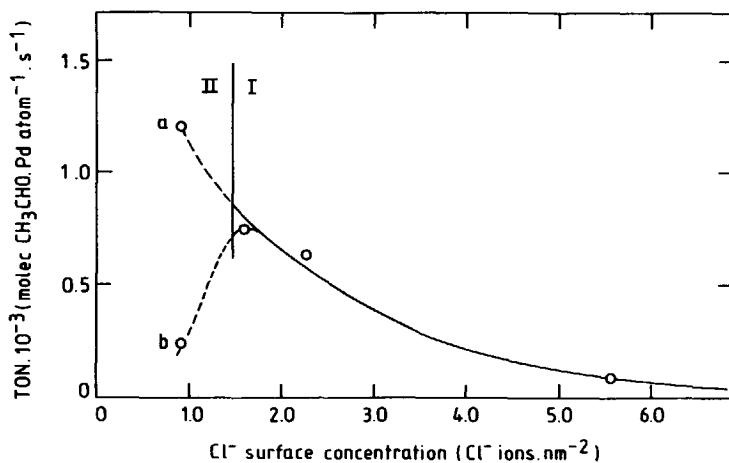


Figure 5. TON as a function of the HCl surface concentration for catalysts of type A. Conditions as indicated in the legend of Fig.1. Surface Pd concentration: $0.22 \text{ Pd atoms.nm}^{-2}$; curve a: initial activity, curve b: stabilized activity.

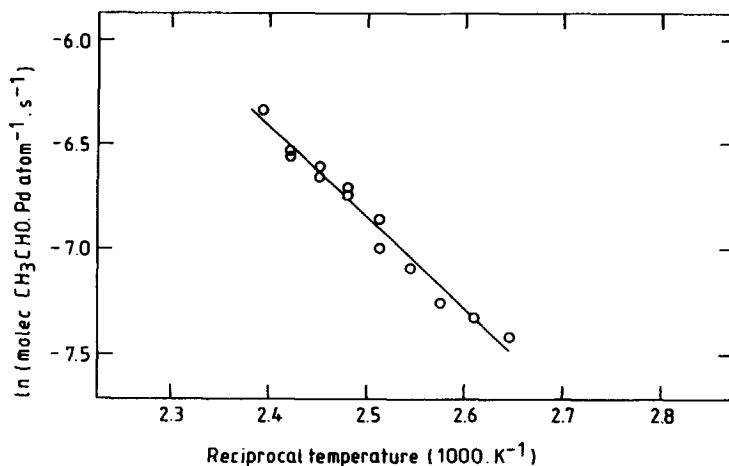
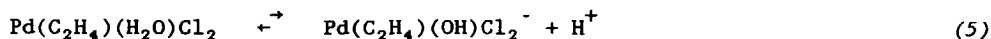


Figure 6. Arrhenius plot for ethylene oxidation over catalyst A1. Conditions: 1 g of catalyst; total pressure 0.11 MPa; flow rate $1.67 \text{ cm}^3(\text{STP}).\text{g}^{-1}.\text{s}^{-1}$. Composition of the feed: 1 % C_2H_4 , 19 % O_2 , 80 % gas of variable $\text{H}_2\text{O}/\text{N}_2$ ratio; $\text{P}/\text{Po}(\text{H}_2\text{O}) = 0.050$.

- 4. Ethylene oxidation -

concentration also changes and follows the chlorine anion concentration by the equation $H^+ = Cl^- - 2 * Pd^{2+}$ ions.nm⁻². With increasing HCl/Pd ratio, to the right of the vertical line in the figure, indicated by I, a negative order varying from about -1 to less than -2 (calculated from a double-logarithmic plot) indicates an increasing inhibiting effect by HCl. In the homogeneous case, in accordance with eqs. (3), (4) and (5), a total order



for H⁺ and Cl⁻ of -3 is observed, but with our heterogeneous types of catalyst a lower inhibiting effect by HCl is observed at lower Cl/Pd ratios.

At the left-hand side of the vertical line in Fig. 5, indicated by II, the catalysts suffer from deactivation; both initial and stabilized

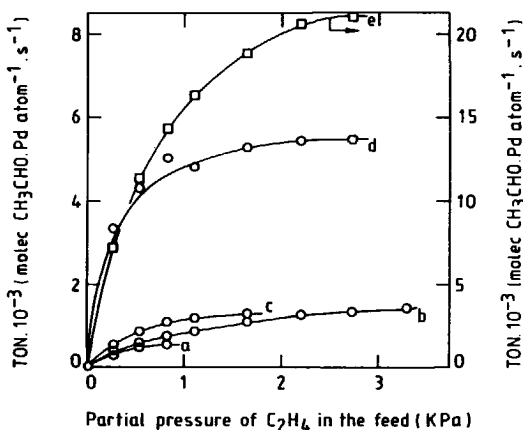


Figure 7. TON as a function of the C₂H₄ pressure for catalysts based on different carriers. Conditions: temp. 373 K; total pressure 0.11 MPa. Feed composition: 6.3 % H₂O, 18.3 % O₂, 75.2 % gas of variable C₂H₄/N₂ ratio. Flow rate: 1.67 cm³.s⁻¹. Surface concentrations: 0.22 Pd atoms.nm⁻², 1.54 Cl⁻ ions.nm⁻². Catalysts: curve a: α-Al₂O₃, 1.6 g of cat B; curve b: γ-Al₂O₃, 1 g of cat A1; curve c: ZrO₂, 3.5 g of catalyst consisting of 96.5 mol% ZrO₂, 1.3 mol% V₂O₅, 0.4 mol% PdCl₂, 1.8 mol% HCl; curve d: TiO₂(r), 2 g of catalyst consisting of 99.8 mol% TiO₂, 0.08 mol% V₂O₅, 0.01 mol% PdCl₂, 0.06 mol% HCl; curve e: TiO₂(a), temp. 348 K, 0.22 g of catalyst consisting of 94.4 mol% TiO₂, 3.6 mol% V₂O₅, 0.34 mol% PdCl₂, 1.7 mol% HCl. The TON values are given on the left scale except for curve e.

activities are shown. For the homogeneous system a similar effect is observed by Jira [10] and possibly in his case deactivation also occurs.

Fig. 6 presents the Arrhenius plot of the TON of catalyst Al at constant H₂O coverage. From the slope an apparent activation energy of 36 kJ.mol⁻¹ is calculated.

Carriers other than γ -Al₂O₃ take up a vanadate monolayer as well. In Fig. 7 TON values as a function of the partial ethylene pressure are presented for catalysts based on α -Al₂O₃ (no vanadate monolayer formed), γ -Al₂O₃, ZrO₂ and TiO₂ (both rutile and anatase). About equal activities per Pd atom are observed, pointing to the absence of an important influence of a change in the chemical nature of the surface redox system on the rate of reaction. Rutile and anatase, however, are the exceptions, the activities respectively being a factor of about 3 and 20 higher at even lower temperature. The reason for this behaviour is not clear. An exceptional behaviour of vanadate on anatase was found in many catalytic reactions, e.g. the selective oxidation of o-xylene to phthalic anhydride over vanadate monolayer catalysts [11].

A γ -Al₂O₃-based catalyst was analyzed by XPS/AES after a 5-days run, when the activity had decreased to about 50 % of the initial activity. Formation of Pd(0) up to 30 - 50 % of the initial Pd(II) concentration is found. Obviously this is at least one of the causes of deactivation, which may perhaps be suppressed by maintaining the surface Cl⁻ concentration at a constant level. The Cl⁻/Pd(II) ratio, derived from this and other XPS/AES measurements, in all cases equals or exceeds a value of 4, so the presence of catalytically active surface PdCl₄²⁻ complexes cannot be excluded, being more probable than the surface Pd compound as proposed by Evnin [1] and Forni [2].

Conclusions

In the heterogeneous case the order in C₂H₄ pressure clearly deviates from 1, and shows a variable value to be described by a Langmuir adsorption isotherm, in accordance with expectation (energetic equivalence of the Pd-sites).

An interesting new variable in the heterogeneous case is the influence of the water vapour pressure on the kinetics. First order in H_2O coverage was found, which is likely to be due to a shift of equilibrium (4) from strongly to the left more to the right.

The influence of the H^+ and Cl^- surface concentrations is complicated (see results), but not contrary to what is to be expected according to equilibria (3), (4) and (5). Deviations from the -2 order in $[Cl^-]$ and -1 order in $[H^+]$ upon lowering of the HCl concentration are also reported for the homogeneous case by Jira *et al.* [10].

From our study no indications are found of a reaction mechanism deviating essentially from the classical homogeneous mechanism. The question whether we are dealing with a direct chemical bond between the Pd complexes and the redox system, as is the case with $CuCl_2$ [12] and has been suggested for V_2O_5 [1], remains to be studied.

From a technological point of view a further development of our heterogeneous catalyst is important for two reasons: the corrosion problem ($HCl + O_2$) is largely absent and heterogeneous catalysts offer the possibility of oxidation of higher alkenes.

From our results it follows that the electric potential of the surface vanadate redox couple is high enough to reoxidize Pd(0). The reoxidation rate should be high enough as well. Higher stability under milder conditions may be achieved for instance by replacing HCl by LiCl. Further work is in progress.

References

1. A.B. Evnin, J.A. Rabo and P.H. Kasai, *J. Catal.*, **30** (1973) 109-117.
2. L. Forni and G. Terzoni, *Ind. Eng. Chem. Process Des. Dev.*, **16** (1977) 288.
3. P.M. Henry, *J. Am. Chem. Soc.*, **86** (1964) 3246-3250.
4. J. Smidt, W. Hafner, R. Jira, J. Sedlmeier, R. Sieber, R. Ruttinger and H. Kojer, *Angew. Chem.*, **71** (1959) 176-182.
5. J.J.F. Scholten and P.J. van der Steen, European Patent Specification 0210,705, d.d. 22.03.1989.

- 4. Ethylene oxidation -

6. P.J. van der Steen, *Thesis*, University Press, Delft, 1987.
7. G. Kumar, J.R. Blackburn, R.G. Albridge, W.E. Moddeman and M.M. Jones, *Inorg. Chem.*, 11 (1972) 296-300.
8. K.S. Kim, A.F. Gossmann and N. Winograd, *Anal. Chem.*, 46 (1974) 197-200.
9. F. Roozeboom, T. Fransen, P. Mars and P.J. Gellings, *Z. Anorg. Allg. Chem.*, 449 (1979) 25-40.
10. R. Jira, J. Sedlmeier and J. Smidt, *Ann.*, 693 (1966) 99-108.
11. M.S. Wainwright and N.R. Foster, *Catal. Rev.*, 19 (1979) 211-292.
12. P.M. Henry: *Palladium Catalyzed Oxidation of Hydrocarbons*, Reidel, Dordrecht, The Netherlands, (1980) 43, 128.

Kinetics and mechanism of the gas phase oxidation of 1-butene to butanone over a new heterogenized surface-vanadate Wacker catalyst

Evert van der Heide, Jan A.M. Ammerlaan, Albert W. Gerritsen and Joseph J.F. Scholten.

Abstract

A study has been made of the kinetics and mechanism of the oxidation of 1-butene to methyl-ethyl-ketone (MEK) over a new heterogeneous vanadate-monolayer Wacker catalyst, in the temperature range of 363 to 408 K and at 0.11 MPa total pressure. The kinetics of the reaction with respect to the dependency of the reaction rate on the partial pressures of 1-butene and of water, as well as on the surface Pd and NaCl concentrations, is logically related to the kinetics of the homogeneous Wacker process. At 10 % conversion, the main product (MEK) is formed with 80 - 95 % selectivity. The formation of byproducts, including crotonaldehyde, acetone, acrolein, acetaldehyde and acetic acid, has been studied and a reaction scheme developed.

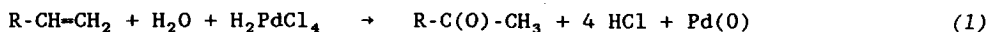
From an XPS/AES analysis of spent catalysts, it follows that deactivation is probably caused by a gradual decrease of the chlorine surface concentration. Compensation for the loss of chlorine by adding HCl to the deactivated catalyst leads to a partly regenerated catalyst.

Replacing the PdCl₂/NaCl sub-monolayer by PdSO₄/H₂SO₄ leads to a stable catalyst.

Introduction

Nowadays the oxidation of 1-butene to butanone (methyl ethyl ketone, MEK) is performed commercially by H₂SO₄-catalyzed hydroxylation of the alkene, followed by dehydrogenation to the corresponding ketone over a Cu-Zn catalyst [1]. The first process step, leading to the butane sulphate ester, is a corrosive one. Moreover, the Cu-Zn dehydrogenation catalyst suffers from deactivation by H₂O. A one-step oxidation of 1-butene to MEK would be more attractive, and attempts to reach this have been reported. Most of these, but not all of them [2], are based on Wacker oxidation.

In homogeneous Wacker oxidation, terminal alkenes can be oxidized to the corresponding methyl ketones by a solution of H₂PdCl₄ in excess HCl (eq. (1)):



Precipitation of Pd(0) in the form of palladium black is avoided by the continuous oxidation of Pd(0) to Pd(II) by oxygen, making use of the Cu(I)/Cu(II) redox couple [3].

The technical disadvantages of the homogeneous Wacker process are the highly corrosive properties of the excess HCl in combination with oxygen, the unwanted formation of chlorinated byproducts and the difficulty of separating the products from the aqueous reaction mixture when starting from C₃ or higher alkenes. Although a detailed process scheme has been developed for 1-butene oxidation [4], the process has never been commercialized because of the above mentioned disadvantages.

Attempts to circumvent these difficulties have been undertaken by replacing the CuCl/CuCl₂ redox couple by chlorine-free ones. A homogeneous catalyst based on PdSO₄ and a heteropolyacid (HPA) was reported by Davison [5] and further developed by Catalytica Associates (USA) by adding chlorine-free Cu(II) to the HPA-Pd(II)-solution [6].

From the viewpoint of the separation of products from the catalyst, a heterogeneous catalyst would be more attractive; such a catalyst based on a Pd-salt on active carbon was developed by Fujimoto [7]. A technical drawback is the mechanical weakness of carbon as a support. A catalyst consisting of V_2O_5 crystallites and dispersed $PdCl_2$ on an $\alpha-Al_2O_3$ support failed to oxidize butene [8].

In the present chapter we report on the performance of a new heterogeneous Wacker catalyst, in which a vanadium oxide redox component is molecularly dispersed on, and chemically bound to, the surface of a support ($\gamma-Al_2O_3$ or $TiO_2(a)$). This dispersed phase, in turn, is covered by a sub-monolayer of a palladium salt [9,10]. Furthermore we discuss the mechanism and kinetics of 1-butene oxidation to MEK.

Experimental

Chemicals

Oxygen, N_2 and 1-butene (in cylinders) were obtained from Air Products (U.S.A.). Nitrogen and 1-butene were of high purity and O_2 was of industrial grade. Water was distilled twice. $PdCl_2$ and $PdSO_4$, analytical grade, were obtained from Drijfhout (The Netherlands). HCl and H_2SO_4 , analytical grade, were purchased from Baker (The Netherlands). NH_4VO_3 , also analytical grade, was purchased from Merck (F.R.G.). $\gamma-Al_2O_3$, type 000-3P, $S(BET) = 250 \text{ m}^2 \cdot \text{g}^{-1}$, was supplied by Akzo (The Netherlands) and TiO_2 (anatase), type CRS 31 LOT 2, $S(BET) = 127 \text{ m}^2 \cdot \text{g}^{-1}$, was obtained from Rhône Poulenc (France).

Apparatus

The catalytic performance has been studied in a continuous-flow fixed-bed stainless steel reactor, internal diameter 1 cm and length 10 cm, at a total pressure of 0.11 MPa and over the temperature range 363 - 393 K. All gases were dried over molecular sieves and the composition of the feed was regulated by means of mass-flow controllers (Inacom, The Netherlands). Water was dosed to the feed by leading finely divided bubbles of nitrogen through a thermostatted flask filled with water. Off-gas analysis was performed gas chromatographically, applying a Porapak QS column, length 100 cm, diameter 3

mm, at 453 K. Peak areas were recorded and integrated by a microcomputer (Digital LCI 11/03, U.S.A.).

Surface element analysis was carried out in a Leybold-Heraeus (F.R.G.), type LHS 10 XPS/AES apparatus. A $MgK\alpha$ excitation source (energy 1253.6 eV) was applied under the operating conditions of 13 kV and 20 mA. Spectral lines were compared with standard values [11]. Samples were pretreated in vacuo at 393 K in a preparation chamber connected to the XPS/AES chamber via a valveless UHV lock.

A VG 70 SE-250 mass spectrometer was used for TPD-MS analysis (desorption from 313 K to 673 K, 50 K/min) and GC-MS analysis. In the latter case a capillary CP sil-5 column, length 25 m, was used.

Catalyst preparation

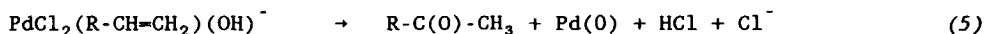
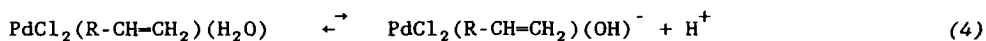
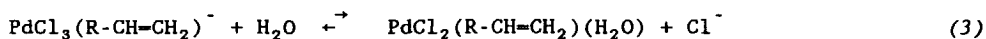
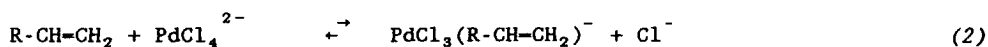
The γ - Al_2O_3 pellets were crushed and sieved to particles with diameters from 425 to 600 μm . By leading an NH_4VO_3 solution of pH = 4 at 343 K over these particles, following the method described by Roozeboom *et al.* [12], the surface was covered with an aluminovanadate monolayer. The particles were then calcined in air at 673 K for 4 hours. From titration with Fe(II) the vanadium coverage was found to correspond to 3.9 vanadium atoms per nm^2 . Next, through impregnation to incipient wetness with a solution of Na_2PdCl_4 (or another Pd(II) salt), followed by drying at 353 K, the aluminovanadate layer was covered by a sub-monolayer of the Pd compound. The catalyst, consisting of 0.33 mol % $PdCl_2$, 2.7 mol % NaCl, 8.1 mol % V_2O_5 and 88.9 mol % Al_2O_3 , is hereinafter designated as catalyst A.

The $TiO_2(a)$ pellets were also crushed and sieved to particles with diameters from 425 to 600 μm . The vanadate monolayer was prepared by wet impregnation of an NH_4VO_3 solution of pH = 4 for 16 hours at 293 K. A vanadium coverage of 4.7 vanadium atoms per nm^2 was arrived at. The catalyst, consisting of 0.47 mol % $PdCl_2$, 2.3 mol % HCl, 3.1 mol % V_2O_5 and 94.1 mol % $TiO_2(a)$ is hereinafter designated as catalyst B.

Results and discussion

Kinetics

Traditionally, the mechanism of homogeneous Wacker oxidation is believed to consist of three equilibria (eq. (2) - (4)) preceding the rate determining step (eq. (5)):



the last reaction consisting of at least three elementary steps.

The mechanism of the homogeneous Wacker oxidation of 1-butene

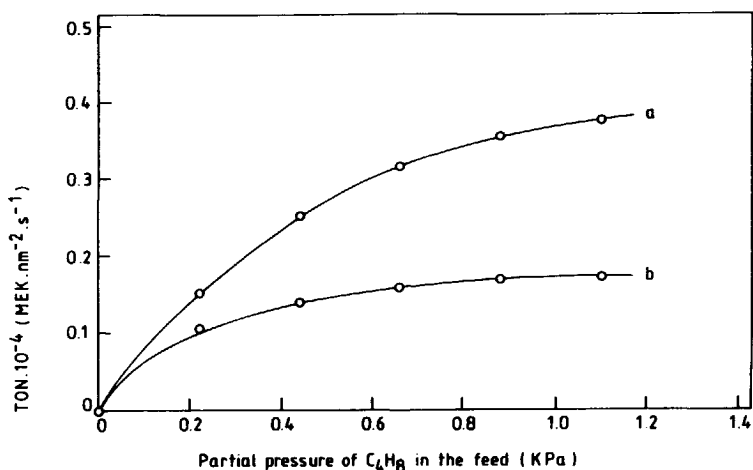


Figure 1. Turnover numbers as a function of the partial 1-butene pressure for two catalysts with different Pd coverages.

Curve a: 0.98 mol % PdCl₂; 7.84 mol % NaCl; 7.63 mol % V₂O₅; 83.55 mol % Al₂O₃. Curve b: catalyst A. Conditions: Temp. 373 K; total pressure 0.11 MPa; flow rate 0.56 cm³(STP)·s⁻¹·g⁻¹; 3 g of catalyst. Feed composition: 7.0 % H₂O; 18.4 % O₂; 74.6 % gas of variable C₄H₈/N₂ ratio.

corresponds to the oxidation mechanism of ethylene and the over-all kinetics are in accordance with the above mechanism (eq. (6)) [13]:

$$r = k \cdot \frac{[\text{PdCl}_4^{2-}][\text{C}_4\text{H}_8]}{[\text{H}^+][\text{Cl}^-]^2} \quad (6)$$

The kinetics of ethylene oxidation over our heterogeneous catalyst have been reported before [10]; they largely correspond to the homogeneous kinetics. The kinetics of butene oxidation with respect to the same variables will now be reported.

Fig. 1 represents the activity as a function of the partial butene pressure for two catalysts differing in Pd-coverage. Both curves are of the Langmuir type and correspond to eq. (2); from the derived Langmuir k-values first-order kinetics in the Pd coverage of the catalyst are found.

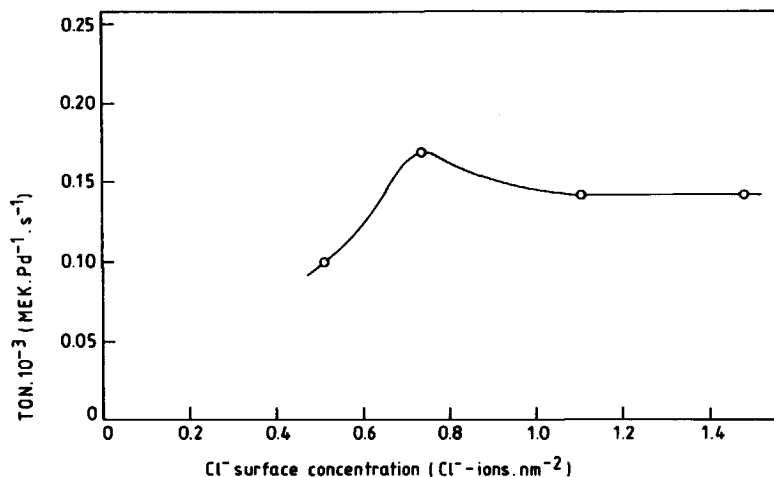


Figure 2. Turnover numbers as a function of the Cl⁻ surface concentration. Catalysts: 0.33 mol % PdCl₂; 1.65-5.94 mol % NaCl; mol % Al₂O₃/mol % V₂O₅ ratio is 10.95; Pd coverage 0.074 Pd(II) ions · nm⁻². Conditions as indicated in the legend of Fig 1; 1 % C₄H₈ in the feed.

The dependence of the reaction rate on the NaCl coverage is depicted in Fig. 2. The relationship is approximately the same as that found for ethylene oxidation, where the HCl coverage was varied [10]. At too low a NaCl coverage, the Cl/Pd ratio is unfavourable for the formation of the

catalytically active PdCl_4^{2-} -complexes, leading to a slight deactivation of the catalyst during the start up procedure, although a relatively stable level is reached thereafter. At increasing NaCl coverage, a maximum is reached and thereafter in accordance with eq. (6), retardation of the reaction rate by chloride is found. However, at $\text{Cl/Pd} > 15$ the decrease of the reaction rate ceases and no further influence of the NaCl coverage is detected.

This last result differs from the kinetics reported earlier when the amount of HCl instead of NaCl was varied [10], and is due to the constancy of NaCl coverage in the presence of non-adsorbed crystalline NaCl. From XRD analysis, the presence of a significant amount of crystalline NaCl on the catalyst only occurred when $\text{Cl/Pd} > 15$.

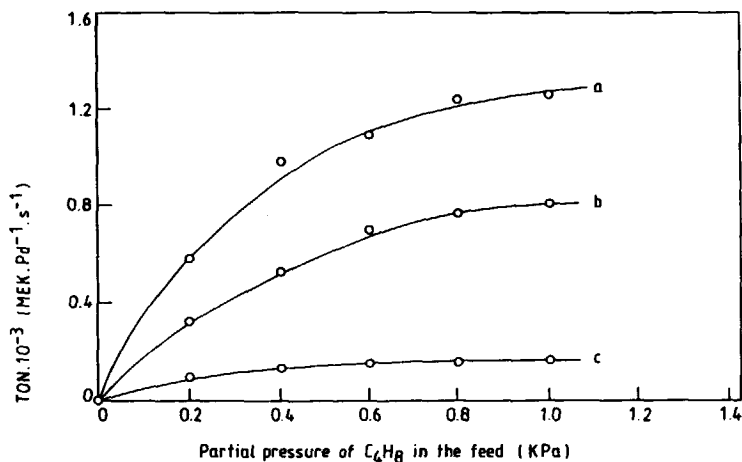


Figure 3. Turnover numbers as a function of the partial 1-butene pressure at three different H_2O partial pressures. Catalyst A. Conditions as indicated in the legend of Fig 1. Feed composition: curve a: 17.0 % H_2O ; 16.6 % O_2 ; 66.4 % gas of variable $\text{C}_4\text{H}_8/\text{N}_2$ ratio. Curve b: 12.0 % H_2O ; 17.6 % O_2 ; 70.4 % gas of variable $\text{C}_4\text{H}_8/\text{N}_2$ ratio. Curve c: 7.0 % H_2O ; 18.4 % O_2 ; 74.6 % gas of variable $\text{C}_4\text{H}_8/\text{N}_2$ ratio.

Measurements at three partial pressures of H_2O (Fig. 3) indicate that water has a positive influence on the reaction rate to ca. first order extent. This result is in accordance with the proposed homogeneous mechanism expressed in eq. (3), but cannot be measured in the homogeneous case because water as a solvent is present in high concentration. A first order

- 5. 1-Butene oxidation -

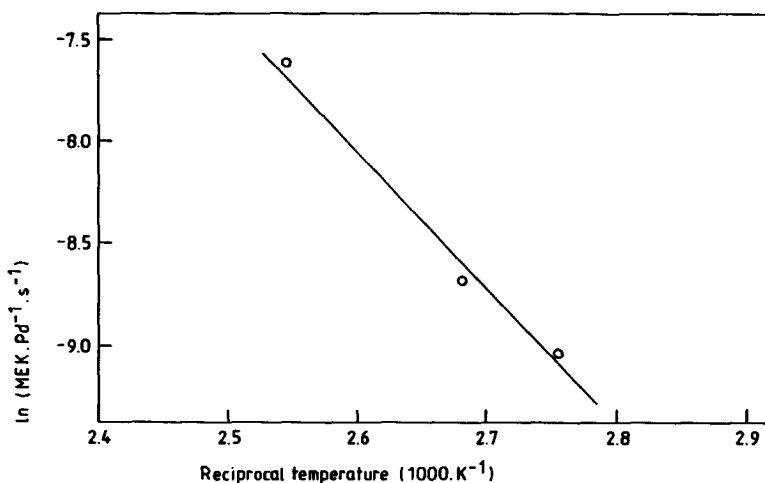


Figure 4. Arrhenius plot for butene oxidation. Catalyst A. Conditions as indicated in the legend of Fig 1 (except for the temperature); constant relative H₂O pressure P/P₀ = 0.07; 1 % C₄H₈ in the feed.

dependence of the kinetics on the H₂O coverage has been measured before in the heterogeneous oxidation of ethylene [10].

Fig. 4 depicts the Arrhenius plot obtained over the temperature range 363 - 393 K at a constant coverage with water. An apparent activation energy of 58 kJ.mol⁻¹ was calculated from this plot, whereas 36 kJ.mol⁻¹ was found in the case of ethylene [10].

Selectivity

During the oxidation of 1-butene over a γ -Al₂O₃ supported catalyst, formation of acetaldehyde and acrolein was observed in addition to MEK and when a TiO₂(a)-supported catalyst was used acetic acid, acetone and crotonaldehyde were also detected as byproducts.

The selectivities to these products as a function of conversion are depicted in Fig. 5. An increase in temperature has a strong negative influence on the selectivity to MEK, with such selectivity increasing with increasing time. When 1-butene was fed over a γ -Al₂O₃-V₂O₅ catalyst in the absence of the Pd sub-monolayer no reaction occurred, indicating that the vanadate monolayer shows no activity for the oxidation of 1-butene under the conditions employed in this work for studying Wacker oxidation. However,

- 5. 1-Butene oxidation -

main product (MEK) can be oxidized under the same conditions over the vanadate monolayer, to yield acetaldehyde and, to a lesser extent, acetic acid. When MEK is oxidized over catalyst B, the products were mainly acetaldehyde, acetic acid and acetone. When catalyst A was used, the MEK

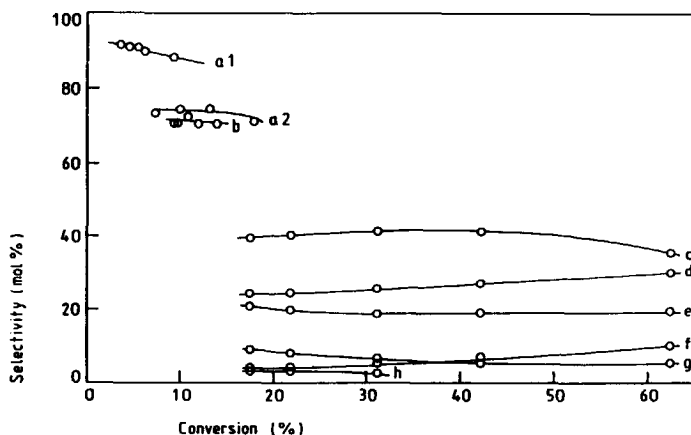


Figure 5. Selectivity to butene oxidation products as a function of the conversion. Curve a1: catalyst A; conditions as indicated in the legend of Fig 1. Curve a2: as a1, temp 393 K. Curve b: 0.33 mol % PdCl₂; 2.7 mol % LiCl; 8.1 mol % V₂O₅; 88.9 mol % Al₂O₃; conditions as indicated in the legend of Fig 1. For the sake of clarity only the selectivity to MEK is given for these catalysts. Curves c-h: 0.46 mol % PdCl₂; 3.7 mol % NaCl; 3.1 mol % V₂O₅; 92.8 mol % TiO₂(a). Conditions: temp 408 K; total pressure 0.11 MPa; flow rate 0.84 cm³(STP).s⁻¹.g⁻¹; 2 g of catalyst. Feed composition as given in Fig 3 for curve b. Selectivity to, respectively, MEK (curve c), acetic acid (curve d), acetaldehyde (curve e), acetone (curve f), acrolein (curve g) and crotonaldehyde (curve h).

conversion was lower than with the vanadate monolayer alone, indicating that the Pd sub-monolayer masks the vanadate monolayer sites which are active in oxidation of MEK. An increase in the partial pressure of water also influences these reactions, and in both cases (with and without palladium) leads to a decreasing reaction rate for MEK oxidation. Acrolein and crotonaldehyde were typical products formed by a palladium-catalyzed π -allyl oxidation reaction. The formation of acetaldehyde and acetic acid by the oxidative scission of MEK over V₂O₅ has been reported previously by Takita et al. [14]. It is possible to obtain acetone from MEK via 1-butene-3-ol [15] or via acetic acid.

- 5. 1-Butene oxidation -

When a homogeneous Wacker catalyst is applied, 3-chloro-2-butanone is formed in yields higher than 20 percent [4]. This unwanted product could not be detected under normal conditions with our catalyst. Only trace amounts were found by GC-MS analysis of collected product when a PdCl₂-containing catalyst was used. From the carbon balance, it can be concluded that the formation of CO and CO₂ (excluding the amount formed simultaneously with acrolein and acetone) is less than 5 %. By summarizing, we arrive at Fig. 6 for the reaction.

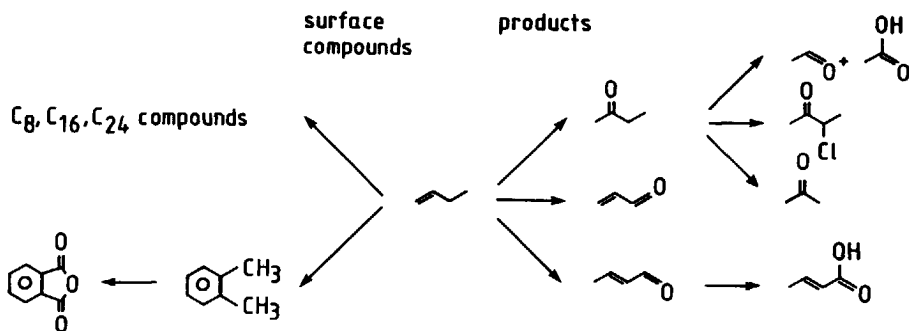


Figure 6. Reaction scheme for butene oxidation.

Temperature-programmed desorption of products deposited on the surface of the spent catalyst, followed by MS analysis of the desorbed products, indicates that, besides the products mentioned above, other (heavy) products are also formed. There are indications of the presence of phthalic anhydride ($m/e = 149$) and its precursor o-xylene ($m/e = 106$); in addition C₈, C₁₆ and C₂₄-products are detected, indicating the occurrence of coupling initially involving two butene units followed by that of the C₈-compounds formed. C₁₂ and C₂₀ compounds are not formed, probably due to a higher coverage with C₈ compounds (which have high boiling points and are therefore available for the coupling reaction) than C₄ units with lower boiling points. Coupling of alkenes by Pd(II) is a well-known reaction [7,16], and in the systems studied in this work this coupling reaction will also be Pd-catalyzed. The

carbon content of the spent catalyst after 135-h use was only 1 wt %, including the amount of adsorbed and unreacted 1-butene.

Stability and regeneration

The PdCl_2 -based catalysts deactivate slowly during use (Fig 7). The reasons for this have been investigated. The presence of the high-boiling products on the surface of the catalyst does not cause deactivation; regeneration of

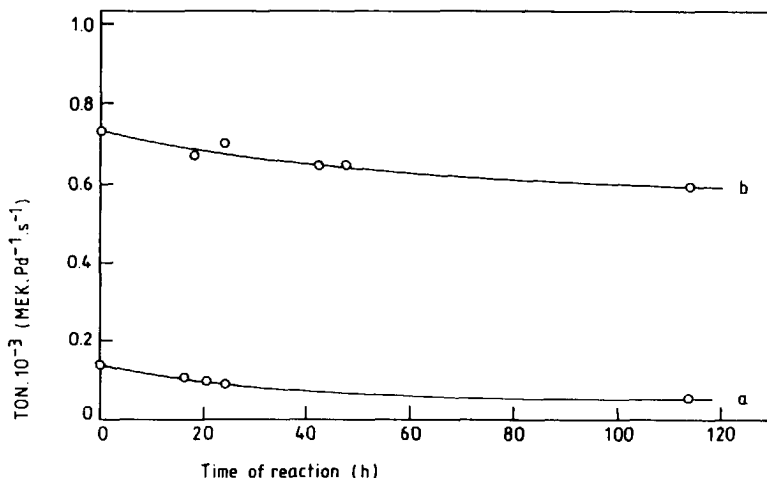


Figure 7. Turnover numbers as a function of time. Curve a: catalyst A. Conditions as given in the legend of Fig 1; 1 % C_4H_8 in the feed. Curve b: 0.34 mol % PdSO_4 ; 5.7 mol % H_2SO_4 ; 7.8 mol % V_2O_5 ; 86.1 mol % Al_2O_3 . Conditions as given in Fig 2 for curve b; 1 % C_4H_8 in the feed.

a slightly deactivated PdCl_2 containing catalyst by heating to 423 K (or 473 K) for 4 hours in a gas stream consisting of an air-10% steam gas mixture does not influence the residual activity. Heating to 553 K under the same conditions leads to complete deactivation. Calcination at 673 K in dry air was also not effective in increasing the residual activity. By TPD and TPO experiments, performed in a thermobalance, we found that under the latter regeneration conditions most of the organic products are removed from the catalyst. XPS analysis indicated that after a 140 h run at 393 K with catalyst B, only 20 % of the original amount of chlorine was present leading to a decrease in the amount of the catalytically active PdCl_4^{2-} -complexes. In addition, the presence of $\text{Pd}(0)$, formed by reduction of $\text{Pd}(\text{II})$ by butene without re-oxidation, could be detected. Impregnation of the catalyst with

HCl leads to a nearly complete recovery of the original activity. Hence, loss of HCl, possibly via formation of chlorinated products, is the main cause of deactivation.

Addition of Cu(II)- or Mo(VI)-salts (or H_3PO_4) to a freshly prepared catalyst leads to good activity, but is not effective in improving the stability. The use of chlorine, whose loss is the main cause of deactivation, may be circumvented by the use of $PdSO_4$ -based catalysts. This indeed results in a more stable catalyst (Fig. 7).

References

1. Kirk Othmer Encyclopedia of Chemical Technology, 3th ed., Wiley, New York, 13 (1981) 894.
2. A.L. Farragher and G.W.J. Heimerikx: Proc. 4th. Int. Conf., Chem. Uses Molybdenum, (Amsterdam), (1982) 432. Y. Moro-Oka, S. Tan and A. Ozaki, J. Catal., 17 (1970) 125. S. Tan, Y. Moro-Oka and A. Ozaki, J. Catal., 17 (1970) 132.
3. J. Smidt, W. Hafner, R. Jira, J. Sedlmeier, R. Sieber, R. Ruttinger and H. Kojer, Angew. Chem., 71 (1959) 176.
4. J. Smidt and H. Krekeler, Chem. Eng. News, July 8 (1963) 50. J. Smidt and H. Krekeler, Hydrocarbon Process. Pet. Refiner, 42 (7) (1963) 149.
5. S.F. Davison, B.E. Mann and P.M. Maitlis, J. Chem. Soc., Dalton Trans., (1984) 1223.
6. Catalytica Associates (U.S.A.), WO 87/01615, (march 26, 1987).
7. K. Fujimoto, H. Takeda and T. Kunugi, Ind. Eng. Chem. Prod. Res. Dev., 13 (4) (1974) 237.
8. A.B. Evnin, J.A. Rabo and P.H. Kasai, J. Catal., 30 (1973) 109.
9. P.J. van der Steen, Thesis, Delft University Press, 1987. J.J.F. Scholten and P.J. van der Steen, European Patent Specification 210705 A, (march 22, 1989).
10. E. van der Heide, M. de Wind, A.W. Gerritsen and J.J.F. Scholten, Proc. Int. Congr. Catal., 9th, (Calgary), 4 (1988) 1648.
11. G. Kumar, F.R. Blackburn, T.G. Albridge, W.E. Moddeman and M.M. Jones, Inorg. Chem., 11 (1972) 296-300. K.S. Kim, A.F. Gossmann and N. Winograd, Anal. Chem., 46 (2) (1974) 197-200.
12. F. Roozeboom, T. Fransen, P. Mars and P.J. Gellings, Z. Anorg. Allg. Chem., 499 (1979) 25-40.
13. P.M. Henry, J. Am. Chem. Soc., 86 (1964) 2346. J.M. Henry, J. Am. Chem. Soc., 88 (1966) 1595.
14. Y. Takita, K. Iwanaga, N. Yamazoe and T. Seiyama, Oxid. Commun., 1 (2) (1980) 135-144.
15. R.J. Theissen, J. Org. Chem., 36 (1971) 752.
16. H.C. Volger, Recl. Trav. Chim. Pays-Bas, 86 (1967) 677. K. Kaneda, T. Kiriyaama, T. Hiraoko and T. Imanaka, J. Mol. Catal., 48 (1988) 343-347.

6

Mechanism of the gas phase oxidation of cyclohexene over a new heterogenized surface-vanadate Wacker catalyst

Abstract

The mechanism of the Wacker oxidation of cyclohexene to cyclohexanone has been studied over a new heterogeneous monolayer-vanadate Wacker catalyst in the temperature range from 333 to 453 K and at 0.11 MPa total pressure. Applying a Na_2PdCl_4 containing catalyst, a conversion of cyclohexene to benzene with 100 % selectivity was arrived at, the reaction probably being catalyzed by a surface sodium vanadate. Cyclohexanone and phenol are formed in trace amounts only.

From a study of cyclohexene oxidation in the presence of ethylene in the feed it follows that the cyclohexene conversion is extremely low due to the very weak interaction of cyclohexene with the catalytic sites.

Introduction

A new route to cyclohexanone, an important intermediate in the production of Nylon-6, might be the selective hydrogenation of benzene to cyclohexene, followed by oxidation of cyclohexene to cyclohexanone. This last reaction can be performed step-wise via acid catalyzed hydration of the alkene to cyclohexanol, followed by dehydrogenation of cyclohexanol to the ketone. A

- 6. Cyclohexene oxidation -

reaction strongly related to Wacker oxidation is the acetoxylation of cyclohexene to 1-cyclohexenyl acetate [1,2] and its isomers [3]. Hydrolysis of these products leads to cyclohexanone and acetic acid and the latter compound can be recirculated.

However, by applying Wacker oxidation, a one-stage process leading to cyclohexanone is possible as well. Homogeneous Wacker oxidation of cyclohexene to cyclohexanone was performed already by Smidt *et al.* [4] and by other investigators [5,6,7]. Side reactions include disproportionation of the alkene to cyclohexane and benzene [2] (but this can be avoided by addition of an active redox compound [2]) and formation of the cyclohexenone isomers and phenol [8].

The kinetics of the homogeneous Wacker oxidation of cyclohexene deviate from the kinetics of ethylene oxidation; in the case of cyclohexene oxidation no inhibition of the reaction rate by hydrogen ion is found [5,6]. This may be attributed to a deviating mechanism, probably proceeding via π -allyl complex formation [9] or via nucleophilic attack on coordinated cyclohexene by water [10].

Heterogeneous Wacker oxidation can be performed over a monolayer-vanadate catalyst supported on γ - Al_2O_3 or on $\text{TiO}_2(\text{a})$; this monolayer, in turn, is covered by a sub-monolayer of a Pd(II) salt, for instance palladium sulphate or palladium chloride. Oxidation of ethylene [11,12], 1-butene [13] and styrene [14], over the same catalyst, are described in the Chapters 4, 5 and 7, respectively. The performance of the catalyst towards cyclohexene oxidation will be discussed now.

Experimental

Materials, catalyst preparation and experimental conditions have been described before [11,13,14].

Cyclohexene (Merck, F.R.G.) was distilled before use and dosed to the feed by bubbling finely divided nitrogen bubbles through a thermostatted flask filled with the alkene. The dependence of the feed composition from the temperature of liquid cyclohexene is calculated from the Antoine equation and the Antoine parameters as given in ref. [15]. Products were analyzed by means of temperature programmed GC, applying a wide bore CP wax

52 CB column, film thickness 1.96 nm, internal diameter 0.53 mm and length 10 m. The temperature programme ran from 373 to 473 at a heating rate of 0.3 K.s⁻¹. Ethylene was detected by means of a Porapak QS column, length 1 m, diameter 3 mm, at 423 K, as described in [14]. Three types of catalyst have been used. Catalyst A contained 85.9 mol % Al₂O₃, 8.2 mol % V₂O₅, 5.2 mol % NaCl and 0.7 mol % PdCl₂; catalyst B 84.5 mol % Al₂O₃, 8.0 mol % V₂O₅, 7.1 mol % H₂SO₄ and 0.4 mol % PdSO₄, and catalyst C 81.2 mol % Al₂O₃, 7.7 mol % V₂O₅, 9.3 mol % HCl and 1.9 mol % PdCl₂.

Results and discussion

In our first experiment (Table I), benzene was produced quantitatively over the Na₂PdCl₄ containing catalyst A, by oxidative dehydrogenation of cyclohexene, at a temperature as low as 373 K. As benzene is the only product formed, the disproportionation of cyclohexene to benzene and cyclohexane [2] has to be excluded. The occurrence of the reaction appeared to be related to the presence of sodium chloride in the catalyst. Therefore, the catalytic activity may be attributed to the formation of a sodium vanadate, a compound related to magnesium orthovanadate, which is known to be an active dehydrogenation catalyst [16].

The conversion to benzene could be partly suppressed by addition of hydrochloric acid to the catalyst, six-fold in excess of the amount of chloride already present. Next to benzene, the formation of traces of cyclohexanone could be detected. In the presence of the excess of hydrochloric acid, cyclohexanone may be produced via the acid-catalyzed hydration of cyclohexene, followed by oxidative dehydrogenation of the intermediate cyclohexanol to cyclohexanone (Fig. 1).

The low Wacker oxidation activity may be ascribed to the weak coordination of cyclohexene to palladium chloride, relative to the coordination of terminal alkenes. Therefore, palladium chloride was replaced by palladium sulphate (catalyst B). On applying this last catalyst, 1-butene was oxidized to butanone and a high activity and stability, relative to the chloride catalyst A, were found [13]. This is due to the weaker coordination of sulphate to Pd(II) compared with chloride. However, as can be seen from

- 6. Cyclohexene oxidation -

Table I. Influence of catalyst composition and experimental conditions on the course of the oxidation reaction of cyclohexene.

<u>cat.</u>	<u>amount of reaction catalyst</u>	<u>temp.</u>	<u>% alkene in the feed¹</u>	<u>remarks</u>
A	2 g	373, 393 K	0.5 % C ₆ H ₁₀	complete conversion to benzene
	2 g	353, 363 K	0.5 % C ₆ H ₁₀	partial conversion to benzene After addition of HCl: conv. to benzene is lowered, 0.6 % conv. to cyclohexanone.
B	2 g	373 K	0.5 % C ₆ H ₁₀	no activity
	2 g	393 - 453 K	0.5 % C ₆ H ₁₀	max. 1 % conversion to phenol
C	2 g	333 - 393 K	0.5 - 1.5 % C ₆ H ₁₀	trace of phenol
	1.5 g ²	393 K	0.5 % C ₆ H ₁₀	trace of phenol
	1 g	373 K	1 % C ₂ H ₄ ³	No influence of cyclohexene on the acetaldehyde production
B	1 g	373 K	0.5 % C ₆ H ₁₀ , 1 % C ₂ H ₄	No conversion of cyclohexene
C	1 g	373 K	0.5 % C ₆ H ₁₀ , 1 % C ₂ H ₄	No conversion of cyclohexene

¹ Composition of the feed: 10 mol % H₂O, supplemented with air. Total pressure: 0.11 MPa.

² The catalyst is pretreated by leading over of ethylene.

³ 5 ml cyclohexene is added to 500 ml H₂O in the water evaporator and evaporated simultaneously with water.

Table I, on applying catalyst B no conversion of cyclohexene could be detected under the conditions mentioned. At higher temperatures, even up to 453 K, only traces of phenol (max. 1 % yield) could be detected. It is likely that phenol is formed by the dehydrogenation of cyclohexanol or of cyclohexanone (Fig. 1).

Besides by the weak interaction of cyclohexene with the palladium sites, the lack of activity of the catalysts towards cyclohexene oxidation can be caused by at least two other effects, viz. by the lack of activation of the

- 6. Cyclohexene oxidation -

catalyst during treatment with cyclohexene and by deactivation, caused by contact with cyclohexene or oxidation products.

To test these hypotheses, the performance of a H_2PdCl_4 catalyst without addition of sodium chloride, catalyst C, was studied, but only traces of phenol were found. Next, the catalyst was used for the oxidation of ethylene, in which process, in accordance with ref. [11], production of acetaldehyde was observed. However, this ethylene oxidation run did not

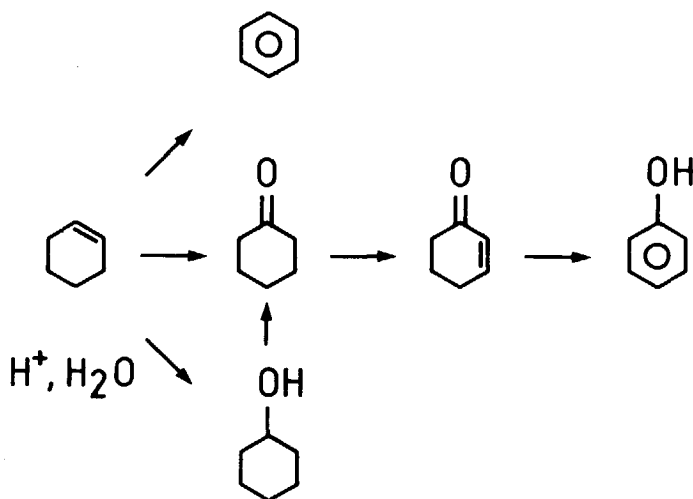


Figure 1. Reaction routes of oxidation of cyclohexene.

influence the rate of the subsequent oxidation of cyclohexene. Subsequently, ethylene was oxidized once more over the same catalyst sample and again the same turnover number to acetaldehyde was found.

In conclusion, it can be stated that neither activation nor deactivation lie at the root of the low activity of the catalyst in cyclohexene oxidation.

To check in how far cyclohexene interacts with the catalytic sites, an experiment was carried out in which a cyclohexene - ethylene mixture was oxidized applying catalyst C (Table I). During the oxidation of ethylene, the cyclohexene was added to the feed, but no influence on the reaction rate to acetaldehyde was found. The test was repeated with catalysts B and C (Table I) and no cyclohexene conversion could be detected.

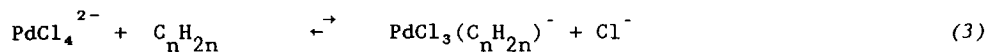
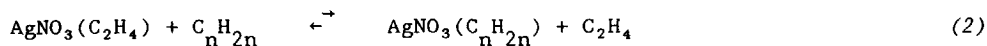
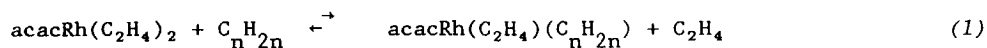
- 6. cyclohexene oxidation -

The coordination of alkenes to transition metals is influenced by steric and by electronic factors. In general the bonding strength between the alkene and the metal decreases with increasing alkene chain length and with an increasing electron donating ability of the substituents on the alkene [17]. As is clearly shown in Table II, the equilibrium constants of

Table II. Equilibrium constants of coordination of alkenes to rhodium, silver and palladium complexes for reactions (1), (2) and (3), respectively.

<u>alkene</u>	rhodium ^a	silver ^b	palladium ^c
	<u>equilibr. const.</u>	<u>equilibr. const.</u>	<u>equilibr. const.</u>
CH ₂ =CH-CH ₃	0.078	0.43 (0.41)	0.83
CH ₂ =CH-CH ₂ -CH ₃	0.092	0.50 (0.35)	0.64
<i>cis</i> -CH ₃ -CH=CH-CH ₃	0.0041	0.28 (0.24)	0.50
<i>trans</i> -CH ₃ -CH=CH-CH ₃	0.0020	0.091 (0.063)	0.26

a: ref. [17]. b: ref [17]; in parenthesis: relative to formation of AgNO₃(C₂H₄), as calculated from ref. [19]. c: relative to formation of PdCl₃(C₂H₄), as calculated from ref. [18].



coordination of an alkene with rhodium, silver or palladium complexes strongly decreases with increasing length and number of the alkyl substituents. As the steric hindrance will be about the same for all metals, from the deviation of the constants it is to be concluded that alkene

- 6. Cyclohexene oxidation -

coordination is dominated by electronic factors in the case of rhodium and silver, and mainly determined by steric factors in the case of palladium [17]. The coordination constant of cyclohexene to palladium will be low relative to the values mentioned in Table II.

Besides the weak coordination of cyclohexene with palladium, the nucleophilic attack of palladium coordinated cyclohexene by a hydroxo group, the rate determining step in Wacker oxidation, will be retarded for both steric and electronic reasons.

We conclude that the low activity of the catalysts towards cyclohexene oxidation has to be attributed to a very weak interaction of cyclohexene with the palladium sites. The low activity towards cyclohexene oxidation in the homogeneous Wacker reaction and the deviation of the kinetics from ethylene oxidation found in this case [5] can probably be explained in the same way.

Conclusions

Catalytic oxidation of cyclohexene over the Na_2PdCl_4 containing catalyst A leads to a full oxidative dehydrogenation of cyclohexene to benzene. This is probably due to the presence of a surface sodium vanadate, the catalytic properties of which are related to those of the well-known magnesium orthovanadate dehydrogenation catalysts. The reaction was found to be partly suppressed when hydrochloric acid was added to the catalyst. Production of traces of cyclohexanone, probably formed via acid catalyzed hydration of cyclohexene followed by dehydrogenation, could be detected.

A very low conversion of cyclohexene over $\text{H}_2\text{SO}_4/\text{PdSO}_4$ and H_2PdCl_4 -containing catalysts has been detected, accompanied by the formation of traces of phenol. The low activity appeared to be due to the very weak interaction between cyclohexene and the catalytic palladium sites.

Excluding the reactions already mentioned, cyclohexene and benzene appeared to be stable under the reaction conditions.

References

1. S. Wolfe and P.G.C. Campbell, *J. Am. Chem. Soc.*, 93 (1971) 1494.
2. M. Green, R.N. Haszeldine and J. Lindley, *J. Organometal. Chem.*, 6 (1966) 107.
3. S. Winstein and C.B. Anderson, *J. Org. Chem.*, 28 (1963) 605.
4. J. Smidt, W. Hafner, R. Jira, J. Sedlmeier, R. Sieber, R. Rüttinger and H. Kojer, *Angew. Chem.*, 71 (1959) 176.
5. M. Kolb, E. Bratz and K. Dialer, *J. Molec. Catal.*, 2 (1977) 399.
6. M.N. Vargaftik, I.I. Moiseev and Ya.K. Syrkin, *Dokl. Akad. Nauk USSR*, 139 (1961) 1396; M.N. Vargaftik, I.I. Moiseev and Ya.K. Syrkin, *Dokl. Akad. Nauk USSR*, 147 (1962) 804.
7. E. Bratz, G. Prauser and K. Dialer, *Chem.-Ing.-Techn.*, 46 (1974) 161; K. Takehira, H. Orita, I.H. Oh, C.O. Leobardo, G.C. Martinez, M. Shimidzu, T. Hayakawa and T. Ishakawa, *J. Molec. Catal.*, 42 (1987) 247; K. Takehira, H. Orita, I.H. Oh, C.O. Leobardo, G.C. Martinez, M. Shimidzu, T. Hayakawa and T. Ishakawa, *J. Molec. Catal.*, 42 (1987) 237.
8. R.J. Theissen, *J. Org. Chem.*, 36 (1971) 752; R.G. Brown and J.M. Davison, *J. Chem. Soc. (A)*, (1971) 1321; R.G. Brown and J.M. Davison, *Adv. Chem. Ser.*, 132 (1974) 49.
9. R. Hüttel, H. Dietl and H. Christ, *Chem. Ber.*, 97 (1964) 2037.
10. P.M. Henry: *Palladium Catalyzed Oxidation of Hydrocarbons*, Reidel, Dordrecht, (1980) 97.
11. E. van der Heide, M. de Wind, A.W. Gerritsen and J.J.F. Scholten, *Proc. Int. Congr. Catal.*, 9th, (Calgary), 4 (1988) 1648.
12. P.J. van der Steen, *Thesis*, University Press, Delft, (1987). J.J.F. Scholten and P.J. van der Steen, European Patent Specification 0210705, d.d. 22.03.1989.
13. E. van der Heide, J.A.M. Ammerlaan, A.W. Gerritsen and J.J.F. Scholten, *J. Molec. Catal.*, 55 (1989) 320.
14. E. van der Heide, J. Schenk, A.W. Gerritsen and J.J.F. Scholten, accepted for publication in *Recl. Trav. Chim. Pays-Bas*.
15. J. Gmeling, K. Onken and W. Arlt: Vapor-liquid equilibrium data collection, Aliphatic Hydrocarbons C₄ - C₆, 1 (6a) (1980).
16. M.A. Chaar, D. Patel, M.C. Kung and H.H. Kung, *J. Catal.*, 105 (1987) 483; M.A. Chaar, D. Patel and H.H. Kung, *J. Catal.*, 109 (1988) 463; M. DelArco, M.J. Holgado, C. Martin and V. Rives, *J. Mater. Sci. Lett.*, 6 (1987) 616.
17. R. Cramer, *J. Am. Chem. Soc.*, 89 (1967) 4621.
18. P.M. Henry, *J. Am. Chem. Soc.*, 86 (1964) 3246; P.M. Henry, *J. Am. Chem. Soc.*, 88 (1966) 1595.
19. M.A. Muhs and F.T. Weiss, *J. Am. Chem. Soc.*, 84 (1962) 4697.

Kinetics and mechanism of the gas phase oxidation of styrene to benzaldehyde, acetophenone and cinnamaldehyde over a new heterogenized surface-vanadate Wacker catalyst

Evert van der Heide, John Schenk, Albert W. Gerritsen and Joseph J.F. Scholten.

Abstract

A study has been made of the kinetics and mechanism of the oxidation of styrene over a heterogeneous vanadate-monolayer Li_2PdCl_4 Wacker catalyst in the temperature range of 348 K to 453 K at 0.11 MPa total pressure. The kinetics of the reaction, with respect to the dependence of the reaction rate on the partial pressures of styrene and water, as well as on the surface LiCl concentration, appear to be logically related to the kinetics of the homogeneous Wacker process.

In addition to acetophenone (initial selectivity 45 mol %), benzaldehyde, probably originating from phenylacetaldehyde, is formed with gradually increasing selectivity (initial selectivity 55 mol %). Formation of benzoic acid can sometimes be detected but in all cases with a selectivity lower than 5 mol %. Initially no other products are detected but, after a short period, cinnamaldehyde is formed with increasing selectivity (15 mol % after three days).

Deactivation of the catalyst is due to carbonaceous deposits and removal of these deposits by oxidation with air at 473 K leads to partial regeneration.

Introduction

Phenylacetaldehyde, a costly crude material in the perfume industry, can be produced in several ways. Industrially important production routes include isomerisation of 2-phenyloxirane at ca. 650 K, making use of a $Mg_2SiO_4 \cdot x H_2O$ catalyst, oxidation of cyclooctatetraene with hydrogen peroxide, catalyzed by mercury, and combined hydrolysis and decarboxylation of 3-phenyl-2-oxiranecarboxylate, formed by the reaction of 2-phenyloxirane with ethyl 2-chloroacetate [1].

From an economical point of view, oxidation of styrene to phenylacetaldehyde seems to be more attractive which, in principle, may be accomplished by Wacker oxidation. In general, Wacker oxidation of terminal alkenes leads mainly to the formation of the corresponding methyl ketones but, in the case of homogeneous Wacker oxidation of styrene, phenylacetaldehyde is formed with selectivities as high as 75 mol %, in addition to the normal Wacker product acetophenone [2]. Acetophenone, benzaldehyde and cinnamaldehyde, the products dealt with in this paper, are also important fine-chemicals.

Technical disadvantages of the homogeneous Wacker process are the highly corrosive properties of the catalyst solution (consisting of $PdCl_2$ and $CuCl_2$ dissolved in hydrochloric acid) in the presence of oxygen, the unwanted formation of chlorinated by-products and the difficult separation of the products from the aqueous reaction mixture when starting from C_3 or higher alkenes. Therefore, a heterogeneous catalytic process would be more attractive.

In this paper we report on the performance of a heterogeneous Wacker catalyst, in which a vanadium oxide redox monolayer is molecularly dispersed on, and chemically bound to, the surface of a support ($\gamma-Al_2O_3$ or $TiO_2(a)$). This dispersed phase, in turn, is covered by a sub-monolayer of a palladium salt [3-5]. The mechanism, kinetics and selectivity of the oxidation of styrene with oxygen over this catalyst are presented.

Experimental

Chemicals

O₂ and N₂ (in cylinders) were obtained from Air Products (U.S.A.). N₂ was of high purity and O₂ was of industrial grade. H₂O was distilled twice. PdCl₂, analytical grade, was obtained from Drijfhout (The Netherlands). HCl, analytical grade, was purchased from Baker (The Netherlands). NH₄VO₃, also analytical grade, was purchased from Merck (F.R.G.). γ -Al₂O₃, type 000-3P, S(BET) = 250 m².g⁻¹, was supplied by AKZO (The Netherlands) and TiO₂(a), type CRS 31 Lot 2, S(BET) = 127 m².g⁻¹, was obtained from Rhône Poulenc (France).

Apparatus

The performance of the catalyst was studied in a continuous-flow, fixed-bed, stainless-steel reactor, internal diameter 1 cm and length 10 cm, at a total pressure of 0.11 MPa and in the temperature range 348 to 453 K. The composition of the feed was regulated by means of mass-flow controllers (Inacom, The Netherlands) and all gases were dried over molecular sieves. Water was dosed to the feed by leading finely divided bubbles of nitrogen through a thermostatted flask filled with water. On-line off-gas analysis was performed gas-chromatographically, applying a 15 % siponato DS 10 chromosorb W HP (100-120 mesh) column, length 4 m, diameter 3 mm. Peak areas were recorded and integrated by a micro computer (Digital LCI 11/03, USA). Collected products were analyzed by GC-MS, and the derived mass spectra correspond with the relevant library spectra.

Catalyst preparation

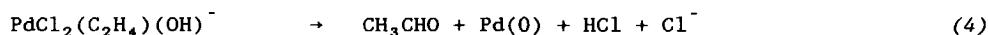
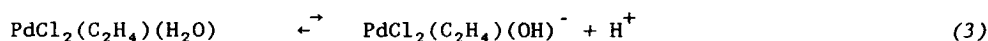
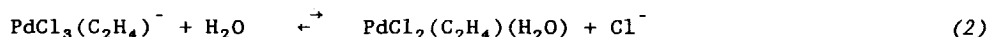
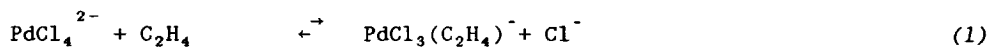
The γ -Al₂O₃ pellets were crushed and sieved to particle diameters from 425 to 500 μ m. By leading an NH₄VO₃ solution at 343 K over these particles during 24 h, the surface was covered with an alumino vanadate monolayer [4]. The particles were then calcined in air at 673 K for 4 h. The vanadium coverage was determined by titration with Fe(II). Next, through impregnation to incipient wetness with a solution of Li₂PdCl₄ and LiCl, followed by drying at 353 K, the alumino vanadate layer was covered with a sub-monolayer of the Pd compound. In preparing TiO₂(anatase)-based catalysts, the same

procedure was followed, except for the temperature and duration of vanadium monolayer deposition, viz, 293 K and 4 hrs.

Results and discussion

Kinetics

Traditionally, the mechanism of homogeneous Wacker oxidation is believed to consist of three equilibria (eqs. (1)-(3)), preceding the rate determining step (eq. (4)) [6]. For the case of C_2H_4 oxidation we then have:



The last (rate determining) step is built up of at least three elementary steps. In the case of styrene oxidation, in addition to acetophenone, the corresponding aldehyde, phenylacetaldehyde, is also formed according to reaction (4). The kinetic equation derived from these equilibria is as follows (eq. (5)):

$$r = k \cdot \frac{[PdCl_4^{2-}][C_2H_4]}{[H^+][Cl^-]^2} \quad (5)$$

The kinetics of the heterogeneous Wacker oxidation of both ethylene and 1-butene have been previously reported [4,5] and a close relationship with the homogeneous kinetics was found. Kinetic measurements on the homogeneous Wacker oxidation of styrene are scarce [7]; when varying the H^+ or the Cl^- concentration, contrary to expectation, a maximum in the activity as a function of these concentrations is found.

In Fig. 1 the reaction rate is plotted as a function of the partial

- 7. Styrene oxidation -

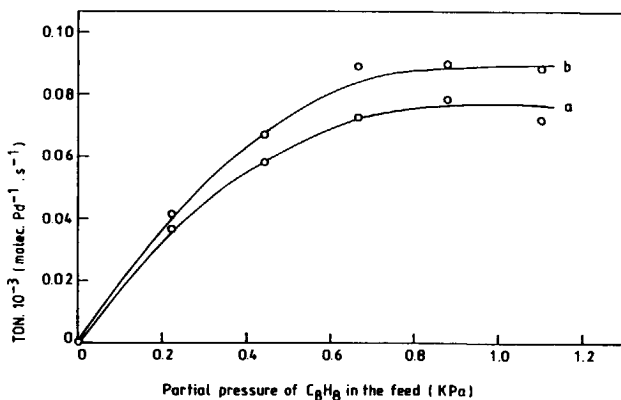


Figure 1. Turnover numbers as a function of the partial styrene pressure. Curve a: rate of formation of acetophenone; curve b: rate of formation of benzaldehyde. Catalyst composition: 0.9 mol % PdCl₂; 7.4 mol % LiCl; 7.0 mol % V₂O₅; 84.6 mol % Al₂O₃. Conditions: temperature: 373 K; total pressure 0.11 MPa; flow rate: 0.83 cm³ (STP)·s⁻¹·g⁻¹; 2 g of catalyst. Feed composition: 6.5 % H₂O; 18.6 % O₂; 74.9 % gas of variable C₈H₈/N₂ ratio.

styrene pressure. The curves, which represent the rate of formation of benzaldehyde and of acetophenone, respectively, are of the Langmuir type. This is in accordance with what is to be expected on the basis of eq. (1) in

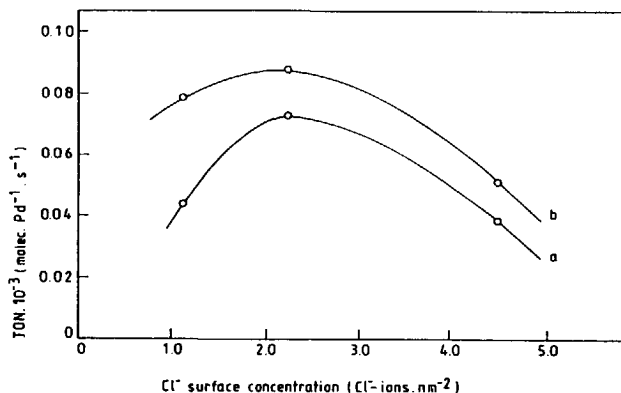


Figure 2. Turnover numbers as a function of the Cl⁻ surface concentration. Curve a: rate of formation of acetophenone; curve b: rate of formation of benzaldehyde. Catalysts composition: 0.9 mol % PdCl₂; 2.9-15.2 mol % LiCl; mol % Al₂O₃/mol % V₂O₅ ratio is 11.9. Pd coverage is 0.22 Pd(II) ions · nm⁻². Conditions as indicated in the legend to Fig. 1; 1 % C₈H₈ in the feed.

- 7. Styrene oxidation -

the case of styrene.

The dependence of the reaction rate on the LiCl coverage is plotted in Fig. 2. The observed relationship is about the same as that reported for the influence of the Cl^- concentration in the homogeneous oxidation of styrene [7], and is in accordance with what has been previously reported for the heterogeneous oxidation of ethylene and 1-butene [4,5]. At too low a LiCl coverage, the Cl/Pd-ratio is unfavourable for the formation of the catalytically active PdCl_4^{2-} complexes. Initially, during the start-up procedure, a high, but very unstable, activity is measured, followed by a slight deactivation of the catalyst, but finally a relatively stable level is reached. On increasing the LiCl coverage, a maximum activity is reached and thereafter no difference is found between the initial and stable activity. As would be expected (eq. 5), a retardation of the rate of

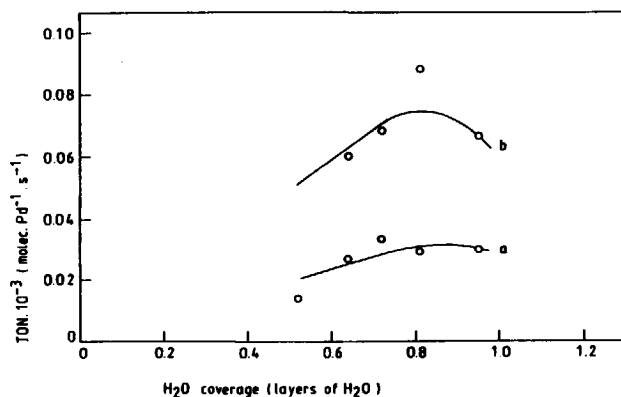


Figure 3. Turnover numbers as a function of the H_2O partial pressure. Curve a: rate of formation of acetophenone; curve b: rate of formation of benzaldehyde. Catalyst and conditions as indicated in the legend to Fig. 1. Feed composition: 1 % C_8H_8 ; 17.4 % O_2 ; 81.6 % gas of variable $\text{H}_2\text{O}/\text{N}_2$ ratio.

reaction with increasing chloride concentration was found, but the precise order of this effect was not determined.

According to eq. (2), a first order dependence of the activity on the water coverage is to be expected. In the case of the homogeneous Wacker oxidation, the order in water concentration cannot be measured, it being the solvent present in excess. In the case of heterogeneous oxidation of

- 7. Styrene oxidation -

ethylene [4], a first-order dependence of the water coverage on the activity is found and also, in the case of styrene oxidation, a first-order dependence appears to be valid at low water coverage (Fig. 3). At higher partial pressures of water, the catalyst deactivates, possibly starting with hydrolysis of the palladium-vanadium bond. This is probably followed by the formation of Pd(0), due to breakdown of the reoxidation, and hence the catalyst deactivates.

The activity of the catalyst as a function of temperature has been measured between 348 and 373 K and is shown in Fig. 4 in the form of an Arrhenius plot. Apparent activation energies of 51 kJ/mol and 90 kJ/mol were calculated for benzaldehyde and acetophenone formation, respectively. The difference in the apparent activation energies may be due to a decrease in the Pd(II)-aromatic ring bonding strength with increasing temperature. This

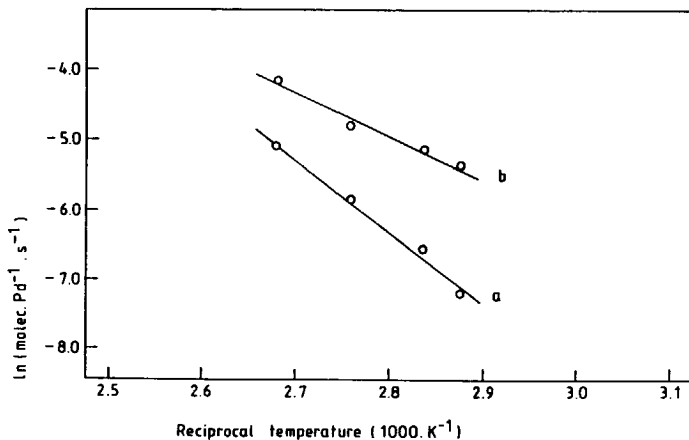


Figure 4. Arrhenius plot for styrene oxidation. Curve a: rate of formation of acetophenone; curve b: rate of formation of benzaldehyde. Catalyst and conditions as indicated in the legend to Fig. 1; LiCl is replaced by HCl; constant relative H₂O-pressure: P/P₀ = 0.093; 1 % C₈H₈ in the feed.

leads to the preferred formation of the normal Wacker product, acetophenone relative to benzaldehyde, at higher temperatures, this latter product being probably derived from phenylacetaldehyde. In a separate experiment, the activity of a TiO₂(a)-supported catalyst was measured. In the case of ethylene oxidation, quite unexpectedly, the reaction rate increased by a factor of 20 on replacing the γ -Al₂O₃ carrier by TiO₂(a) [4], which indicates that the reoxidation of Pd(0) to Pd(II) by the vanadate monolayer

- 7. Styrene oxidation -

is not a separate reaction, but linked to the main reaction, steps (1) to (4). The activity for styrene oxidation appeared to be the same for both catalysts. Hence, for unknown reasons, in the case of styrene oxidation, no influence of the type of vanadate monolayer on the activity of the Pd site was found.

Selectivity

In the Wacker oxidation of styrene, the product to be expected, acetophenone, is formed initially with 45 mol % selectivity, in addition to benzaldehyde, which is formed with 55 mol % selectivity. These initial selectivities are the same under all conditions, except at low chloride concentration, where the selectivity to benzaldehyde is slightly higher (65 mol % at a Pd/Cl ratio of 1/4). The Pd-aromatic ring interaction will be more important at low chloride concentration, leading to the preferred formation of phenylacetaldehyde, the precursor of benzaldehyde. As reported above, an increase in the selectivity to benzaldehyde is also found at lower temperatures (85 mol % at 348 K); this phenomenon is reversible: with increasing temperature, the selectivity to benzaldehyde again decreases.

When phenylacetaldehyde is dosed with the feed, benzaldehyde is formed quantitatively, possibly via oxidative cleavage of the $\text{CH}_2\text{-CHO}$ bond. A similar behaviour is observed in the case of the reaction of 2-butanone to acetic acid and acetaldehyde over the present catalyst [5], which was found

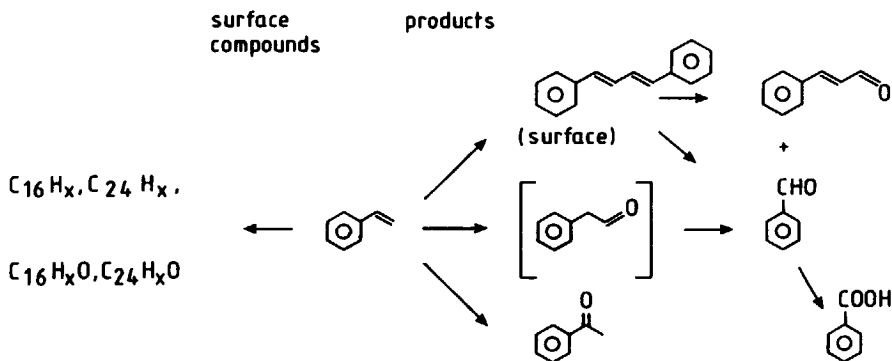


Figure 5. Reaction scheme for styrene oxidation.

- 7. Styrene oxidation -

to be catalyzed by the vanadate monolayer. Thus, the formation of benzaldehyde from styrene proceeds via phenylacetaldehyde, which, in the case of homogeneous Wacker oxidation, is formed with high selectivities [7].

In some cases, the formation of benzoic acid, derived from benzaldehyde, could be detected, although its selectivity was less than 5 mol % in all cases. Initially, no other products are detectable, however, after a period of time, cinnamaldehyde is formed with increasing selectivity, up to 15 mol % after three days. This increase in the selectivity to cinnamaldehyde coincides with an increase in the selectivity to benzaldehyde. On applying temperature-programmed desorption, combined with mass spectrometry (TPD-MS), in order to detect adsorbed products on the surface of a spent catalyst, large amounts of 1,4-diphenyl-1,3-butadiene desorbed. This led us to conclude that cinnamaldehyde and benzaldehyde are formed simultaneously via dimerisation of styrene, followed by asymmetric oxidative cleavage of 1,4-diphenyl-1,3-butadiene, which is built up at the surface over time. Although Pd(II) catalyzed head-to-tail coupling of styrene is known [8], head-to-head coupling of styrene catalyzed by Pd(II) has also been reported [9]. The oxidative scission of 1,4-diphenyl-1,3-butadiene can be catalyzed by the vanadate monolayer.

The reactions discussed in this section, and their mutual coherence, are summarized in Fig. 5.

Stability

The activity of the catalyst decreased slowly; for most catalysts an activity half-life of 24 to 48 hours was measured. The deposition of carbonaceous products, formed by oligomerisation of styrene or of oxidation products, could well explain this fact.

The quantity of surface hydrocarbons has been measured gravimetrically and an 8 wt % increase was found after a 4-days run. Elemental analysis of the same spent catalyst indicated the presence of 6.8 wt % carbon. From TPD-MS measurements, it was found that mainly aromatized C₁₈ and C₂₄ compounds are deposited (m/z = 204, 206, 306), as well as to oxidized products (m/z = 220, 222, 320).

From gravimetric measurements, it was found that the deposited carbonaceous products can be removed by oxidation with air at 473 K. A

deactivated catalyst was treated in air over 4 h at 473 K and this led to a 65 % recovery in activity.

Conclusions

The kinetics of the Wacker oxidation of styrene largely corresponds to those previously reported for homogeneous systems. The first order dependence of the activity on the coverage of water, as found here, is a new phenomenon and confirms the generally accepted reaction mechanism for Wacker oxidation.

The products of heterogeneous Wacker oxidation of styrene include acetophenone and benzaldehyde (formed via phenylacetaldehyde). After a longer time-on-stream, cinnamaldehyde is formed with gradually increasing selectivity. This last aldehyde is produced via asymmetric oxidative scission of 1,4-diphenyl-1,3-butadiene, which is formed by dimerisation of styrene. In some cases, only traces of the oxidation product of benzaldehyde, benzoic acid, could be detected.

Deactivation occurs by deposition of carbonaceous products on the surface of the catalyst. Partial regeneration is possible via oxidative removal of the deposit with air at 473 K.

References

1. S. Coffey, ed.: *Rodd's Chemistry of Carbon Compounds*, Elsevier, Amsterdam, (1976).
2. W. Hafner, R. Jira, J. Sedlmeier and J. Smidt, *Chem. Ber.*, 95 (1962) 1575.
3. P.J. van der Steen, *Thesis*, University Press, Delft, 1987.
J.J.F. Scholten and P.J. van der Steen, *European Patent Specification* 0210705, d.d. 22.03.1989.
4. E. van der Heide, M. de Wind, A.W. Gerritsen and J.J.F. Scholten, *Proc. Int. Congr. Catal.*, 9th, (Calgary), 4 (1988) 1648.
5. E. van der Heide, J.A.M. Ammerlaan, A.W. Gerritsen and J.J.F. Scholten, *J. Molec. Catal.*, 55 (1989) 320.
6. P.M. Henry, *J. Am. Chem. Soc.*, 86 (1964) 2346. P.M. Henry, *J. Am. Chem. Soc.*, 88 (1966) 1595.
7. H. Okada, T. Noma, Y. Katsuyama and H. Hashimoto, *Bull. Chem. Soc. Jpn.*, 41 (1968) 1395.
8. K. Kaneda, T. Kiriyama, T. Hiraoka and T. Imanaka, *J. Molec. Catal.*, 48 (1988) 343.
9. K. Kawamoto, A. Tatani, T. Imanaka and S. Teranishi, *Bull. Chem. Soc. Jpn.*, 44 (1971) 1239. H.C. Volger, *Rec. Trav. Chim.*, 86 (1967) 677.

Kinetics and mechanism of the gas-phase oxidation of ethylene to acetaldehyde over TiO_2 (anatase) supported surface vanadate Wacker catalysts

Abstract

A study has been made of the kinetics and mechanism of the oxidation of C_2H_4 to CH_3CHO over a heterogeneous monolayer-vanadate Wacker catalyst supported on $\text{TiO}_2(\text{a})$ in the temperature range from 348 to 393 K and at 0.11 MPa total pressure. The kinetics of the reaction with respect to the dependency of the reaction rate on the C_2H_4 and H_2O pressures and with respect to the PdCl_4^{2-} coverage are logically related to the kinetics of the homogeneous Wacker process.

However, an exceptional behaviour of the reaction rate with respect to the Cl^- coverage and with respect to PdCl_4^{2-} at high coverage is observed. Furthermore, the activity of $\text{TiO}_2(\text{a})$ -supported catalysts is about 20 times as high as the activity of $\gamma\text{-Al}_2\text{O}_3$ supported catalysts. This strongly points to the presence of a positive chemical influence of $\text{TiO}_2(\text{a})$ supported vanadate on the catalytically active palladium sites.

Although most catalysts deactivate slowly at low partial pressures of oxygen, a high stability was arrived at by omitting the calcination procedure during catalyst preparation.

Introduction

Terminal alkenes can be oxidized to the corresponding methyl ketones through Wacker oxidation (eq. (1)) [1].



As is well-known, the homogeneous Wacker catalyst consists of an aqueous solution of PdCl_2 and CuCl_2 dissolved in an excess of hydrochloric acid. Technological disadvantages of the Wacker process are the highly corrosive properties of the excess HCl in combination with oxygen, the unwanted formation of chlorinated byproducts and the difficulty of separation of the products from the aqueous reaction mixture when starting from C_3 or higher alkenes.

These difficulties are largely circumvented by heterogenization of the catalyst. For this purpose Evin *et al.* and Forni *et al.* replaced the Cu(I)/Cu(II) redox couple by the $\text{V}_2\text{O}_4/\text{V}_2\text{O}_5$ couple, which was attached to the surface of an $\alpha\text{-Al}_2\text{O}_3$ support [2]. However, though such a catalyst appears to be active indeed, it suffers from deactivation in relatively short periods.

Recently, a new stable heterogeneous surface vanadate Wacker catalyst, supported on $\gamma\text{-Al}_2\text{O}_3$, was introduced by van der Steen *et al.* [3]. The performance of this catalyst in the oxidation of ethylene to acetaldehyde [4], in the oxidation of 1-butene to butanone [5] and in the oxidation of styrene to acetophenone and benzaldehyde [6] has been reported earlier. The kinetics of these heterogeneous oxidation reactions appeared to correspond largely to the kinetics found when applying the homogeneous Wacker catalyst.

However, $\text{TiO}_2(\text{a})$ supported catalysts appeared to be much more active in Wacker oxidation than catalysts supported on $\gamma\text{-Al}_2\text{O}_3$ [4]. An exceptional behaviour of $\text{TiO}_2(\text{a})$ supported vanadate has also been reported in the case of selective oxidation of *o*-xylene to phthalic anhydride [7] and in the selective reduction of NO_x in the presence of oxygen [8].

The question arises in which way $\text{TiO}_2(\text{a})$ exerts its activating action, because the actual active site is the palladium complex and not the $\text{TiO}_2(\text{a})$ supported vanadate. This problem forms the subject of the present Chapter.

Experimental

Chemicals

Oxygen, nitrogen and ethylene (in cylinders) were obtained from Air Products (U.S.A.). The nitrogen and the ethylene were of high purity and the oxygen was of industrial grade. Water was distilled twice. PdCl₂, analytical grade, was obtained from Drijfhout (The Netherlands). HCl and H₂SO₄, analytical grade, were purchased from Baker (The Netherlands). NH₄VO₃, also analytical grade, was purchased from Merck (F.R.G.). γ -Al₂O₃, type 000-3P, S(BET) = 250 m².g⁻¹, was supplied by Akzo (the Netherlands) and TiO₂(anatase), type CRS 31 LOT 2, S(BET) = 127 m².g⁻¹, was obtained from Rhône Poulenc (France).

Apparatus

The catalytic performance has been studied in a continuous-flow fixed-bed stainless-steel reactor, internal diameter 1 cm and length 10 cm, at a total pressure of 0.11 MPa and over the temperature range from 363 to 393 K. All gases were dried over molecular sieves and the composition of the feed was regulated by means of mass-flow controllers (Inacom, The Netherlands). Water was dosed to the feed by leading finely divided bubbles of nitrogen through a thermostatted flask filled with water. Off-gas analysis was performed gas chromatographically, applying a Porapak QS column, length 100 cm, diameter 3 mm, at 423 K. Peak areas were recorded and integrated by a microcomputer (Digital LCI 11/03, U.S.A.). The C₂H₄ conversion was found to range from 15 % to 30 %. This, together with the fact that the reaction is first order with respect to ethylene, means that we are dealing with integral reactor behaviour. Therefore, the reaction rates were recalculated to their differential values.

Catalyst preparation

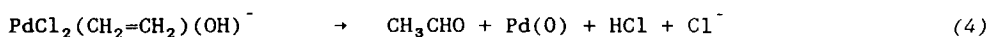
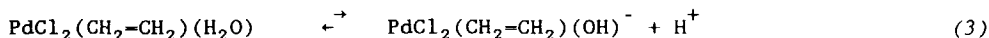
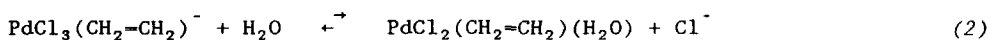
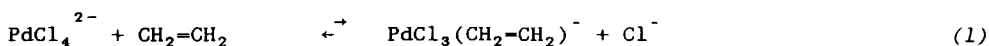
The TiO₂(a) pellets were crushed and sieved to particles with diameters of from 425 to 600 μ m. By leading an NH₄VO₃ solution of pH = 4 over these particles at 293 K, following the method described by Roozeboom *et al.* [9], the surface was covered with a vanadate monolayer. The particles were then calcined in air at 673 K for 4 h. From titration with Fe(II), the vanadium coverage was found to correspond to 4.7 vanadium atoms per nm². Next, through impregnation to incipient wetness with a solution of H₂PdCl₄,

followed by drying at 353 K, the vanadate layer was covered with a sub-monolayer of the Pd compound.

The $\gamma\text{-Al}_2\text{O}_3$ pellets were also crushed and sieved to particles with diameters of from 425 to 600 μm . The vanadate monolayer on $\gamma\text{-Al}_2\text{O}_3$ was prepared analogously to the $\text{TiO}_2(\text{a})$ supported vanadate monolayer, except for the preparation temperature, which was 343 K. A vanadium coverage of 3.9 vanadium atoms per nm^2 was attained.

Results and discussion

Traditionally, the mechanism of homogeneous Wacker oxidation is believed to consist of three equilibrium reactions preceding the rate-determining step:



Reaction step (4) is made up of at least three elementary steps. The overall kinetics are in accordance with the above mechanism (eq. (5)) [10]:

$$r = k \cdot \frac{[\text{PdCl}_4^{2-}][\text{CH}_2=\text{CH}_2]}{[\text{H}^+][\text{Cl}^-]^2} \quad (5)$$

The kinetics of ethylene [4], 1-butene [5] and styrene [6] oxidation over the $\gamma\text{-Al}_2\text{O}_3$ supported heterogeneous catalyst have been reported before. From these studies it appeared that in the heterogeneous case equation (5) is valid as well, provided concentrations are replaced by coverages. The kinetics of ethylene oxidation over a $\text{TiO}_2(\text{a})$ supported catalyst will now be reported.

In Fig. 1 the activity of the catalyst, expressed per Pd site and calculated from the Langmuir equation at a low coverage of C_2H_4 , is plotted as a function of the vanadate coverage on $\gamma\text{-Al}_2\text{O}_3$ and on $\text{TiO}_2(\text{a})$. In the

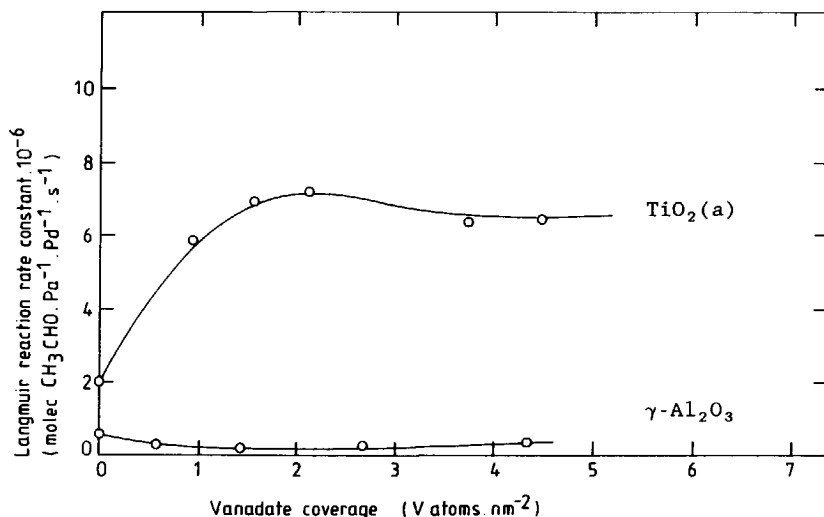


Figure 1. Activity, given in the form of the reaction rate per Pd site, calculated from the Langmuir equation at low coverage of C₂H₄ (molecules of CH₃CHO . Pa(C₂H₄)⁻¹ . Pd atom⁻¹ . s⁻¹), as a function of the vanadate coverage. Catalysts: γ-Al₂O₃: 0.19 mmol PdCl₂ . g⁻¹, 0.96 mmol Cl⁻ . g⁻¹, variable Al₂O₃/V₂O₅ ratio; 1 g of catalyst. TiO₂(a): 0.089 mmol PdCl₂ . g⁻¹, 0.48 mmol Cl⁻ . g⁻¹, variable TiO₂(a)/V₂O₅ ratio; 0.5 g of catalyst. Composition of the feed: 6.5 mol % H₂O, variable C₂H₄/air ratio; 1.67 ml STP . s⁻¹; 373 K; 0.11 MPa total pressure.

case of γ-Al₂O₃ only a weak influence of vanadate on the reaction rate is found. At low vanadate coverages, from 0 to 1.5 V atoms . nm⁻², the initial activity decreases somewhat with increasing coverage, and in this range the catalysts suffer from deactivation in relatively short periods. At coverages higher than 1.5 V atoms . nm⁻² only a slight increase of the activity with increasing coverage is found.

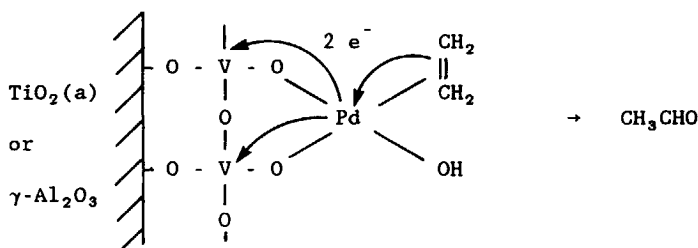


Figure 2. Interaction between the vanadate monolayer and the catalytically active Pd(II) site.

- 8. Anatase supported catalysts -

However, when $\text{TiO}_2(\text{a})$ is used as a support, the activity of the catalyst strongly increases with increasing coverage up to about $1.5 \text{ V atoms.nm}^{-2}$, whereas at increasing coverage above $1.5 \text{ V atoms.nm}^{-2}$ a stable and high activity level is observed. At these high coverages the activity of $\text{TiO}_2(\text{a})$ supported catalysts is about twenty times as high as the activity of $\gamma\text{-Al}_2\text{O}_3$ based catalysts and this points to a positive influence of $\text{TiO}_2(\text{a})$

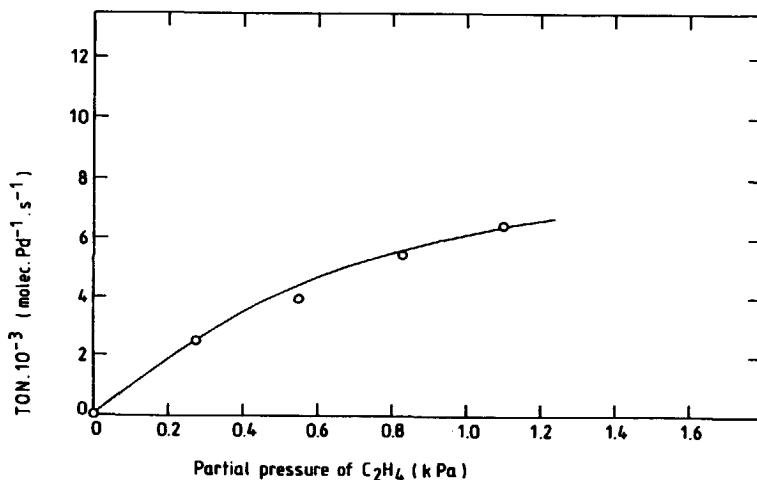


Figure 3. TON as a function of the partial ethylene pressure. The solid line represents the theoretical Langmuir curve. Catalyst: 88.2 mol % TiO_2 , 3.3 mol % V_2O_5 , 7.76 mol % HCl , 0.68 mol % PdCl_2 ; 0.5 g of catalyst. Composition of the feed: 6.5 mol % H_2O , variable $\text{C}_2\text{H}_4/\text{air}$ ratio; 373 K, 0.11 MPa total pressure, $1.67 \text{ ml STP.s}^{-1}$.

supported vanadate on the catalytic activity of the Pd(II) sites. This leads us to the supposition that a permanent chemical bond exists between the chemisorbed vanadate layer and the catalytically active palladium centre, as schematically represented in Fig. 2. The $\text{TiO}_2(\text{a})/\text{V}_2\text{O}_5$ -layer is thought to have an activating influence on the palladium site via this bond and thus influences the kinetics of the reaction. Furthermore, this would mean that we are dealing with a concerted reaction, viz. the oxidation of ethylene to acetaldehyde and simultaneous reduction of the V(V) to V(IV). Hence, no zero-valent palladium is formed as is assumed in the classical formulation of the Wacker mechanism. Other redox couples based on copper [11], $\text{Cr}_2\text{O}_7^{2-}$

[12] and heteropolyacids [13] also positively influence the reaction rate and in these cases a chemical bond between the redox couple and the catalytic palladium centre will also be present.

As shown clearly in Fig. 3 the turnover number (TON) increases with increasing partial ethylene pressure; the course of the curve points to a

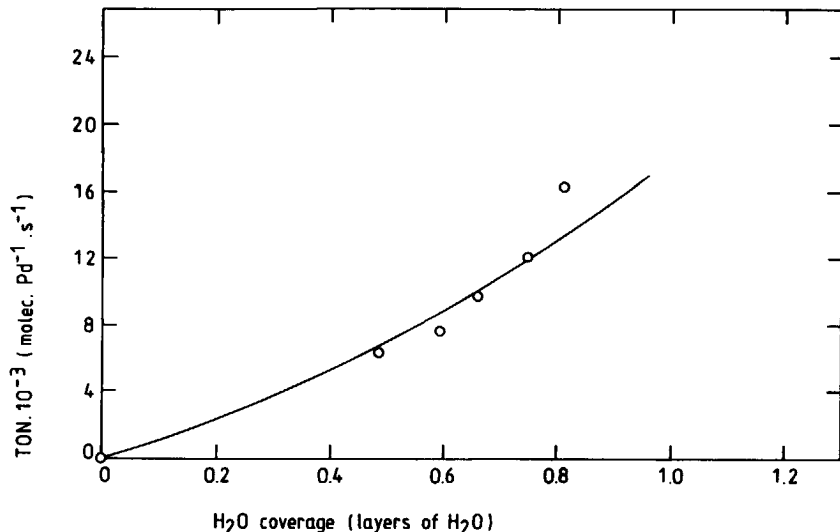


Figure 4. TON as a function of the water coverage. Catalyst: 90.3 mol % TiO₂, 3.4 mol % V₂O₅, 5.6 mol % HCl, 0.70 mol % PdCl₂; 0.5 g of catalyst. Composition of the feed: 1 % C₂H₄, variable H₂O/air ratio; total flow 1.67 ml STP · s⁻¹, 373 K, 0.11 MPa total pressure.

Langmuir-type relationship between the TON and $p(\text{C}_2\text{H}_4)$, in accordance with equilibrium (1).

In Fig. 4 the TON is plotted as a function of the water coverage. From equilibrium (2) a first order dependence of the reaction rate on the water coverage is to be expected. In the homogeneous Wacker oxidation the solvent water is present in excess and therefore no influence of the water concentration on the reaction rate can be measured. However, in the present study (Fig. 4) and also in preceding studies [4-6] a first order dependence of the reaction rate on the water coverage was found indeed, in accordance with eq. (2).

The dependence of the TON on the partial oxygen pressure is depicted in Fig. 5. When $\gamma\text{-Al}_2\text{O}_3$ is used as a support a zero order dependence of the

TON on the partial pressure of oxygen is found, but a negative order with respect to oxygen is found in the $\text{TiO}_2(\text{a})$ case. This is probably due to reaction of oxygen with the catalytically active palladium sites. This reaction appeared to be reversible.

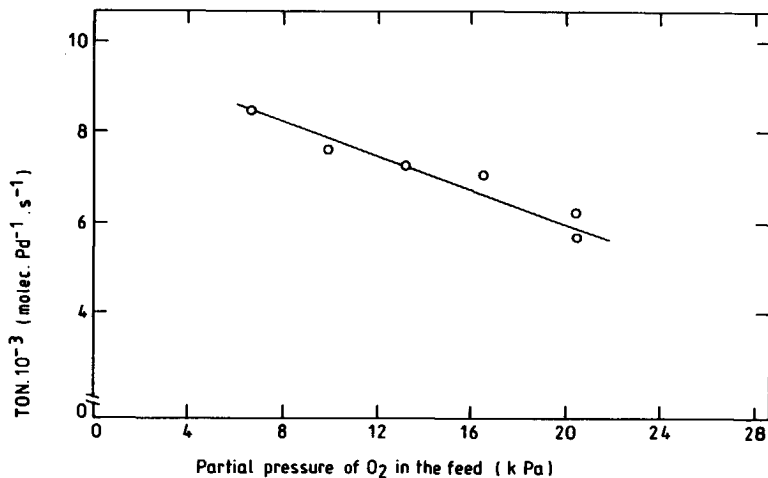


Figure 5. TON as a function of the partial oxygen pressure. Catalyst as given in the legend of Fig. 4. Composition of the feed: 1 mol % C_2H_4 , variable O_2/N_2 ratio; total flow: $1.67 \text{ ml STP} \cdot \text{s}^{-1}$, 373 K, 0.11 MPa total pressure.

Fig. 6 represents the turn-over number as a function of the PdCl_4^{2-} coverage. At low coverages, below $0.5 \text{ Pd atoms} \cdot \text{nm}^{-2}$, a positive influence of the coverage on the reaction rate is found, in accordance with *equilibrium (1)*. However, at a higher coverage, the influence becomes zero order with respect to coverage; this is contrary to *equilibrium (1)* and difficult to explain. Perhaps only part of the palladium complexes is strongly bound to the redox surface. From Fig. 1 one might conclude that such strongly bound palladium sites are already present at a low vanadate coverage. Further research is needed to clarify this point.

The dependence of the reaction rate on the chloride coverage is plotted in Fig. 7. It is seen that the chloride coverage hardly influences the reaction rate, contrary to what is to be expected on the basis of *equilibria (1) and (2)*, which predict an order of minus 2 with respect to chloride coverage. For the time being no explanation is available.

- 8. Anatase supported catalysts -

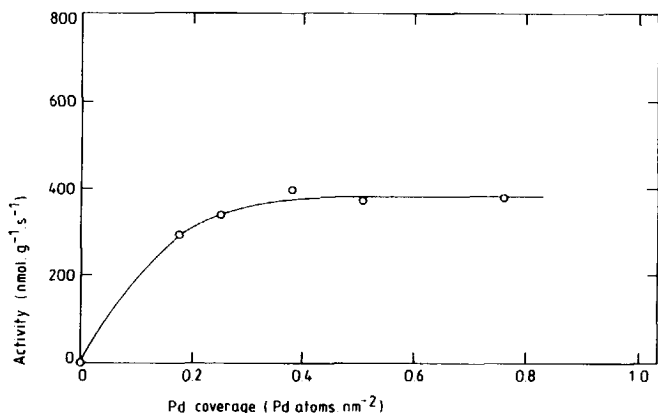


Figure 6. TON as a function of the PdCl_4^{2-} coverage. Catalyst: $0.43 \text{ mmol V}_2\text{O}_5 \cdot \text{g}^{-1}$, $1.789 \text{ mmol Cl}^- \cdot \text{g}^{-1}$, variable $\text{TiO}_2/\text{PdCl}_2$ ratio; 0.5 g of catalyst. Composition of the feed: $0.75 \text{ mol \% C}_2\text{H}_4$, $6.5 \text{ mol \% H}_2\text{O}$, 18.5 mol \% O_2 , 74.2 mol \% N_2 ; total flow $1.67 \text{ ml STP} \cdot \text{s}^{-1}$, 373 K , 0.11 MPa total pressure.

The stability of the catalyst appeared to be related to the partial oxygen pressure. At 18.6 \% oxygen in the feed (at 20.5 KPa partial oxygen pressure) the catalyst half life is 120 h , but at lower oxygen pressures the stability decreases to a half life of 30 h at 6 \% oxygen (6.6 KPa partial

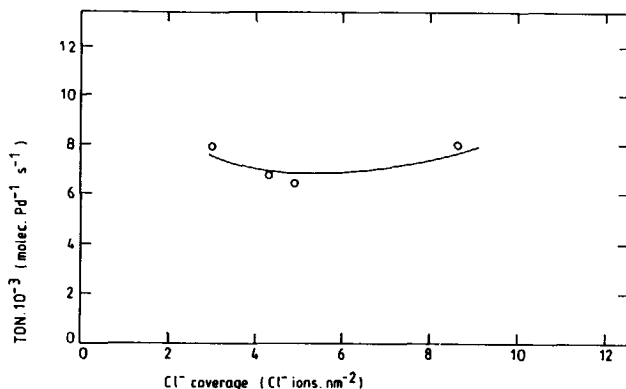


Figure 7. TON as a function of the chloride coverage. Catalyst: $0.43 \text{ mmol V}_2\text{O}_5 \cdot \text{g}^{-1}$, $0.089 \text{ mmol PdCl}_2 \cdot \text{g}^{-1}$, variable TiO_2/HCl ratio; 0.5 g of catalyst. Composition of the feed: $1 \text{ mol \% C}_2\text{H}_4$, $6.5 \text{ mol \% H}_2\text{O}$, 18.5 mol \% O_2 , 74.0 mol \% N_2 ; $1.67 \text{ ml STP} \cdot \text{s}^{-1}$, 373 K , 0.11 MPa total pressure.

oxygen pressure) in the feed. Deactivation was found to be related to the formation of catalytic crystalline Pd(0) in the case of $\gamma\text{-Al}_2\text{O}_3$ as a support. Zero-valent palladium is probably also formed when $\text{TiO}_2(\text{a})$ supported catalysts are used.

The stability and activity of the catalysts are strongly influenced by the calcination procedure during catalyst preparation. As is plotted in Fig. 8, omittance of the calcination procedure led to an excellent stability

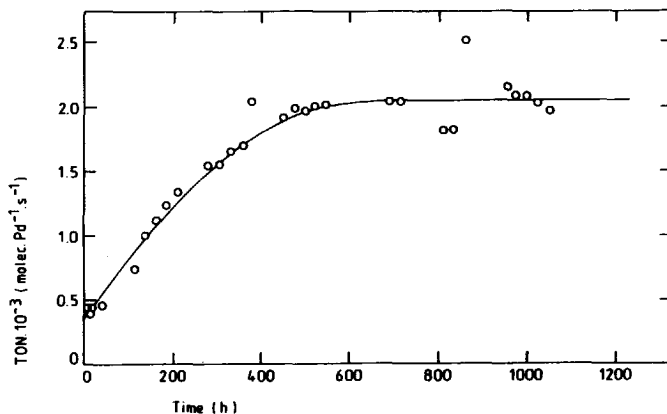


Figure 8. TON as a function of time. Conditions as indicated in the legend of Fig. 5. 6 % mol O_2 in the feed.

during 1200 h at a somewhat lower activity, related to the calcined catalyst. The reasons for these unexpected differences in activity and stability are yet unclear, but are due to alterations of the catalyst during calcination of the monolayer. By calcination ammonia, originating from ammonium metavanadate, is set free and probably also recrystallisation of the vanadate monolayer occurs. In Fig. 8 the somewhat lower activity and probably also the higher stability can be ascribed to the presence of ammonia, as ammonia causes retardation of the Wacker reaction rate [14].

From rate measurements at temperatures ranging from 353 K to 413 K an apparent activation energy of $36 \text{ kJ}\cdot\text{mol}^{-1}$ was calculated. The same value was found in the case of oxidation of ethylene over $\gamma\text{-Al}_2\text{O}_3$ supported catalysts [4], which is indicative of the occurrence of analogous mechanisms in both cases. On the other hand, the high activity of $\text{TiO}_2(\text{a})$ supported catalysts relative to $\gamma\text{-Al}_2\text{O}_3$ supported ones and the anomalies in the kinetics point to the occurrence of different mechanisms.

Conclusions

The activity of $\text{TiO}_2(\text{a})$ supported Wacker catalysts in the oxidation of ethylene to acetaldehyde is surprisingly high, about 20 times as high as the activity of $\gamma\text{-Al}_2\text{O}_3$ supported catalysts. This points to a chemical interaction between the catalytically active palladium centre and the monolayer vanadate. A concerted formation of acetaldehyde and reduction of the monolayer vanadate is proposed.

The kinetics with respect to the partial C_2H_4 and H_2O pressures and with respect to the PdCl_4^{2-} coverage are in accordance with expectation. Increasing partial oxygen pressures lead to a decrease in the activity, probably due to a reaction of oxygen with palladium yielding palladium oxide.

However, an exceptional behaviour of the reaction rate with respect to the Cl^- coverage and with respect to the PdCl_4^{2-} at higher coverage is observed. In both cases a nearly zero order behaviour is found. The reason for this is unclear, and further research is needed to clarify these phenomena.

The catalysts appeared to be stable for longer periods of time. However, at low partial oxygen pressures the catalyst deactivates, perhaps due to the formation of crystalline zero-valent palladium clusters.

References

1. J. Smidt, W. Hafner, R. Jira, J. Sedlmeier, R. Sieber, R. Ruttinger and H. Kojer, *Angew. Chem.*, 71 (1959) 176.
2. A.B. Evnin, J.A. Rabo and P.H. Kasai, *J. Catal.*, 30 (1973) 109; L. Forni and G. Terzoni, *Ind. Eng. Chem. Process Des. Dev.*, 16 (1977) 288.
3. P.J. van der Steen, *Thesis*, Delft University, (1987); J.J.F. Scholten and P.J. van der Steen, *Eur. Pat. Spec.*, 0210705, d.d. 22.03.1989.
4. E. van der Heide, M. de Wind, A.W. Gerritsen and J.J.F. Scholten, *Proc. 9th Int. Congr. Catal.*, Calgary, (1988), 4, 1648.
5. E. van der Heide, J.A.M. Ammerlaan, A.W. Gerritsen and J.J.F. Scholten, *J. Molec. Catal.*, 55 (1989) 320.

- 8. Anatase supported catalysts -

6. E. van der Heide, J. Schenk, A.W. Gerritsen and J.J.F. Scholten, Recl. Trav. Chim. Pays-Bas, 109 (1990) 93.
7. G.C. Bond and P. König, J. Catal., 77 (1982) 309; A.J. van Hengstum, J.G. van Ommen, H. Bosch and P.J. Gellings, Proc. 8th Int. Congr. Catal., Berlin, 4 (1984) 297.
8. H. Bosch, F.J.J.G. Janssen, F.M.G. van den Kerkhof, J. Oldenziel, J.G. van Ommen and J.R.H. Ross, Appl. Catal., 25 (1986) 239.
9. F. Roozeboom, T. Fransen, P. Mars and P.J. Gellings, Z. Anorg. Allg. Chem., 499 (1979) 25.
10. J.M. Henry, J. Am. Chem. Soc., 86 (1964) 2346; J.M. Henry, J. Am. Chem. Soc., 88 (1966) 1595.
11. P.M. Henry: Palladium Catalyzed Oxidations of Hydrocarbons, Reidel, Dordrecht, (1980); P. François, Ann. Chim. (Paris), 4 (1969) 371.
12. N.B. Shitova, L.I. Kuznetsova and K.I. Matveev, Kinet. Katal., 15 (1974) 72.
13. K.I. Matveev, Kinet. Katal., 18 (1977) 862.
14. P.M. Henry: Palladium Catalyzed Oxidation of Hydrocarbons, Reidel, Dordrecht (1980).

Kinetics and mechanism of the reduction of vanadate monolayers by hydrogen spilt over from palladium

Abstract

Vanadate monolayers chemisorbed on γ -Al₂O₃ were reduced by hydrogen spilt over from palladium, in the temperature range from 353 K to 413 K. In all experiments the final vanadate valency was found to be about 3.55.

The rate of reduction is determined by the rate of surface migration of the hydrogen atoms; a theoretical model was developed which describes the kinetics of this migration process. With this model the change of the vanadium valence state as a function of time could be described quite well. Reduction rates were measured and calculated, starting from initial loadings of 0.5 wt % to 6.8 wt % palladium chloride, and from the results a diffusion coefficient for the surface migration of hydrogen atoms of $1.10 \cdot 10^{-16} \text{ m}^2 \cdot \text{s}^{-1}$ was calculated. The surface diffusion coefficient was found to decrease with decreasing vanadate coverage.

When TiO₂(anatase) was used as a support a faster reduction of the vanadate monolayer occurred, the surface diffusion coefficient being $2.10 \cdot 10^{-15} \text{ m}^2 \cdot \text{s}^{-1}$.

From measurements at temperatures ranging from 363 K to 403 K an apparent activation energy for surface migration of 87 kJ.mol⁻¹ was calculated. When dihydrogen was replaced by dideuterium, an apparent kinetic isotope effect $D_{\text{H}} / D_{\text{D}}$ of 1.1 was found.

Introduction

In catalysis many examples of hydrogen spillover are known. For instance, in the case of supported platinum metals, hydrogen is dissociatively chemisorbed on the metal, followed by spillover to the support and migration of hydrogen atoms over the support to H accepting sites. The spilt-over hydrogen atoms may reside on the surface, diffuse into the bulk, give rise to partial reduction of the support or react with adsorbed molecules. Reviews are published in refs. [1,2,3].

The role of hydrogen spillover in catalysis has been studied in *e.g.* the hydrogenation of ethylene, cyclohexene and benzene and in the hydrogenolysis of thiophene [2].

Spilt-over hydrogen atoms are difficult to detect. Indirect methods like dihydrogen chemisorption and desorption and reduction of suitable oxidation agents are widely applied [3]. Well-known examples of oxidation agents are MoO_3 , WO_3 and V_2O_5 ; through reduction by spilt-over hydrogen the corresponding hydrogen bronzes are formed. These bronzes may be represented by H_xMoO_3 , H_xWO_3 and $\text{H}_x\text{V}_2\text{O}_5$, with reported x values of 1.63, 0.46 and 3.80, respectively [4,5].

The kinetics of the reduction of these oxides by spilt-over hydrogen in the presence of palladium or platinum are reported. These kinetics appear to be rather complicated [5,6], probably due to the occurrence of a combination of a fast reduction of the surface and a slow reduction of the bulk of the oxide. By studying the reduction of oxides in the form of a chemisorbed monolayer this complication is circumvented, because when vanadate monolayers are reduced by hydrogen spilt over from palladium, only the fast surface reduction will occur.

It was shown recently that a sub-monolayer of a palladium salt adsorbed on a supported vanadate monolayer forms an active heterogeneous catalyst for the Wacker oxidation of alkenes [7]. Reduction/oxidation cycles of the vanadate layer play a part in the reaction mechanism. It also appeared that Wacker oxidation of an alkene is possible in the absence of gaseous dioxygen (Chapter 10). In that case oxygen from the vanadate monolayer is gradually depleted, most probably by reaction with hydrogen atoms spilt over from palladium complexes to the vanadate monolayer.

In view of the foregoing we thought it worthwhile to make a separate study of the reduction of adsorbed vanadate monolayers by hydrogen spilt over from small palladium crystallites. We now report on the kinetics and mechanism of this last process. The results will be described by computer modelling of the reaction.

Experimental

Chemicals

Hydrogen and deuterium (in cylinders) were obtained from Air Products (U.S.A.) and from Union Carbide Corporation (U.S.A.), respectively. Water was distilled before use. PdCl_2 and PdSO_4 , analytical grade, were obtained from Drijfhout (The Netherlands). HCl and H_2SO_4 , analytical grade, were purchased from Baker (The Netherlands). NH_4VO_3 , also analytical grade, was purchased from Merck (F.R.G.). $\gamma\text{-Al}_2\text{O}_3$, type 000-3P, $S(\text{BET}) = 250 \text{ m}^2.\text{g}^{-1}$, was supplied by Akzo (The Netherlands) and TiO_2 (anatase), type CRS 31 LOT 2, $S(\text{BET}) = 127 \text{ m}^2.\text{g}^{-1}$, was obtained from Rhône Poulenc (France).

Apparatus

Volumetric dihydrogen adsorption measurements, in the pressure range from 0.133 to $1.33 \cdot 10^4$ Pa, were carried out in a glass apparatus provided with a Baratron type 310CA - 00100 pressure gauge connected to a signal conditioner type 270 B, from MKS (U.S.A.). Teflon stopcocks enabled evacuation to 10^{-4} Pa. In batch experiments, the catalysts were dried *in situ* at 423 K at 10^{-2} Pa for 16 h and were afterwards reduced by dihydrogen at 373 K and at $8 \cdot 10^3$ Pa initial pressure.

The palladium dispersion, after reduction of freshly prepared catalysts in a 3 % H_2/He stream, was determined from the extent of CO chemisorption as determined by pulsing CO in a stream of dihydrogen. The CO/Pd surface stoichiometry was assumed to be unity.

Reaction modelling was performed making use of an Olivetti M24 personal computer (Italy).

Catalyst preparation

The γ - Al_2O_3 pellets were crushed and sieved to particles with diameters from 425 to 600 μm . By leading an NH_4VO_3 solution of $\text{pH} = 4$ at 343 K over these particles, following the method described by Roozeboom *et al.* [8], the surface was covered with an aluminovanadate monolayer. Next, the particles were calcined in air at 673 K for 4 h. From titration with Fe(II), the vanadium coverage was found to correspond to 3.9 vanadium atoms per nm^2 . Lower vanadate coverages were realized by wet impregnation of the particles at 293 K with measured amounts of an NH_4VO_3 solution at $\text{pH} = 4$.

Next, through impregnation to incipient wetness with a solution of H_2PdCl_4 , followed by drying at 353 K, the aluminovanadate layer was covered with a sub-monolayer of the Pd compound.

$\text{TiO}_2(\text{a})$ supported catalysts were prepared in the same way, except for the temperature of monolayer preparation, which was 293 K. A monolayer coverage of 4.7 V atoms. nm^{-2} was attained.

Theory

Reduction of vanadate monolayers by hydrogen spilt over from palladium proceeds via a number of consecutive reaction steps (Fig. 1). First the palladium salt is rapidly reduced to Pd metal. Then dihydrogen is dissociatively chemisorbed on two palladium sites and the hydrogen atoms migrate over the surface of the palladium cluster (reactions 1 and 2, respectively).

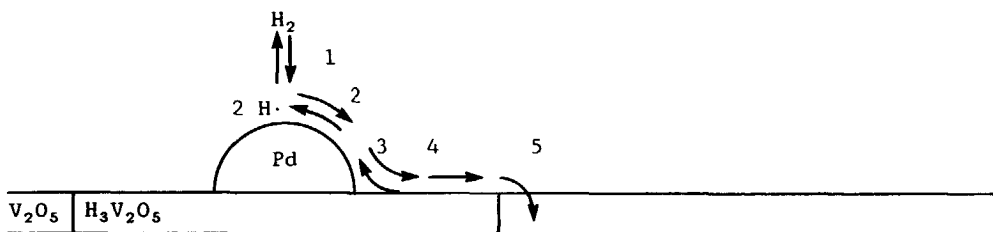


Figure 1. Reaction steps in the reduction of a vanadate monolayer by hydrogen atoms spilt over from palladium

Via spillover the hydrogen atoms arrive at the vanadate monolayer, where $V(V)$ is reduced. Then the hydrogen atoms migrate over reduced vanadate sites, until new $V(V)$ sites are reached, which, in turn, are reduced (reactions 3, 4 and 5, respectively).

Surface migration of hydrogen originating from a point source, a palladium crystallite in our case, can be described by the diffusion eq. (1) [9]:

$$\frac{\partial c}{\partial t} = -D \left[\frac{\partial^2 c}{\partial r^2} + \frac{1}{r} \cdot \frac{\partial c}{\partial r} \right] \quad (1)$$

where c represents the surface concentration of hydrogen atoms at a distance r from the point source at time t and D indicates the surface diffusion coefficient.

The boundary conditions are represented by eqs. (2) and (3):

$$r = r_0 \rightarrow c = c_0 \quad (2)$$

$$r = R_t \rightarrow c = 0 \quad (3)$$

where r_0 stands for the mean radius of the palladium crystallites, c_0 is the surface concentration of hydrogen atoms at distance r_0 and R_t signifies the radius of the circle of reduced vanadate around the palladium crystallite. It should be noted that c_0 and R_t are functions of time.

In solving differential eq. (1) it is assumed that the number of hydrogen atoms reacting with the vanadate monolayer per nm^2 by far exceeds the mobile hydrogen atom coverage, which means that accumulation of hydrogen atoms is negligible. Hence, dc/dt is assumed to be zero and eq. (1) can be solved, resulting in eq. (4):

$$\frac{c}{c_0} = \frac{\ln(R_t/r)}{\ln(R_t/r_0)} \quad (4)$$

- 9. Hydrogen spillover -

Taking the material balances into consideration, the hydrogen flow can be represented in three ways (eqs. (5) - (7)) :

$$\Phi_{H_2} = - D \cdot \pi \cdot R_t \cdot nPd \cdot m \cdot \left(\frac{dc}{dr} \right)_{R_t} \quad (5)$$

$$\Phi_{H_2} = \pi \cdot R_t \cdot c_v \cdot \beta \cdot nPd \cdot m \cdot \frac{dR_t}{dt} \quad (6)$$

$$\Phi_{H_2} = - \frac{V}{RT} \cdot \frac{dP}{dt} \quad (7)$$

where nPd represents the number of palladium crystallites per g of catalyst, m is the catalyst weight, c_v is defined as mol V per m^2 and the factor β is the number of H atoms consumed during reduction of one V atom. P represents the dihydrogen gas pressure and V is the total gas volume. R is the gas constant ($8.3144 \text{ Pa} \cdot \text{m}^3 \cdot \text{mol}^{-1} \cdot \text{K}^{-1}$) and T is the temperature.

The derivative of R_t with respect to time (eq. (8)), and the derivative of the pressure with respect to time (eq. (9)) are found by combining eqs. (5), (6) and (7) :

$$\frac{dR_t}{dt} = - \frac{D}{c_v \cdot \beta} \cdot \left[\frac{dc}{dr} \right]_{R_t} \quad (8)$$

$$\frac{dP}{dt} = \frac{D \cdot \pi \cdot R_t \cdot nPd \cdot m \cdot R \cdot T}{V} \cdot \left[\frac{dc}{dr} \right]_{R_t} \quad (9)$$

The dependence of the surface concentration of hydrogen on the distance r from the centre of the palladium crystallite was already given in eq. (4). Via the Runge-Kutta procedure both equations (8) and (9) were solved simultaneously and in this way the change of P as a function of t could be calculated.

The mathematical model presented above gives an accurate description of the experimental results at the start of reduction. However, after longer

reduction times an increasing departure of experimental results from theory is observed. This is due to overlap of the extending circles of reduced vanadate around the palladium crystallites, leading to experimental reduction rates lower than the theoretical rates. Therefore, a correction factor was introduced, starting from a Gauss distribution of the position of the palladium crystallites. When two palladium crystallites at mutual distance r are considered, the vanadate layer in between the crystallites will be reduced up to a distance $1/2 r$ from the crystallites. Further reduction in the direction of the line connecting the two crystallites is not possible. Therefore, the correction factor, corresponding to the fraction of non-reduced vanadate, could be presented as given in eq. (10):

$$X_r = 1 - \int_0^{2r} (Pd)_r \cdot dr \quad (10)$$

where X_r is the fraction of the non-reduced vanadate found at a distance r from the palladium crystallite and $(Pd)_r$ represents the Gauss distribution of the palladium crystallites over the surface as a function of the distance r . The calculated changes of the P values are corrected by this factor. Only the nearest neighbour palladium crystallites are considered.

Integration of the Gauss distribution was performed by applying a Taylor series. In the simulation of hydrogen spillover the Gaussian σ -value was varied, but it never exceeded a value of 0.4 times the average distance between the palladium clusters. The surface diffusion coefficient D was found to be independent of the Gaussian σ -value chosen and was inversely proportional to the c_0 values.

One should keep in mind that, before hydrogen spillover commences, hydrogen is consumed for the reduction of the palladium salt. All spillover measurements were corrected for this.

In order to be able to carry out the computer calculations, knowledge of the following quantities is needed:

- the mean radius of the palladium crystallites, r_0 ,
- the maximum hydrogen surface concentration, c_0 , and
- the Gaussian σ -value.

- 9. Hydrogen spillover -

After reduction of the freshly prepared catalyst in a stream of 3 % dihydrogen in helium at 373 K, the palladium dispersion was determined from the extent of carbon monoxide chemisorption at 273 K. The metallic dispersion was found to be 0.65, which corresponds to a mean radius of the palladium crystallites of 1.0 nm (about 175 Pd atoms per crystallite). In the calculations it was assumed that the Pd crystallites are hemispherical in shape and are bound to the vanadate layer via the flat part of their surface. For c_0 , a value of 2.10^{-2} H atoms per nm^2 , at a dihydrogen pressure of 8.10^3 Pa, as reported by Kramer and Andre [10], was taken. Although a Langmuir relation between c_0 and P is to be expected, a linear relationship between c_0 and P was assumed, which holds for the low-pressure part of a Langmuir isotherm.

In all experiments the final average vanadium valency, as calculated from the total dihydrogen uptake up to termination of spillover, was found to be about 3.55, which corresponds to a stoichiometry $\text{H}_x\text{V}_2\text{O}_5$, with x being 2.9 ± 0.2 .

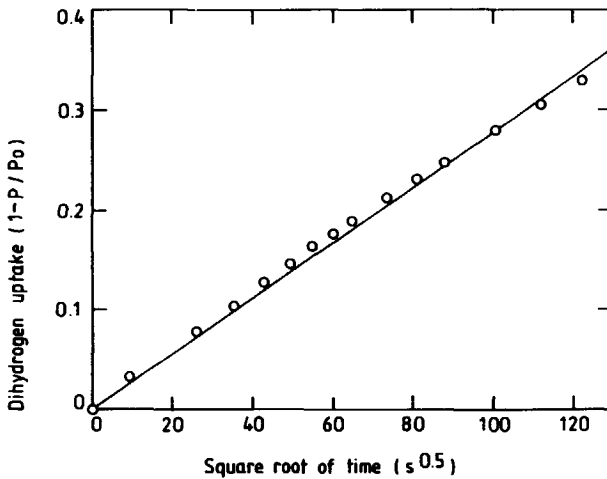


Figure 2. Reduction of a vanadate monolayer by hydrogen spilt over from palladium crystallites. Catalyst: 0.17 mol % PdCl_2 , 1.4 mol % HCl , 8.2 mol % V_2O_5 and 89.9 mol % Al_2O_3 . Conditions: temperature: 373 K; starting pressure: 8.10^3 Pa.

Results and discussion

In Fig. 2 the dihydrogen uptake during reduction of a vanadate monolayer by hydrogen spilt over from palladium is plotted as a function of the square root of time. From the linearity of the plot it has to be concluded that diffusional retardation of the reaction plays a part. When the mean diameter of the catalyst particles was varied between 425 μm and 900 μm the rate of reaction did not change, which points to the absence of pore diffusional retardation. It is likely, therefore, that the reaction rate is retarded by reaction step (4), the migration of hydrogen atoms over the reduced vanadate surface.

From thermogravimetric analysis, it followed that in the absence of palladium at temperatures of up to 600 K no vanadate reduction by dihydrogen occurs. Starting with H_2PdCl_4 on the surface, a fast reduction of the vanadate at 373 K or at even lower temperatures was observed. Therefore it

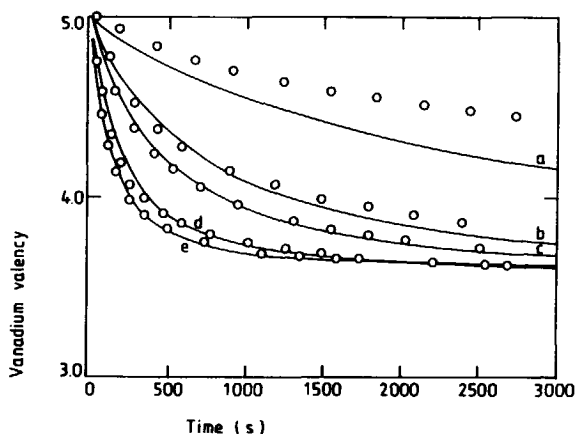


Figure 3. Change of the vanadium valency as a function of time. Catalysts: HCl/PdCl_2 mol ratio = 8; $\text{Al}_2\text{O}_3/\text{V}_2\text{O}_5$ mol ratio = 10.9; curve a: 0.55 wt % PdCl_2 ; curve b: 1.5 wt % PdCl_2 ; curve c: 2.3 wt % PdCl_2 ; curve d: 4.5 wt % PdCl_2 ; curve e: 6.8 wt % PdCl_2 . Conditions: temp. 373 K; initial pressure: 8.10^3 Pa.

has to be concluded that reduction of the vanadate layer is preceded by dissociative chemisorption of dihydrogen on palladium sites created by pre-reduction of the adsorbed sub-monolayer of the palladium salt.

- 9. Hydrogen spillover -

The proposed reaction mechanism is presented in Fig. 1. If one of the reaction steps 1, 2 or 3 (Fig. 1) is rate determining, the rate of hydrogen uptake would be a linear function of pressure. From Fig. 2 it is seen that this is not the case. Hence, migration of spilt-over hydrogen atoms over the reduced vanadate is expected to be the rate determining process. The migration of hydrogen atoms is terminated by a fast reaction with non-reduced vanadate (step 5 in Fig. 1), resulting in the formation of a hydrogen bronze $H_xV_2O_5$ [1].

The change of the vanadium valency, in catalysts with palladium loadings ranging from 0.5 wt % to 6.8 wt %, calculated as palladium chloride, was

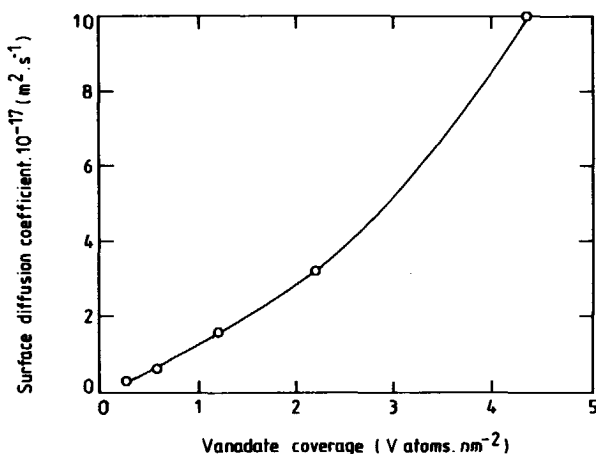


Figure 4. The surface diffusion coefficient as a function of the vanadate coverage. Catalyst: 2.3 wt % PdCl₂; HCl/PdCl₂ mol ratio = 8; variable V₂O₅/Al₂O₃ ratios. Conditions: temp. 373 K; initial pressure 5.10³ Pa.

measured as a function of time and is depicted in Fig. 3. The drawn lines represent the change of the vanadium valencies, as calculated by adopting a surface diffusion coefficient D of $1.10^{-16} \text{ m}^2.\text{s}^{-1}$. The figure clearly shows a good accordance between calculated and measured values, with the exception of the measurements at low palladium coverages, where the rates were found to be lower than calculated. For the time being, the reason for this deviation is not clear. Perhaps the metallic dispersion of the palladium crystallites is influenced by the palladium loading, especially at low loadings. Indeed, from the calculated curves in Fig. 3 and the corresponding

Gauss σ -values the palladium crystallite distribution was found to be broadened at decreasing coverages. The final vanadate valency (3.55) was found to be independent of the palladium loading.

In Fig. 4 the change of the surface diffusion coefficient D is depicted as a function of the vanadate coverage. D increases strongly with increasing coverage, indicating that hydrogen atoms migrate over the vanadate surface more easily than over the surface of $\gamma\text{-Al}_2\text{O}_3$. Vanadium, being a transition metal, can change its valency easily, in contrast to aluminium. Therefore, the higher migration rate over reduced vanadate must be due to the occurrence of oxidation - reduction cycles during the migration process. From Fig. 4 it is seen that the diffusion coefficient increases more strongly as the vanadate coverage increases. Obviously, isolated isles of vanadate on the surface hamper hydrogen migration.

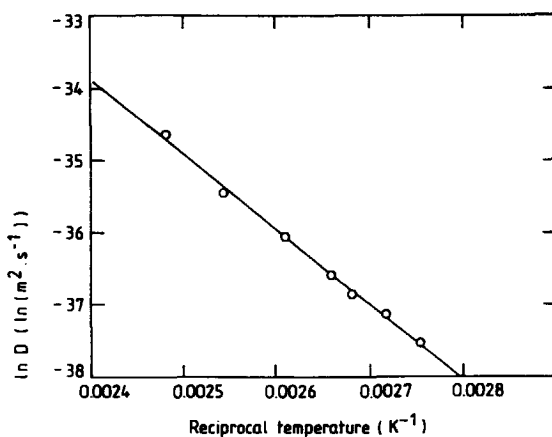


Figure 5. Arrhenius plot of the surface diffusion coefficient. Catalyst: 1.0 mol % PdCl_2 , 8.0 mol % HCl , 7.8 mol % V_2O_5 , 83.3 mol % Al_2O_3 . Conditions: initial pressure: 8.10^3 Pa.

An Arrhenius plot of D , in the temperature range of from 363 K to 403 K, is given in Fig. 5. An apparent activation energy E_a of $87 \text{ kJ} \cdot \text{mol}^{-1}$ was calculated. The high value of E_a points to the occurrence of bond breaking and making during surface migration. Activation energies of the same magnitude are reported in literature [1,10].

From an experiment in which dihydrogen was replaced by dideuterium an

- 9. Hydrogen spillover -

apparent kinetic isotope effect D_H / D_D of only 1.1 was found. This low value is likely to be due to the simultaneous occurrence of a thermodynamic and a kinetic isotope effect. The thermodynamic isotope effect is related to reaction step 1 (Fig. 1) and stems from the fact that the heat of chemisorption of deuterium on palladium is significantly higher than that of dihydrogen. This results in a higher deuterium coverage on palladium as compared with hydrogen coverage at equal pressure. It follows that the surface concentration of spilt-over deuterium will also be high compared

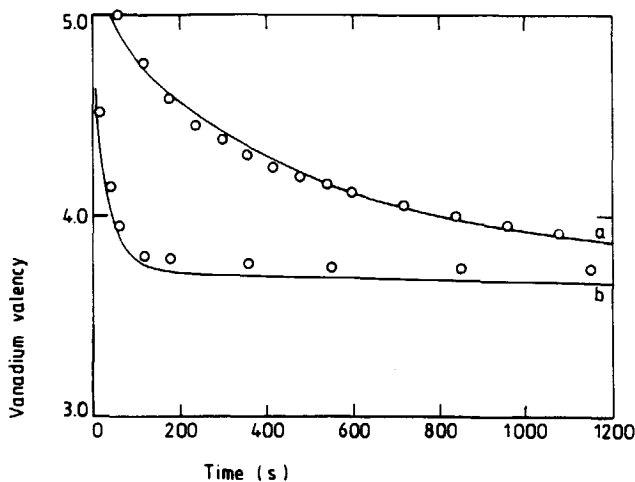


Figure 6. Vanadium valency as a function of time. Catalysts: curve a: 1.3 mol % PdCl₂, 10.0 mol % HCl, 7.6 mol % V₂O₅ and 81.1 mol % Al₂O₃; curve b: 0.5 mol % PdCl₂, 3.8 mol % HCl, 3.1 mol % V₂O₅ and 92.6 mol % TiO₂. Conditions: 373 K, initial pressure: curve a: 8.10³ Pa; curve b: 5.3.10³ Pa.

with hydrogen, which results in an increase of the reaction rate. However, this rate increase is, in turn, diminished by the slower surface migration of D as compared with H. As migration involves bond making and bond breaking of OH· or OD· groups, the migration of deuterium atoms is slower than that of hydrogen atoms.

It is likely that the thermodynamic and the kinetic isotope effects described above counteract one another in such a way that the resulting apparent kinetic isotope effect is nearly unity.

In Fig. 6 the vanadium valency is given as a function of time for a γ -Al₂O₃ supported catalyst as well as for a TiO₂(a) supported one. The

figure clearly shows the high reduction rate of the $\text{TiO}_2(\text{a})$ supported vanadate relative to $\gamma\text{-Al}_2\text{O}_3$ supported vanadate. A surface diffusion coefficient of $2.10^{-15} \text{ m}^2.\text{s}^{-1}$ was found, which exceeds the surface diffusion coefficient found with $\gamma\text{-Al}_2\text{O}_3$ supported vanadate by a factor of 20. Obviously, titanium dioxide, being a transition metal oxide, accelerates the migration of hydrogen atoms over the supported vanadate while, at vanadate-free areas the hydrogen can migrate over the titanium dioxide as such.

Conclusions

- Vanadate monolayers chemisorbed on $\gamma\text{-Al}_2\text{O}_3$ or on $\text{TiO}_2(\text{a})$ are reduced by hydrogen atoms spilt over from supported palladium crystallites. The reaction proceeds at measurable rates already at 353 K or at even lower temperatures.
- The reduction rate was found to be determined by the rate of hydrogen migration over the reduced vanadate.
- By numerical modelling, the reduction rate was calculated for a wide range of palladium loadings. The calculated reduction rates agree quite well with experimental rates, adopting a surface diffusion coefficient of $1.10^{-16} \text{ m}^2.\text{s}^{-1}$.
- For the migration of hydrogen atoms over a reduced vanadate layer supported on $\gamma\text{-Al}_2\text{O}_3$ a diffusion coefficient of $1.10^{-16} \text{ m}^2.\text{s}^{-1}$ was found. With decreasing vanadate coverage this diffusion coefficient diminishes strongly. Interestingly, for the case of $\text{TiO}_2(\text{a})$ supported catalysts the surface diffusion coefficient is about twenty times as high as found for $\gamma\text{-Al}_2\text{O}_3$ supported samples.
- From rate measurements in the temperature range of from 353 K to 413 K an apparent activation energy for the overall reaction rate of 87 kJ.mol^{-1} was found.
- An apparent kinetic isotope effect, $D_{\text{H}}/D_{\text{D}}$, of 1.1 was found. This low value is probably due to a thermodynamic isotope effect in the chemisorption of hydrogen on palladium, which counteracts the kinetic isotope effect in the hydrogen surface migration.

List of symbols

c	surface concentration of free hydrogen atoms at distance r	(mol hydrogen atoms.m ⁻²)
c ₀	c at distance r = r ₀ (c ₀ = α.P)	(mol hydrogen atoms.m ⁻²)
α	a constant, is the ratio of c ₀ to P	(mol hydrogen atoms.m ⁻² .Pa ⁻¹)
c _v	surface concentration of vanadium atoms	(mol vanadium atoms.m ⁻²)
D	surface diffusion coefficient	(m ² .s ⁻¹)
m	mass of catalyst	(g)
nPd	palladium crystallites per gram	(g ⁻¹)
P	dihydrogen pressure	(Pa)
(Pd) _r	normal distribution of palladium crystallites	(function of r)
r	distance from the centre of the palladium crystallite	(m)
r ₀	mean radius of the palladium crystallite	(m)
R	gas constant	(Pa.m ³ .mol ⁻¹ .K ⁻¹)
R _t	radius of the circle of reduced vanadate at time t	(m)
t	time	(s)
T	temperature	(K)
V	gas volume	(m ³)
X _r	fraction of non-reduced vanadate	
β	number of hydrogen atoms consumed per vanadium atom	
Φ _{H₂}	dihydrogen uptake as a function of time	(mol H ₂ .s ⁻¹)

References

1. G.C. Bond in: Spillover of Adsorbed Species, G.M. Pajonk, S.J. Teichner and J.E. Germain (eds.), Elsevier, Amsterdam, (1983) 1; W.C. Conner, G.M. Pajonk and S.J. Teichner, Adv. Catal., 34 (1986) 1; H. Charcosset and B. Delmon, Ind. Chim. Belg., 38 (1973) 481.
2. B.K. Hodnett and B. Delmon in: Catalytic Hydrogenation, L. Gervey (ed.), Elsevier, Amsterdam, (1986) 53.
3. P.A. Sermon and G.C. Bond, Catal. Rev., 8 (1973) 211.
4. P.A. Sermon and G.C. Bond, J. Chem. Soc., Faraday Trans. I, 72 (1976) 730; D. Tinet, S. Partyka, J. Rouquerol and J.J. Fripiat, Mater. Res. Bull., 17 (1982) 561.
5. J.L. Seoane, P. Boutry and R. Montarnal, J. Catal., 63 (1980) 182.
6. C. Blejean, P. Boutry and R. Montarnal, C. R. Acad. Sci. Paris, Ser. C, 270 (1970) 257.
7. P.J. van der Steen, Thesis, Delft University Press, (1987); E. van der Heide, M. de Wind, A.W. Gerritsen and J.J.F. Scholten, Proc. 9th Int. Congr. Catal. (Calgary), 4 (1988) 1648; E. van der Heide, J.A.M. Ammerlaan, A.W. Gerritsen and J.J.F. Scholten, J. Molec. Catal., 55 (1989) 320; E. van der Heide, J. Schenk, A.W. Gerritsen and J.J.F. Scholten, Recl. Trav. Chim. Pays-Bas 109 (1990) 93.
8. F. Roozeboom, T. Fransen, P. Mars and P.J. Gellings, Z. Anorg. Allg. Chem., 499 (1979) 25.
9. H.S. Carslaw and J.C. Jaeger: Conduction of Heat in Solids, Clarendon Press, Oxford, (1959).
10. R. Kramer and M. Andre, J. Catal., 58 (1979) 287.

Oxidation of ethylene to acetaldehyde over a heterogenized surface vanadate Wacker catalyst, in the presence and in the absence of gaseous oxygen.

Abstract

In heterogeneous Wacker oxidation reduction and oxidation of vanadate alternate (eqs. (2), (3) and (4)). In the present chapter a study of these oxidation-reduction cycles is presented and an all-embracing reaction model is drawn up. In the absence of vanadate and dioxygen the total number of acetaldehyde molecules produced appeared to equal the number of Pd(II) ions. In the absence of dioxygen, but in the presence of vanadate, a strong increase of the production of acetaldehyde was observed and the vanadate valence state after depletion of oxygen was found to be V^{4+} . This vanadium valency appeared to be nearly independent of the palladium coverage. Only at low temperatures and at a low palladium coverage an incomplete reduction of the vanadate monolayer was found.

In the presence of dioxygen a fast oxidation of reduced vanadate takes place and the average valence state under normal Wacker oxidation conditions was found to approach V^{5+} .

From experiments in which dioxygen was dosed pulse-wise to the reactor it appeared that oxidation of ethylene is possible in the absence of dioxygen in the gas phase. Afterwards, the oxygen-depleted catalyst can be reoxidized.

Introduction

Alkenes can be oxidized to ketones or to aldehydes by Wacker oxidation. The homogeneous Wacker catalyst, which consists of a solution of palladium chloride and copper chloride in hydrochloric acid, has widely been applied in the commercial production of acetaldehyde from ethylene [1]. Terminal alkenes can also be oxidized via the Wacker route and the corresponding methyl ketones result according to eq. (1).



The application of the homogeneous Wacker catalyst has a number of disadvantages. The catalyst solution in combination with oxygen has very corrosive properties. When higher alkenes are oxidized unwanted chlorinated byproducts are formed and separation of the higher ketones from the reaction mixture is difficult. For these reasons oxidation of alkenes higher than ethylene has never been practised commercially.

In a number of publications [2,3,4] we have shown that the difficulties mentioned above may largely be circumvented by applying a heterogeneous Wacker catalyst. This catalyst, based on a concept introduced originally by van der Steen *et al.* [5], consists of a vanadate monolayer on $\gamma\text{-Al}_2\text{O}_3$, this monolayer in turn being covered by a sub-monolayer of palladium chloride or palladium sulphate.

In the Wacker oxidation of the alkenes the vanadate monolayer is partly reduced, in accordance with the reduction of crystalline V_2O_5 in the presence of palladium by ethylene or by *o*-xylene as reported by Blejean [6] and by Seoane *et al.* [7]. The rate of reduction increases with increasing partial pressure of ethylene and the final reduction state of the vanadate was found to be approximately V_4O_9 . However, nothing is known about possible differences in the degree of reduction of surface vanadate as compared with bulk V_2O_5 .

In this chapter a closer study of the reduction and reoxidation of the vanadate monolayer during Wacker oxidation of ethylene will be reported.

Experimental

Chemicals

Dioxygen, dinitrogen and ethylene (in cylinders) were obtained from Air Products (U.S.A.). Dinitrogen and ethylene were of high purity and dioxygen was of industrial grade. H₂O was distilled before use. PdCl₂, analytical grade, was obtained from Drijfhout (The Netherlands). HCl and H₂SO₄, analytical grade, were purchased from Drijfhout (The Netherlands). NH₄VO₃, also analytical grade, was purchased from Merck (F.R.G.). γ -Al₂O₃, type 000-3P, S(BET) = 250 m².g⁻¹, was supplied by Akzo (The Netherlands).

Apparatus

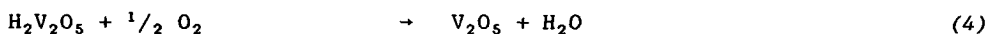
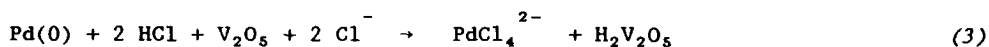
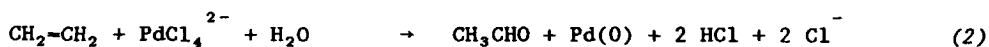
Catalytic performance has been studied in a continuous-flow fixed-bed stainless-steel reactor, internal diameter 1 cm and length 10 cm, at a total pressure of 0.11 MPa and over the temperature range 331 - 373 K. All gases were dried over molecular sieves and the composition of the feed was regulated by means of mass-flow controllers (Inacom, The Netherlands). Water was dosed to the feed by leading finely divided bubbles of nitrogen through a thermostatted flask filled with water. Off-gas analysis was performed gas chromatographically, applying a Porapak QS column, length 100 cm, diameter 3 mm, at 423 K. Peak areas were recorded and integrated by a microcomputer (Digital LCI 11/03, U.S.A.).

Catalyst preparation

The γ -Al₂O₃ pellets were crushed and sieved to particles with diameters from 425 to 600 μ m. By leading an NH₄VO₃ solution of pH = 4 at 343 K over these particles the surface was covered with a vanadate monolayer. The particles were then calcined in air at 673 K for 4 h. From titration with Fe(II), the vanadium coverage was found to correspond to 3.9 V atoms per nm². Next, through impregnation to incipient wetness with a solution of H₂PdCl₄, followed by drying at 353 K, the aluminovanadate layer was covered by a sub-monolayer of the Pd compound.

Results and discussion

By Wacker oxidation ethylene is oxidized to acetaldehyde and terminal alkenes are converted into the corresponding methyl ketones. As indicated in eq. (2) zero-valent palladium is formed simultaneously with the aldehyde. Subsequently the vanadate monolayer reacts with the zero-valent palladium



(to Pd(II)) to form reduced vanadate (eq. (3)), which probably has the structure of a hydrogen bronze. Finally, the reduced vanadate reacts with dioxygen and water is produced (eq. (4)).

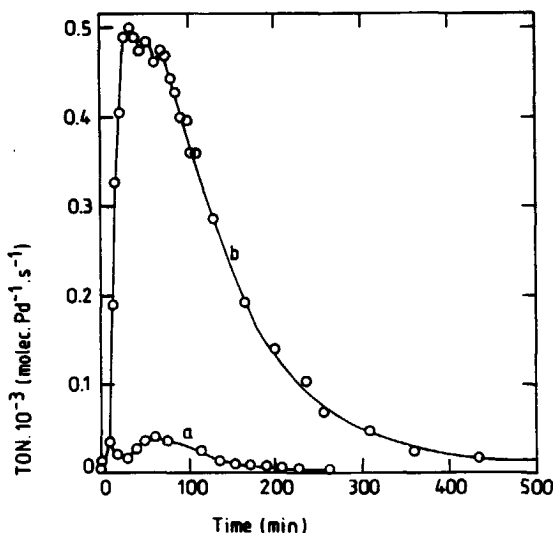


Figure 1. Wacker oxidation of ethylene in the absence of dioxygen. TON as a function of time. Composition of the feed: 92.5 mol % N₂, 6.5 mol % H₂O and 1 mol % C₂H₄. 373 K, 0.11 MPa total pressure. Catalysts: curve a: no vanadate present; 1.2 mol % PdCl₂, 6.1 mol % HCl and 92.6 mol % Al₂O₃; curve b: vanadate present; 1.3 mol % PdCl₂, 6.5 mol % HCl, 7.6 mol % V₂O₅ and 84.6 mol % Al₂O₃.

- 10. Ethylene oxidation in the absence of dioxygen -

In the absence of vanadate and of oxygen the formation of one molecule of acetaldehyde per Pd(II) ion is to be expected, according to eq. (2). As indicated in Fig. 1, curve a, in the absence of oxygen and vanadate the formation of a small amount of acetaldehyde is observed. The total amount of acetaldehyde formed was calculated by integration and indeed one molecule of acetaldehyde per Pd(II) ion is formed, according to eq. (2). In the presence of vanadate the final average valence state of the reduced vanadate was calculated from the total amount of acetaldehyde formed, corresponding to curve b in Fig. 1. In Fig. 2, this vanadium valency is given as a function of the palladium coverage. A mean final valence state of V^{4+} was found, probably corresponding to the formation of a hydrogen bronze with the stoichiometric composition $H_2V_2O_5$.

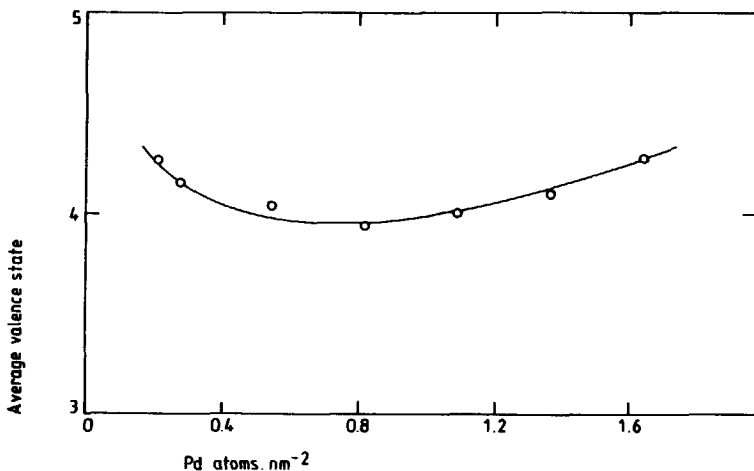


Figure 2. Average valence states of monolayer vanadate after reduction by ethylene as a function of the palladium coverage. It is assumed that all Pd(II) is reduced to Pd(0). Composition of the feed: 92.5 % N_2 , 6.5 % O_2 and 1 % C_2H_4 ; temp. 373 K, 0.11 MPa total pressure. 1 g of catalyst. The Al_2O_3 to V_2O_5 mol ratio is 6.4, the HCl to $PdCl_2$ ratio is 8. Variable amount of $PdCl_2$.

Experiments carried out with 0.5 and 2 g of catalyst led to the same final vanadate valence states. At a Pd coverage below 0.3 Pd atoms per nm^2 a somewhat higher final valence state is calculated. Also at higher Pd coverages, to above 1.3 Pd atoms per nm^2 , a higher average vanadium valence

state is found, up to 4.2. The reason for this is unknown; the higher valency is probably due to screening of the vanadate monolayer by palladium, or to an inefficient reduction of Pd(II) ions at high Pd(II) coverage.

As stated in Chapter 9, reduction of the vanadate monolayer by hydrogen atoms, spilt-over from Pd(0) crystallites, leads to the formation of $V^{3.5+}$, in contrast with the final valence state V^{4+} found by C_2H_4 reduction via Pd(II). During Wacker oxidation Pd(0) has to be reoxidized to Pd(II), before the oxidation cycle of the alkene to ketone or to aldehyde can be repeated. It can be concluded that V^{5+} can oxidize Pd(0) to Pd(II), but Pd(0) is stable in the presence of V^{4+} .

The influence of the reduction state of the catalyst on the apparent

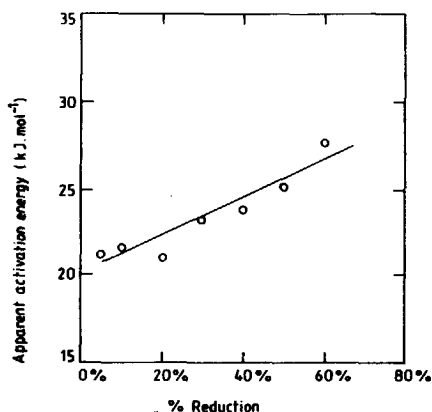


Figure 3. Apparent activation energies as a function of the reduction state of the catalyst in the temperature range of 331 to 373 K. Composition of the feed: 92.5 % N_2 , 6.5 % H_2O and 1 % C_2H_4 . Total pressure 0.11 MPa. Catalyst: 0.44 mol % $PdCl_2$, 3.55 mol % HCl , 7.8 mol % V_2O_5 and 88.2 mol % Al_2O_3 . 0.5 g of catalyst.

activation energy, as measured for ethylene oxidation in the absence of dioxygen and in the temperature range of from 331 K to 373 K, is depicted in Fig. 3. At 373 K a high initial activity and a fast oxygen exhaustion of the catalyst is found relative to measurements at 345 and 331 K. Final average vanadate stoichiometrics correspond to $V_2O_{4.27}$, $V_2O_{4.36}$ and $V_2O_{4.40}$, respectively. This increase of the average vanadate valency with decreasing temperature is probably due to a lower efficiency of oxidation of zerovalent palladium by vanadate at lower temperatures. This is in agreement with the apparent activation energies found for the Wacker oxidation of ethylene to

acetaldehyde (4 kJ per mol at constant water partial pressure) and for hydrogen spillover (87 kJ per mol) (Chapter 9). However, as water accelerates hydrogen spillover, the apparent activation energy of hydrogen spillover may be lower than 87 kJ per mol in the presence of water, as is the case here. At lower temperatures the reoxidation of palladium and simultaneous reduction of the vanadate monolayer are slowed down relative to the reaction rate of oxidation of the alkene and higher final vanadium valence states are to be expected. The increase of the apparent activation energy (Fig. 3) also points to an increasing importance of the reoxidation reaction of palladium at increasing reduction states of the catalyst.

In the commercial production of acetaldehyde there are two different process options: one-step and two-step. In the two-step homogeneous Wacker oxidation the $H_2PdCl_4/CuCl_2$ catalyst is reduced by ethylene in the main reactor where the ethylene is oxidized to acetaldehyde. The catalyst

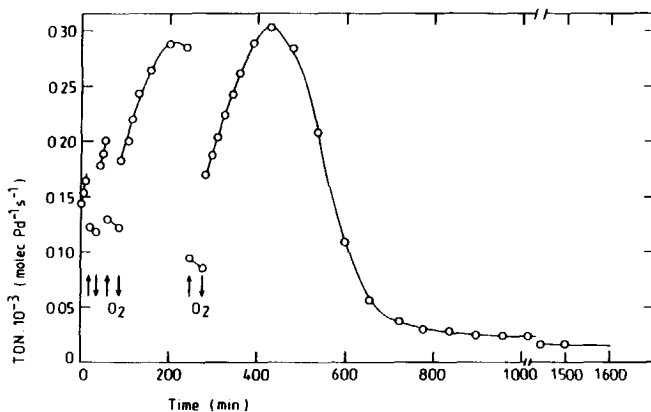


Figure 4. TON as a function of time in the presence and in the absence of dioxygen. Composition of the feed in the absence of dioxygen: 92.5 mol % N_2 , 6.5 mol % H_2O and 1 % C_2H_4 ; in the presence of dioxygen: 74.0 mol % N_2 , 18.5 mol % O_2 , 6.5 mol % H_2O and 1 % C_2H_4 . Temperature 373 K, 0.11 MPa total pressure. Catalyst: 0.34 mol % $PdCl_2$, 2.69 mol % HCl , 7.85 mol % V_2O_5 and 89.1 mol % Al_2O_3 .

solution, depleted from oxygen, is constantly circulated through an auxiliary reactor where regeneration by oxidation with air takes place [8].

The question arises whether such a two-step process is possible also when a heterogenized Wacker catalyst is used. This seems to be the case indeed as appears from the results depicted in Fig. 4.

- 10. Ethylene oxidation in the absence of dioxygen -

As demonstrated by this figure, only a short period of pulse-wise reoxidation by dioxygen is sufficient for complete regeneration of the catalyst. Reoxidation of the catalyst by dioxygen appeared to be at least 7 times as fast as the oxidation reaction of ethylene to acetaldehyde. It should be noted, however, that retardation of the ethylene oxidation by dioxygen by a factor of about two is found during addition of the dioxygen pulse to the feed. Apparently dioxygen interacts with the catalytically active palladium sites. If we describe the mechanism in terms of one organometallic complex containing a vanadium and a palladium centre (Chapter 8) we have to assume that in some way the Pd(II) centre can take up dioxygen in some liganded form, as a result of which the reaction rate is retarded. Possibly the reoxidation of the vanadate monolayer proceeds via palladium catalyzed oxygen spillover, but more research is needed for the clarification of this interesting experimental result. The negative order

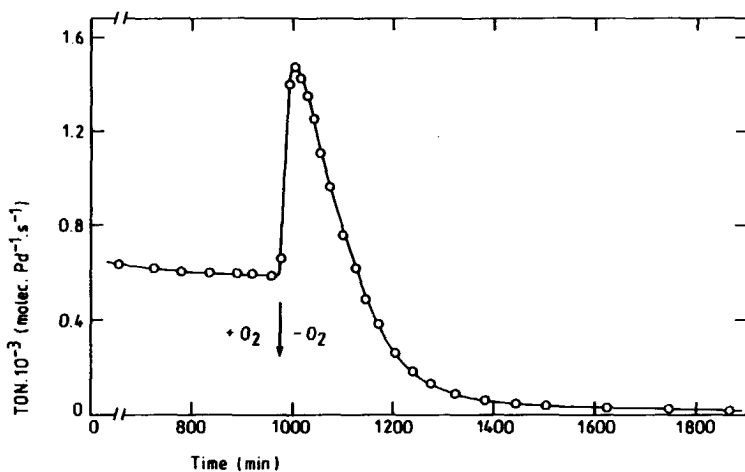


Figure 5. TON as a function of time in the presence and absence of dioxygen. Conditions as given in the legend of Fig. 4.

with respect to dioxygen during the oxidation of ethylene over $\text{TiO}_2(\text{a})$ supported catalysts also points to an interaction of oxygen with palladium (Chapter 8).

It was stated by Seoane *et al.* [7] that V_2O_5 on $\alpha\text{-Al}_2\text{O}_3$ is in a partly reduced state during catalytic oxidation of ethylene to acetic acid in the

- 10. Ethylene oxidation in the absence of dioxygen -

presence of palladium and dioxygen. Therefore it is interesting to investigate the vanadium oxidation state under our reaction conditions. To this end we first oxidized ethylene to acetaldehyde in the presence of dioxygen. After a 16 h run the oxygen supply was stopped and the production of acetaldehyde in the absence of dioxygen was followed as a function of time. The results are depicted in Fig. 5. First an increase of the TON by a factor of 2.5 due to the absence of reaction rate retardation by dioxygen is measured. Next, oxygen exhaustion of the catalyst occurs simultaneously with a decrease of the reaction rate. From the total amount of acetaldehyde produced after stopping the dioxygen supply, and assuming the valency of the vanadium to be 4 at zero TON value (as follows from the results plotted in Fig. 2), the valency of the vanadium during catalytic oxidation in the presence of oxygen was calculated to be +5.

The results discussed up to now are consistent with the simplified mechanism represented in Fig. 6. The kinetics of the heterogeneous oxidation of ethylene to acetaldehyde corresponds to the kinetics of homogeneous

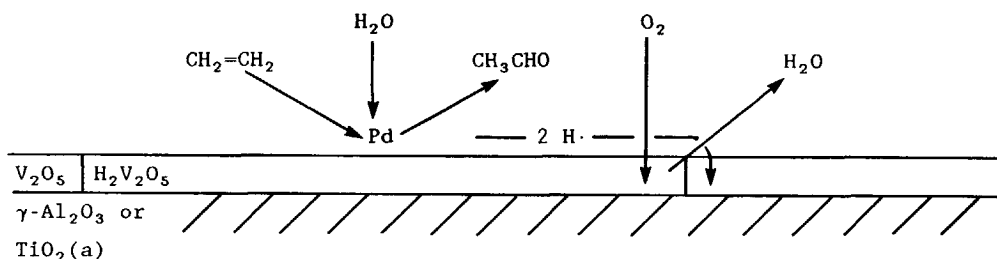


Figure 6. Mechanism of ethylene oxidation over a vanadate monolayer Wacker catalyst.

Wacker oxidation [2] and the mechanism is virtually the same. The rate of heterogeneous oxidation of the alkene is found to be slow relative to the rate of reduction of the vanadate monolayer. Only under extreme conditions, at low temperatures and at high degrees of vanadate reduction, as reported here, the rate of reduction of the monolayer is slow relative to the rate of oxidation of the alkene. Reoxidation of the monolayer by dioxygen appeared to be fast under all conditions.

Conclusions

- Ethylene can be oxidized over a H_2PdCl_4 sub-monolayer on $\gamma-Al_2O_3$ in the absence of dioxygen and vanadate. One molecule of acetaldehyde is formed per $PdCl_4^{2-}$ ion.
- In the absence of oxygen, but in the presence of vanadate, a strong increase of the production of acetaldehyde is found.
- The final average vanadium valency after reduction of the catalyst by C_2H_4 was found to be 4. This valency is nearly independent of the palladium coverage.
- Reoxidation of a partly reduced catalyst by dioxygen appeared to proceed at least 7 times as fast as the oxidation reaction of ethylene to acetaldehyde.
- From the present study it appears that heterogeneous Wacker oxidation can be performed as a two-step process, just as is the case in homogeneous Wacker oxidation.
- During Wacker oxidation of ethylene the vanadium valence state was found to equal V^{5+} .
- Retardation of the reaction rate by dioxygen by a factor of two was found, probably due to interaction of dioxygen with the catalytically active palladium sites.

References

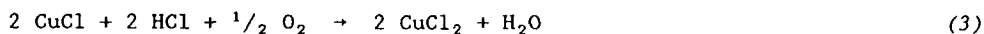
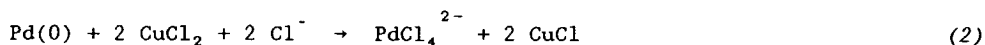
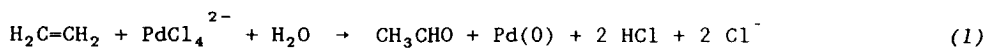
1. J. Smidt, W. Hafner, R. Jira, J. Sedlmeier, R. Sieber, R. Ruttinger and H. Kojer, *Angew. Chem.*, 71 (1959) 176.
2. E. van der Heide, M. de Wind, A.W. Gerritsen and J.J.F. Scholten, *Proc. 9th Int. Congr. Catal. (Calgary)*, 4 (1988) 1648.
3. E. van der Heide, J.A.M. Ammerlaan, A.W. Gerritsen and J.J.F. Scholten, *J. Molec. Catal.*, 55 (1989) 320.
4. E. van der Heide, J. Schenk, A.W. Gerritsen and J.J.F. Scholten, *Recl. Trav. Chim. Pays-Bas*, 109 (1990) 93.
5. P.J. van der Steen, *Thesis*, Delft University Press, (1987); J.J.F. Scholten and P.J. van der Steen, *European Patent Specification 0210705 A* 22.03.1989.
6. C. Blejean, P. Boutry and R. Montarnal, *C.R. Acad. Sci. Paris, Ser. C*, 270 (1970) 257.
7. J.L. Seoane, P. Boutry and R. Montarnal, *J. Catal.*, 63 (1980) 182.
8. A. Aguilo, *Adv. Organometal. Chem.*, 5 (1967) 321.

11

Heterogeneous Wacker oxidation; an outline

Introduction

The formation of acetaldehyde during the reduction of palladium chloride by ethylene was already noticed in 1894 by Phillips [1], but the reaction remained practically unknown until the late nineteen fifties. At that time a new catalytic process for the oxidation of ethylene to acetaldehyde, based on the Phillips reaction, was introduced by Smidt and co-workers [2]. They



found that the oxidation of ethylene by palladium chloride dissolved in hydrochloric acid became a catalytic process when CuCl_2 was added to the palladium chloride/hydrochloric acid solution. In the presence of CuCl_2 the

- 11. Heterogeneous Wacker oxidation; outline -

zero-valent palladium, formed simultaneously with acetaldehyde (eq. (1)) is reoxidized *in situ* to palladium chloride (eq. (2)), after which CuCl reacts with oxygen and returns to CuCl₂ (eq. (3)). When the reactions are added, the net reaction is oxidation of ethylene with oxygen to acetaldehyde (eq. (4)). Higher (terminal) alkenes can be oxidized to the corresponding (methyl-) ketones (eq. (5)) [2,3,4].



The oxidation of alkenes other than ethylene has never been applied industrially, due to a number of technological disadvantages of the homogeneous Wacker process: the combination of oxygen and hydrochloric acid requires special precautions to prevent corrosion, unwanted chlorinated byproducts are formed during the oxidation of higher alkenes and it is difficult to separate products of higher alkenes from the aqueous reaction mixture.

It has been attempted to circumvent these difficulties by heterogenizing the catalyst. A catalyst based on a Pd salt on active carbon was developed by Fujimoto *et al.* [5]. A technical drawback is the mechanical weakness of carbon as a support.

Evnin *et al.* and Forni *et al.* replaced the Cu(I)/Cu(II) redox couple of the homogeneous catalyst by V₂O₄/V₂O₅ supported on α -Al₂O₃ [6]. Although good activities have been reported, their catalysts suffer from deactivation in relatively short periods of time.

In the catalysis research group of TU Delft it was discovered that when vanadate is deposited in the form of a monolayer on γ -Al₂O₃ stable catalysts are obtained [7]. The performance of such catalysts in the oxidation of ethylene [8], 1-butene [9] and styrene [10] has been reported in Chapters 4, 5 and 7 respectively. The reactions proceed under the mild conditions of 0.11 MPa total pressure and 373 K. However, cyclohexene appeared to be hardly reactive under these conditions (Chapter 6).

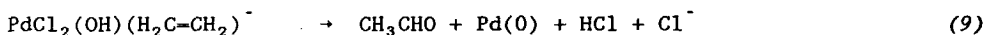
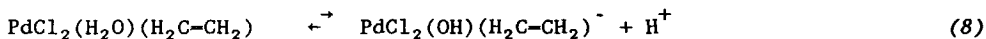
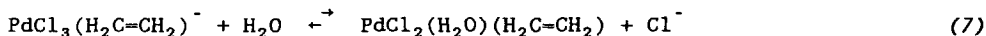
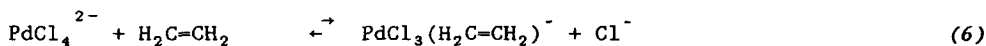
The reduction of the catalysts by dihydrogen appears to proceed via a spillover process and can be described by computer modelling of the reaction (Chapter 9). Hydrogen spillover probably plays an important role during Wacker oxidation, as could be demonstrated by experiments carried out in the absence of oxygen (Chapter 10).

In this Chapter the performance of the monolayer vanadate Wacker catalyst will be reviewed and discussed in depth by comparison of the oxidation of different alkenes. Recommendations for further research will also be given.

Outline

Kinetics

The mechanism of the homogeneous Wacker oxidation, as far as eq. (1) is concerned, can be described by the equilibria (6) to (8) inclusive, followed by the rate determining step (9). From this mechanism the kinetic rate equation (10) is derived [11].



A first order dependence of the reaction rate on the water partial pressure is to be expected, but in the homogeneous case this cannot be established as water, as the solvent, is available in excess.

$$r = k \cdot \frac{[\text{PdCl}_4^{2-}][\text{H}_2\text{C}=\text{CH}_2]}{[\text{H}^+][\text{Cl}^-]^2} \quad (10)$$

In the heterogeneous Wacker oxidation of ethylene, 1-butene and styrene the kinetics with respect to the same variables were measured by us. In all oxidations, the dependence of the reaction rate on the alkene partial pressure could be described by a Langmuir-type equation. At a low palladium coverage the reaction appeared to be first order with respect to palladium

coverage, but at higher coverages the reaction rate was no longer influenced by it. The dependence of the reaction rate on the surface chloride concentration appeared to be first order at low chloride coverages and decreases to about minus 2 at high coverages.

The dependence of the reaction rate on the type of cation coverage appeared to decrease in the sequence: $\text{Li}^+ > \text{H}^+ \approx \text{Na}^+ > \text{K}^+$ (relative activities: 11.5, 6.4, 6.4 and 1, respectively). The same sequence was found by Akimoto *et al.* for the case where the corresponding vanadium bronzes are applied [12].

The heterogeneous reaction appeared to be first order with respect to water coverage and about zero order with respect to O_2 partial pressure. Our results are summarized in eq. (11):

$$r = k \cdot \frac{K \cdot p_{\text{alkene}}}{1 + K \cdot p_{\text{alkene}}} \cdot \frac{c \cdot p_r}{(1-p_r)(1-p_r + c \cdot p_r)} \cdot \theta_{\text{Pd(II)}} \cdot \theta_{\text{Cl}^-}^x \cdot p_{\text{O}_2}^0 \quad (11)$$

in which r is the reaction rate, k a reaction rate constant, K ranges from 0.2 MPa^{-1} to 2 MPa^{-1} and p_r is the relative water partial pressure. The constant c , which stems from the BET equation, was found to be 12. The order with respect to Cl^- , indicated by x , ranges from 1 to minus 2.

From these results we may conclude that the kinetics of the heterogeneous Wacker oxidation largely correspond to the kinetics of the homogeneous Wacker reaction.

Activity

The activity of the heterogeneous Wacker catalyst in the oxidation of the alkenes appeared to decrease in the sequence:

ethylene > 1-butene > styrene >> cyclohexene (relative activities: 1.0, 0.55, 0.24 and < 0.05, respectively).

This result is comparable to the activity sequence reported by Kolb *et al.* [3] with respect to the oxidation of ethylene, 1-butene and cyclohexene. The activity is linearly related to the ability of complex formation of the alkenes with palladium and decreases with increasing chain length and increasing substitution in the alkene. Oxidation of ethylene over $\text{TiO}_2(\alpha)$

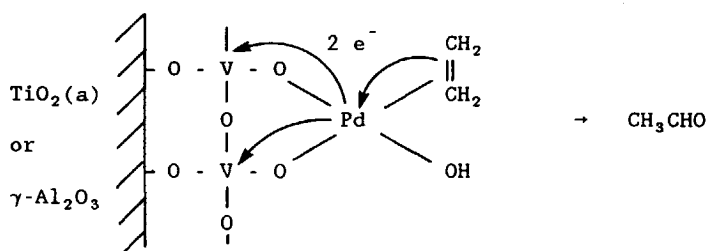


Figure 1 Interaction between palladium and vanadate.

instead of over $\gamma\text{-Al}_2\text{O}_3$ supported catalysts leads to an increase of the activity by a factor of twenty. This can be explained by the introduction of a chemical interaction between the catalytically active Pd site and the vanadate monolayer, which is represented schematically in Fig. 1. The formation of products and reduction of the vanadate now proceeds as a concerted reaction and no zero-valent palladium is formed as assumed in the classical mechanism. Otherwise it should be noted that also in homogeneous Wacker oxidation an influence of the redox compound on the reaction rate is found [13].

Selectivity

The acetaldehyde selectivity in the oxidation of ethylene appeared to be high; at 10 % conversion selectivities as high as 99 % were observed. Acetic acid could be detected in trace amounts only, and no chlorinated byproducts were found under our experimental conditions.

When $\gamma\text{-Al}_2\text{O}_3$ is used as a support 1-butene is oxidized to butanone with selectivities ranging from 80 to 95 % at 10 % conversion. Byproducts include crotonaldehyde, acetone, acrolein, acetaldehyde and acetic acid in roughly equal amounts. Formation of acetaldehyde and acetic acid appeared to proceed over the vanadate monolayer and acetone formation was found to be Pd catalyzed, probably via acetic acid. Acrolein and crotonaldehyde are products typically formed by π -allyl oxidation over palladium. When $\text{TiO}_2(\text{a})$ is used as a support the selectivity to butanone is disappointingly low, being 45 %.

Oxidation of styrene over $\gamma\text{-Al}_2\text{O}_3$ supported catalysts leads to the formation of acetophenone and benzaldehyde in about equal amounts (45 % and

55 % selectivity, respectively). Benzaldehyde is probably formed via oxidation of the styrene oxidation product phenylacetaldehyde. However, after some time the selectivity to benzaldehyde increases, simultaneously with the selectivity of the formation of cinnamaldehyde, the latter being 15 % after a three days run. Benzaldehyde and cinnamaldehyde are formed by asymmetric oxidative scission of 1,4-diphenyl-1,3-butadiene, which is formed by dimerization of styrene.

From the carbon material balance the selectivities to CO and CO₂ appeared to be lower than 5 % in all cases, except for the amounts formed simultaneously with acrolein and acetone during the oxidation of 1-butene and formed simultaneously with benzaldehyde during styrene oxidation.

Stability and regeneration

In the oxidation of ethylene H₂PdCl₄-based catalysts appeared to be stable for weeks and by replacing H₂PdCl₄/HCl by Li₂PdCl₄/LiCl or by Na₂PdCl₄/NaCl the life-time could be improved to months. As shown by XPS/AES, deactivation appeared to be linearly related to the formation of inactive Pd(0).

However, during 1-butene oxidation palladium chloride containing catalysts appeared to suffer from deactivation. This deactivation is also related to Pd(0) formation due to a loss of chloride in the course of the reaction. Deactivated catalysts could be regenerated by adding of hydrochloric acid. The presence of chloride can be avoided by replacing Na₂PdCl₄/NaCl by PdSO₄/H₂SO₄, which leads to an active and stable catalyst.

Deactivation during styrene oxidation appeared to be due to formation of carbonaceous deposits, which cover the surface, and partial regeneration was achieved by removal of the deposits by oxygen at higher temperatures.

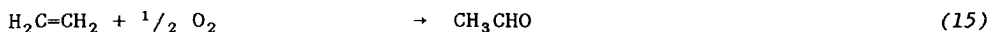
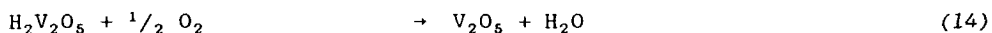
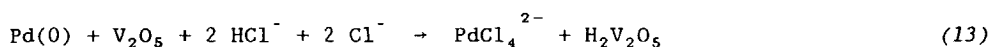
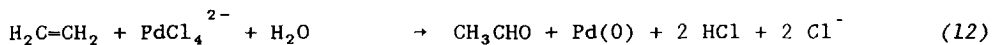
Apparent activation energies

The apparent activation energy of the oxidation of ethylene is 36 kJ.mol⁻¹, applying γ -Al₂O₃ or TiO₂(a) supported catalysts. The apparent activation energy of 1-butene oxidation is 58 kJ.mol⁻¹, whereas in styrene oxidation the apparent activation energies of the formation of acetophenone and benzaldehyde appeared to be 90 kJ.mol⁻¹ and 51 kJ.mol⁻¹, respectively.

Reaction mechanism

As mentioned before the mechanism of the heterogeneous Wacker oxidation of the alkenes (eq. (1)) can be described by combining the rate determining step (eq. (9)) and the preceding equilibria (6) to (8) inclusive. In the course of the rate determining step Pd(II) is formally reduced to zero-valent palladium.

In heterogeneous Wacker oxidation these equilibria and rate determining step are represented by eqs. (12) to (15) inclusive:



The second step, eq. (13), is the reoxidation of Pd(0) by the vanadate monolayer. During the alkene oxidation not only two electrons but also two hydrogen ions are set free, and both, the electrons and the hydrogen ions, are taken up by the vanadate monolayer. This reduction of the vanadate monolayer proceeds already at a temperature as low as 373 K or at even lower temperatures. In the absence of oxygen the monolayer is totally reduced to V^{4+} , irrespective of the palladium coverage (Chapter 10). For these reasons it is proposed that the vanadate monolayer is reduced via a hydrogen spillover process [14]. This is the only process known to us by which vanadate can be reduced at such low temperatures. The spillover process was found to be fast relative to Wacker oxidation (Chapter 9).

The third reaction, the oxidation of the reduced vanadate by oxygen, represented by eq. (14), appeared to be fast relative to reaction step (12). Therefore, in the ethylene oxidation over $\gamma\text{-Al}_2\text{O}_3$ catalysts a reaction rate of zero-order with respect to oxygen partial pressure is found. However, oxygen appeared to interact with the catalytically active (reduced ?) palladium sites. During Wacker oxidation of ethylene over $\text{TiO}_2(\text{a})$ supported

catalysts a retardation by oxygen is found and also in experiments where oxygen is dosed to the catalyst in pulses.

The results are summarized in Fig. 2. It is clearly shown that first ethylene and water are adsorbed on the palladium site, with formation of acetaldehyde. Two electrons and two hydrogen ions are formed simultaneously

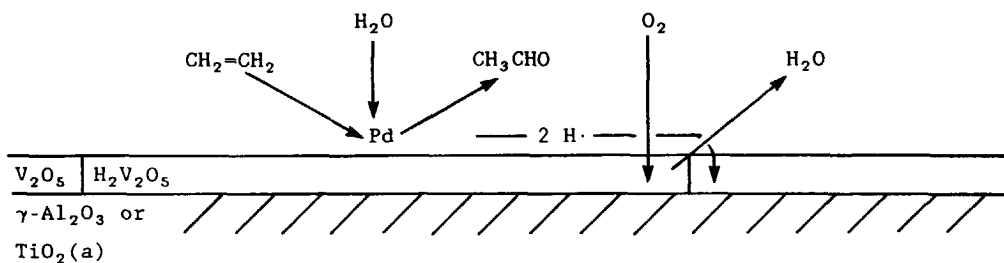


Figure 2. Mechanism of Wacker oxidation over a vanadate monolayer Wacker catalyst.

with acetaldehyde. As a result, hydrogen atoms migrate over the reduced vanadate until they react with $V(V)$. Ultimately dioxygen oxidizes the reduced surface vanadate and water is set free.

Outlook

Urgent questions demanding further research include the clarification of the precise structure of the catalysts. The structure of the vanadate monolayer will be strongly influenced by impregnation of the particles with the palladium containing acid solution, particularly when $PdSO_4/H_2SO_4$ solutions are used. In the presence of H_2SO_4 a surface vanadyl sulphate is probably formed, and in the presence of alkali metal ions catalytically active surface vanadate bronzes will result.

The dispersion of palladium over the catalyst surface and the interaction between palladium salt and vanadium oxide form important but only partly understood subjects. The precise surface structures are difficult to investigate, but the application of ESR, ^{51}V NMR, electron microscopy, EXAFS or IR spectroscopy is likely to provide a deeper insight.

For both fundamental and technological reasons further development of the oxidation of the butenes is attractive. The performance of the $\text{PdSO}_4/\text{H}_2\text{SO}_4$ (or $\text{Pd}(\text{NO}_3)_2/\text{HNO}_3$) variants of the catalyst in the oxidation of 1-butene, isobutene and the 2-butenes should be studied further, as well as the kinetics at high alkene partial pressures, high alkene conversions and low oxygen partial pressures. Alkenes other than those mentioned in this Chapter (e.g. propylene and substituted alkenes) are yet to be investigated.

Hydrogen spillover during the reduction of $\text{TiO}_2(\text{a})$ supported catalysts appeared to be fast as compared to spillover over vanadate monolayers on $\gamma\text{-Al}_2\text{O}_3$. Factors influencing the spillover reaction rate and the mechanisms are still not known in sufficient detail.

Heterogeneous Wacker oxidation of cyclohexene appeared to be an intriguing reaction. The low activity measured was ascribed to the low coordination ability of cyclohexene to palladium. In homogeneous Wacker oxidation of cyclohexene also a low reaction rate was found [3]. Therefore, to improve the reaction rate, the coordination sphere of palladium has to be influenced by suitable ligands, leading to a stronger coordination of cyclohexene to palladium. Also complexes in which both palladium and vanadium (or another redox compound) are coordinated may be active and selective in homogeneous oxidation of cyclohexene to cyclohexanone.

Reactions other than Wacker oxidation may also proceed over the heterogeneous Wacker catalyst. Typical reactions include acetoxylation, selective oxidation, carbon-carbon coupling and selective dehydrogenation reactions.

References

1. F.C. Phillips, *Am. Chem. J.*, **16** 255 (1894).
2. J. Smidt, W. Hafner, R. Jira, J. Sedlmeier, R. Sieber, R. Ruttinger and H. Kojer, *Angew. Chem.*, **71** (1959) 176.
3. M. Kolb, E. Bratz and K. Dialer, *J. Molec. Catal.*, **2** (1977) 399.
4. J. Tsuji, *Synthesis*, (1984) 369.
5. K. Fujimoto, O. Kuchi-ishi and T. Kunugi, *Ind. Eng. Chem. Prod. Res. Dev.*, **15** (1976) 259.
6. A.B. Evnin, J.A. Rabo and P.H. Kasai, *J. Catal.*, **30** (1973) 109; L. Forni, G. Terzoni, *Ind. Eng. Chem. Process Des. Dev.*, **16** (1977) 288.
7. P.J. van der Steen, *Thesis*, Delft University Press, 1987; J.J.F. Scholten and P.J. van der Steen, *Eur. Pat. Appl.* 0210705, d.d. 22.03.1989.
8. E. van der Heide, M. de Wind, A.W. Gerritsen and J.J.F. Scholten, *Proc.*

- 11. Heterogeneous Wacker oxidation; outline -

- 9th Int. Congr. Catal., Calgary, 4 (1988) 1648.
9. E. van der Heide, J.A.M. Ammerlaan, A.W. Gerritsen and J.J.F. Scholten, *J. Molec. Catal.*, 55 (1989) 320.
 10. E. van der Heide, J. Schenk, A.W. Gerritsen and J.J.F. Scholten, *Rec. Chim. Trav. Pays-Bas*, 109 (1990) 93.
 11. P.M. Henry, *J. Am. Chem. Soc.*, 86 (1964) 3246; P.M. Henry, *J. Am. Chem. Soc.*, 88 (1966) 1595.
 12. M. Akimoto, M. Usami and E. Echigoya, *Bull. Chem. Soc. Jpn.*, 51 (1978) 2195; G.K. Boreskov, A.A. Ivanov, O.M. Ilyinich and V.G. Ponomareva, *React. Kinet. Katal. Lett.*, 3 (1975) 1.
 13. P.M. Henry: *Palladium Catalyzed Oxidation of Hydrocarbons*, Reidel, Dordrecht, 1980; P. François, *Ann. Chim. (Paris)*, 4 (1969) 371; K.I. Matveev, *Kinet. Katal.*, 18 (1977) 862; N.B. Shitova, L.I. Kuznetsova and K.I. Matveev, *Kinet. Katal.*, 15 (1974) 72.
 14. J.L. Seoane, P. Boutry and R. Montarnal, *J. Catal.*, 63 (1980) 182; C. Blejean, P. Boutry and R. Montarnal, *C. R. Acad. Sci. Paris, Ser. C*, 270 (1970) 257.

Summary

Via homogeneous Wacker oxidation ethylene can be selectively oxidized with dioxygen to acetaldehyde, while other alkenes can be converted to ketones or to aldehydes. The catalyst consists of a mixture of PdCl_2 and CuCl_2 , dissolved in hydrochloric acid. Making use of this catalyst acetaldehyde is produced industrially, but the importance of this application is decreasing as acetic acid, which used to be manufactured from acetaldehyde, is nowadays produced by carbonylation of methanol.

Via homogeneous Wacker oxidation alkenes higher than ethylene can also be oxidized, but industrial application is unattractive as it is difficult to separate the formed high-boiling aldehydes or ketones from the aqueous catalyst solution. Moreover, chlorinated byproducts are formed in high yields and the corrosive properties of the combination of hydrochloric acid and oxygen cause practical problems.

In the light of the foregoing the development of a heterogeneous catalyst would be attractive. The alkene could then be led over the catalyst in the gas phase, and gaseous products would be set free. The application of such a catalyst, consisting of the combination of a vanadate monolayer on $\gamma\text{-Al}_2\text{O}_3$ or on TiO_2 (anatase) and a submonolayer of tetrachloropalladic acid or palladium sulphate, forms the subject of this thesis.

The structure of the vanadate monolayer on $\gamma\text{-Al}_2\text{O}_3$ has been investigated by means of ^{51}V NMR and DRIFT (Diffuse Reflectance Infrared Fourier Transform). It seems likely that at low coverages mainly isolated (monomeric or dimeric) vanadate units are present, whereas one- or two-dimensional structures are formed at higher coverages. The number of $\text{V}=\text{O}$ groups present appears to be related to the vanadate coverage and to the degree of dehydration, and a surface structure is proposed.

The kinetics and mechanism of the oxidation of ethylene, 1-butene and styrene over the heterogeneous Wacker catalyst appear to correspond to that described in the literature for homogeneous Wacker oxidation. The

selectivities are found to be high. Acetaldehyde is produced with a selectivity higher than 99 %, butanone is formed from 1-butene with selectivities ranging from 80 % to 95 %, and styrene is oxidized to acetophenone and benzaldehyde with a total selectivity higher than 95 %.

The stability of the catalyst during ethylene oxidation appeared to improve when $\text{HCl}/\text{H}_2\text{PdCl}_4$ was replaced by $\text{LiCl}/\text{H}_2\text{PdCl}_4$ or by $\text{NaCl}/\text{Na}_2\text{PdCl}_4$. In 1-butene oxidation an excellent stability was arrived at through the application of $\text{H}_2\text{SO}_4/\text{PdSO}_4$ instead of palladium chloride salts. During the oxidation of styrene the catalyst deactivated due to the formation of carbonaceous deposits. Oxidative removal of these deposits was possible at higher temperatures, resulting in a partial regeneration of the catalyst.

The oxidation of cyclohexene to cyclohexanone and phenol appeared to proceed at a low reaction rate, due to the weak coordination of cyclohexene to palladium. However, in the presence of sodium chloride cyclohexene could be completely converted to benzene.

When $\gamma\text{-Al}_2\text{O}_3$ is replaced as a support by $\text{TiO}_2(\text{a})$ the activity increases by a factor of 20. For the time being a full explanation of this effect is not available, but the phenomenon might be due to chemical bonding between the palladium complex and the vanadate monolayer, which positively influences the activity. Under this assumption no zero-valent palladium would be formed during Wacker oxidation, but monolayer vanadate is reduced simultaneously with the oxidation of ethylene.

With tetrachloropalladic acid as a catalyst, ethylene can reduce the vanadate layer over distances as long as 15 Å. This long-distance reduction probably proceeds via hydrogen spillover. Through Pd catalyzed reduction of the vanadate monolayer with dihydrogen, spillover could be investigated separately. This reaction was computer modelled and the results were compared with the experimental results of heterogeneous Wacker oxidation.

By combining the results summarized above, an overall picture of the various reactions taking place in heterogeneous Wacker catalysis could be obtained.

Samenvatting

Door middel van homogene Wacker oxidatie kan ethyleen met zuurstof selectief worden geoxideerd tot acetaldehyde en kunnen andere alkenen worden omgezet in ketonen of aldehyden. De katalysator, die bestaat uit een mengsel van palladiumchloride en koperchloride opgelost in zoutzuur, wordt industrieel gebruikt voor de productie van acetaldehyde. Zij raakt echter steeds meer in onbruik nu azijnzuur, dat vroeger uit acetaldehyde werd verkregen, wordt geproduceerd door carbonylering van methanol.

Oxidatie van hogere alkenen is goed mogelijk met behulp van homogene Wacker oxidatie, maar industrieel onaantrekkelijk. Bij oxidatie van hogere alkenen zijn namelijk de hoogkokende produkten die ontstaan moeilijk te scheiden van de waterige katalysatoroplossing. Verder ontstaan er grote hoeveelheden gechloreerde bijprodukten en bovendien is de combinatie van zoutzuur en zuurstof bijzonder korrosief.

Het was daarom aantrekkelijk om voor de oxidatie van hogere alkenen een heterogene katalysator te ontwikkelen. Daarbij wordt het alkeen gasvormig over de vaste katalysator geleid, terwijl tevens de produkten in de gasvorm vrijkomen. Een dergelijke katalysator, bestaande uit de combinatie van een vanadaatmonolaag op $\gamma\text{-Al}_2\text{O}_3$ of TiO_2 (anataas) gedeeltelijk bedekt met een sub-monolaag palladiumchloride of palladiumsulfaat, is in dit proefschrift beschreven.

De structuur van de vanadaatmonolaag op $\gamma\text{-Al}_2\text{O}_3$ werd onderzocht met behulp van ^{51}V NMR en DRIFT (Diffuse Reflectance Infrared Fourier Transform). Bij lage belading zijn waarschijnlijk geïsoleerde (monomere of dimere) vanadaateenheden aanwezig, terwijl bij toenemende belading één- of twee-dimensionale vanadaat structuren worden gevormd. Het aantal V=O groepen dat aanwezig is, bleek te zijn gerelateerd aan de belading en de mate van dehydratatie, en een oppervlaktestructuur wordt voorgesteld.

De kinetiek en het mechanisme van de oxidatie van ethyleen, 1-buteen en styreen over de heterogene Wacker katalysator bleek in grote lijnen overeen

te komen met wat in de literatuur beschreven is voor homogene Wacker oxidatie. De selektiviteiten bleken hoog. Aceetaldehyde wordt geproduceerd met een selektiviteit hoger dan 99 %, butanon werd gevormd uit 1-buteen met selektiviteiten van 80 tot 95 %, terwijl styreen wordt geoxideerd tot acetofenon en benzaldehyde met een gezamenlijke selektiviteit die hoger is dan 95 %.

De stabiliteit van de katalysator gedurende oxidatie van ethyleen bleek sterk te verbeteren indien $\text{HCl}/\text{H}_2\text{PdCl}_4$ wordt vervangen door $\text{LiCl}/\text{H}_2\text{PdCl}_4$ of door $\text{NaCl}/\text{Na}_2\text{PdCl}_4$. Voor 1-buteen oxidatie werd een uitstekende stabiliteit verkregen door het toepassen van $\text{H}_2\text{SO}_4/\text{PdSO}_4$ in plaats van chloride bevattende palladiumzouten. Gedurende oxidatie van styreen bleek de katalysator te deaktiveren door koolafzetting. Gedeeltelijke regeneratie bleek mogelijk door bij hogere temperatuur de afzetting oxidatief te verwijderen.

Oxidatie van cyclohexeen tot cyclohexanon en fenol bleek bijzonder traag te verlopen als gevolg van de zwakke interactie van cyclohexeen met palladium. Wel kon cyclohexeen volledig worden omgezet tot benzeen als natriumchloride aanwezig was.

Wanneer $\gamma\text{-Al}_2\text{O}_3$ als drager wordt vervangen door $\text{TiO}_2(\text{a})$ neemt de aktiviteit voor de oxidatie van ethyleen met een faktor 20 toe. Een volledige verklaring voor dit effect ontbreekt nog. Wellicht is het een gevolg van een chemische interactie tussen palladium en monolaag-vanadaat, waardoor de aktiviteit positief wordt beïnvloed. Als dit inderdaad het geval is verloopt Wacker oxidatie niet via nulwaardig palladium, maar wordt de vanadaat monolaag gereduceerd, gelijktijdig met de oxidatie van ethyleen.

Met palladiumchloride als katalysator waren wij in staat om onder reaktie-kondities monolaag-vanadaat over grotere afstanden, in ieder geval tot 15 Å, met ethyleen te reduceren. Deze reductie over grotere afstanden vanuit het katalytisch centrum verloopt waarschijnlijk via een waterstof 'spillover' mechanisme. Spillover kon apart worden onderzocht door de katalysator via Pd klusters te reduceren met waterstof. Een computer modellering van deze reaktie werd opgesteld. De resultaten werden gerelateerd aan heterogene Wacker oxidatie.

Door combinatie van bovengenoemde resultaten kon een totaalbeeld van de verschillende reakties die tijdens Wacker oxidatie in combinatie optreden verkregen worden.

Uitleg voor niet-vakgenoten.

Tijdens heterogene Wacker oxidatie volgen een aantal reacties elkaar op. Een overzicht daarvan is weergegeven in de tekening op de voorkant van dit proefschrift.

U ziet een hard en ruw katalysatordeeltje met scherpe randen en hoeken. Het is ongeveer een halve millimeter groot. Het deeltje is zo poreus als een spons, met poriën van ongeveer een 100.000ste millimeter. Ik heb vier jaar lang onderzocht wat er allemaal in deze poriën gebeurt.

Het deeltje bestaat grotendeels uit het dragermateriaal $\gamma\text{-Al}_2\text{O}_3$. Het werd volledig bedekt met een dun laagje vanadiumpentoxide (V_2O_5), waardoor het deeltje, dat eerst wit was, helder geel gekleurd werd. Op de tekening is deze laag op de binnenkant van de porie zichtbaar. Verder zien we in de porie op deze laag een halve cirkel getekend, met in het midden een rondje. Dit rondje is palladium-chloride (PdCl_2). Palladiumchloride is duur en er is daarom maar een kleine hoeveelheid in de poriën aanwezig.

Zoals u ziet bruist het van leven daarbinnen. Wat gebeurt er allemaal? Tussen de gasmolekulen ziet u ethyleen ($\text{H}_2\text{C}=\text{CH}_2$) en water (H_2O). Ethyleen en water zijn in de porie gekropen en hechten zich aan palladiumchloride. Daar zitten ze zo dicht bij elkaar, dat ze met elkaar reageren en daardoor moeten ze het palladiumchloride loslaten. Er is nu een molecuul acetaldehyde, $\text{H}_3\text{C}-\overset{\text{O}}{\parallel}{\text{C}}-\text{H}$, geboren. Acetaldehyde lijkt op azijn en dat kan er dan ook van gemaakt worden.

Er gebeurt nog meer. Het palladiumchloride houdt aan de reactie twee waterstofradikalen ($\text{H}\cdot$) over, die van het watermolecuul afkomstig zijn. Palladiumchloride is niet bestand tegen deze radikalen. Daarom is er de monolaag van vanadiumpentoxide. Vanadiumpentoxide reageert met de waterstofradikalen en het is binnen de cirkel rond palladiumchloride inmiddels verzadigd met deze radikalen. De nieuw gevormde radikalen migreren binnen de cirkel heen en weer, totdat ze buiten de cirkel terecht komen en

daar gebonden worden. Daardoor wordt de cirkel rond palladiumchloride steeds groter.

De cirkel mag echter niet te groot worden, want dan worden de waterstofradikalen niet snel genoeg gebonden. Daarom is er ook zuurstof ($O=O$) aanwezig tussen de molekulen in de gasfase. Zuurstof reageert met de vastgeplakte waterstofradikalen waarbij water ontstaat. Het gevormde water komt vrij en gaat naar de gasfase.

Ook andere produkten dan aceetaldehyde kunnen met deze katalysator gemaakt worden, maar dat staat niet meer op de tekening. Dat kunt u in dit proefschrift lezen.

Dankwoord

Het is onmogelijk om onderzoek te doen zonder hulp van anderen. Ook aan het onderzoek dat in dit proefschrift is beschreven hebben veel mensen meegewerkt. Deze samenwerking heb ik, behalve als noodzakelijk, vooral als plezierig ervaren. Iedereen ben ik daarvoor dankbaar en een aantal wil ik graag met name noemen.

Allereerst wil ik Jaap Teunisse en Nico van Westen bedanken. Jaap en Nico, de textuuranalyses zijn door jullie gedaan, en doordat ik de theoretische achtergrond aan jullie moest uitleggen ben ik het zelf gaan begrijpen. Maar ik denk vooral terug aan de gezelligheid tijdens de vele uren die we samen hebben doorgebracht met koffiedrinken.

Ook gaat mijn dank uit naar het verdere niet-wetenschappelijk personeel, mensen die -ten onrechte worden aangeduid met datgene wat ze niet kunnen. Veel ondersteuning heb ik ontvangen van de instrumentmakers Peter Beekmans, Arie Molenwijck en Piet Verbooy en binnen Chemische Technologie van Gerard van den Bosch, Wim van den Bosch, Kees, Leen (sr) en Leen (jr) Boshuizen, Wim Dumee, Willem Kerkhoven, Bram van der Lee, Ruud Monna, Wim Mulhuyzen, Dolf Pruysken, Wijnand Rietbroek, Jan Smit, Ton van Velzen en natuurlijk de tekenaar Jan van Holst die posters maakte waar prijzen mee gewonnen werden en die de illustraties in dit proefschrift verzorgde. Ik heb goede contacten gehad met de analytische O en O groep, waar Pim van den Bulk, Louk Peffer en Loes Schouten altijd klaar stonden, en verder met de fotografen en met de secretaresses. Van de systeemgroep heb ik computerondersteuning ontvangen.

Ook de afstudeerders, Menno de Wind, Jan Ammerlaan, John Schenk en Marco Zwinkels hebben zich geweed, wat gevolgen had voor dit proefschrift. Menno hield zich onledig met ossidazione catalitica dell' etilene ad acetaldeide in fase vapore, Jan maakte MEK uit 1-buteen en vermaakte zich met organische syntheses, John varieerde de dragers en leerde styreen oxideren (en bikken)

en Marco deed van alles en nog wat en verder computermodellering van waterstof spillover. Verder heb ik met veel studenten kortere contacten gehad. Daaronder behoren Ronald Hultermans en David Hollestelle, die een fabrieksvoorontwerp schreven voor de oxidatie van 1-buteen naar MEK en de vele praktikanten, die een bijdrage aan de resultaten die in hoofdstuk 2 beschreven zijn geleverd hebben.

De contacten met mijn collega's, Martine Schoenmaker-Stolk, Paul Groen en Jaap Struyk heb ik gewaardeerd. Van Peter van der Steen, mijn voorganger, heb ik interessant onderzoek geërfd, terwijl ik het zelf mocht overdragen aan mijn opvolgster, Anja Kreemers. De vele mogelijkheden die ik nog uit wilde werken kon ik aan jou kwijt. Je zult ongetwijfeld je eigen weg in dit onderzoek vinden. Succes!

De begeleiding van Albert Gerritsen (UHD-er Chemische Reaktorkunde) heb ik als inspirerend ervaren. Zijn bijdrage aan de hoofdstukken 2, 9 en andere heeft mij op het juiste spoor gezet en gehouden. Ik heb er veel van geleerd.

De inbreng van mijn promotor, prof. Scholten, is van wezenlijk belang geweest voor het onderzoek. Zijn toewijding en opbouwende kritiek hebben er toe bijgedragen dat dit proefschrift werd wat het nu is.

Omdat ik deel uitmaakte van een relatief kleine onderzoeksgroep was het van wezenlijk belang om veel contacten te onderhouden, zowel voor de theorievorming als voor de gebruikmaking van moderne analysemethoden. Ik heb met veel onderzoekers, nationaal en internationaal, het onderzoek geëvalueerd, maar in het bijzonder wil ik het contact met prof. J.A.R. van Veen (TUE), prof. J. Reedijk en prof. V. Ponc (beide RUL) noemen, wier voortdurende interesse ik als stimulerend heb ervaren. Verder wil ik de vakgroep Organische Chemie in Delft noemen, en de groep organometaalchemie (de SOC) in Utrecht, waar ik drie maanden onderzoek mocht doen. We deden NMR metingen in Nijmegen en infrarood spectroscopie in Twente. Ook de contacten met DSM, waar de XPS/AES metingen gedaan zijn, zijn vruchtbaar geweest. De engelse tekst van dit proefschrift werd gecorrigeerd door de heer H.J. Rhebergen.

Promoveren is, behalve een inspanning, vooral een voorrecht. Ik dank God voor de talenten die Hij gaf om dit werk te mogen doen. Moge het bijdragen tot een beter inzicht in Zijn schepping en tot lof van Hem die dit alles zo mooi gemaakt heeft.

Curriculum vitae

Evert van der Heide werd op 14 juni 1961 in Zwartsluis geboren. Na het VWO examen en een jaar Evangelische Hogeschool in Amersfoort begon hij in 1980 met de studie scheikunde aan de Rijks Universiteit Utrecht. In de afstudeerperiode werd een analytisch-chemisch onderzoek verricht bij de sub-faculteit biologie in Utrecht naar secundaire plantestoffen in *Hoya* species. Vervolgens werd de synthese van deze fysiologisch actieve verbindingen aangevangen bij de vakgroep organische chemie, waarbij gebruik werd gemaakt van organometaal-gekatalyseerde deelstappen. Het doctoraalexamen werd op 24 februari 1986 behaald.

Aansluitend werd een promotieonderzoek verricht naar heterogene Wacker oxidatie, bij de Faculteit der Chemische Technologie en der Materiaalkunde van de Technische Universiteit Delft. Behalve actieve deelname aan vele binnenlandse bijeenkomsten op het gebied van katalyse werd in het buitenland een bijdrage geleverd aan het negende Internationale Congres over Katalyse in Calgary (1988) en een bijdrage in de vorm van een lezing op het zesde Internationale Symposium over Relaties tussen Homogene en Heterogene Katalyse in Pisa (1989). In mei 1990 werd hem één van de DSM prijzen voor Chemie en Technologie toegekend.

Enige bestuurlijke ervaring werd opgedaan tijdens de afstudeerperiode als voorzitter van een studentenvereniging en als studentlid van de sub-faculteitsraad Scheikunde, en tijdens het promotieonderzoek als lid van het vakgroepsbestuur van Chemische Technologie.

Na vervulling van de militaire dienstplicht hoopt hij in dienst te treden bij het Koninklijke/Shell-Laboratorium, Amsterdam.